

(18) (19)
AFAPL-TR-79-2072
AFESC/ESL-TR-79-29

LEVEL

(2)

AD A089182

(6)
**FUEL CHARACTER EFFECTS ON CURRENT,
HIGH PRESSURE RATIO, CAN-TYPE TURBINE
COMBUSTION SYSTEMS.**

DETROIT DIESEL ALLISON DIV.
DIVISION OF GENERAL MOTORS CORPORATION
INDIANAPOLIS, INDIANA 46206

DTIC
ELECTE
SEP 17 1980

(11) APR 1980

(12) 163

TECHNICAL REPORT AFAPL-TR-79-2072, ESL-TR-79-29
(9) Final Report, Jun 1978 - Jun 1979

(10) Rodney E. / Vogel
Dennis L. / Troth
Alfred J. / Verdun

(15) T3361E-78-L-2476

Approved for public release; distribution unlimited.

(16) 3p48

(14) DDA-EDR-9162

(17) 15

DDC FILE COPY

AERO PROPULSION LABORATORY
AIR FORCE WRIGHT AERONAUTICAL LABORATORIES
AIR FORCE SYSTEMS COMMAND
WRIGHT-PATTERSON AIR FORCE BASE, OHIO 45433

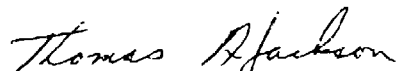
019200 80 9 17 002

NOTICE

When Government drawings, specifications, or other data are used for any purpose other than in connection with a definitely related Government procurement operation, the United States Government thereby incurs no responsibility nor any obligation whatsoever; and the fact that the government may have formulated, furnished, or in any way supplied the said drawings, specifications, or other data, is not to be regarded by implication or otherwise as in any manner licensing the holder or any other person or corporation, or conveying any rights or permission to manufacture use, or sell any patented invention that may in any way be related thereto.

This report has been reviewed by the Office of Public Affairs (ASD/PA) and is releasable to the National Technical Information Service (NTIS). At NTIS, it will be available to the general public, including foreign nations.

This technical report has been reviewed and is approved for publication.

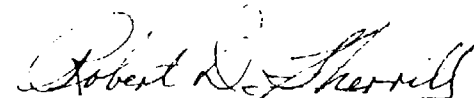


THOMAS A. JACKSON
Fuels Branch
Fuels and Lubrication Division



ARTHUR V. CHURCHILL
Chief, Fuels Branch
Fuels and Lubrication Division

FOR THE COMMANDER



ROBERT D. SHERRILL, Chief
Fuels and Lubrication Division

"If your address has changed, if you wish to be removed from our mailing list, or if the addressee is no longer employed by your organization please notify AFWAL/POSF, W-PAFB, OH 45433 to help us maintain a current mailing list".

Copies of this report should not be returned unless return is required by security considerations, contractual obligations, or notice on a specific document.

REPORT DOCUMENTATION PAGE		READ INSTRUCTIONS BEFORE COMPLETING FORM
1. REPORT NUMBER AFAPL-TR-79-2072, ESL-TR-79-29	2. GOVT ACCESSION NO. AD A659 152	3. RECIPIENT'S CATALOG NUMBER
4. TITLE (and Subtitle) Fuel Character Effects on Current, High Pressure Ratio, Can-Type Turbine Combustion Systems		5. TYPE OF REPORT & PERIOD COVERED Final 15 June 1978 - 15 June 1979
7. AUTHOR(s) Rodney E. Vogel Dennis L. Troth Albert J. Verdouw		6. PERFORMING ORG. REPORT NUMBER DDA EDR 9762
9. PERFORMING ORGANIZATION NAME AND ADDRESS Detroit Diesel Allison (DDA) Division of General Motors Corporation Indianapolis, IN 46206		8. CONTRACT OR GRANT NUMBER(s) F33615-78-C-2006
11. CONTROLLING OFFICE NAME AND ADDRESS Air Force Aero-Propulsion Laboratory, Air Force Wright Aeronautical Laboratory, Air Force Systems Command, Wright-Patterson AFB, Ohio 45433		10. PROGRAM ELEMENT, PROJECT, TASK AREA & WORK UNIT NUMBERS Project 3048 Task 05 Work Unit 95
14. MONITORING AGENCY NAME & ADDRESS (if different from Controlling Office)		12. REPORT DATE April 1980
		13. NUMBER OF PAGES 148
		15. SECURITY CLASS. (of this report) Unclassified
		15a. DECLASSIFICATION/DOWNGRADING SCHEDULE
16. DISTRIBUTION STATEMENT (of this Report) Approved for public release; distribution unlimited.		
17. DISTRIBUTION STATEMENT (of the abstract entered in Block 20, if different from Report)		
18. SUPPLEMENTARY NOTES Partial funding and technical support in the area of the measurement and analysis of gaseous emissions and smoke data were provided by the Environmental Sciences Branch of the Environics Division in the Research and Development Directorate of HQ Air Force Engineering and Services Center (HQ AFESC/RDVC).		
19. KEY WORDS (Continue on reverse side if necessary and identify by block number) TF41 Combustor, High Pressure Ratio Combustor, JP-4, JP-8, Alternative Fuels, Aromatic Fuels, Fuel Property Variation, Exhaust Emissions		
20. ABSTRACT (Continue on reverse side if necessary and identify by block number) The effect of limited fuel property variation on the performance of current, high pressure-ratio, can-type combustors was evaluated. The TF41 turbofan combustor was employed. This combustor has conventional, dual-orifice fuel injection and film cooling. The combustion zone is approximately stoichiometric at takeoff. Twelve experimental fuels, including JP-4 and JP-8, were tested. Distillation range, hydrogen content, and aromatic type were varied by blending JP-4 and JP-8 fuels with mineral seal oil and two types of aromatic solvents.		

20. ABSTRACT (continued)

Performance tests were accomplished at idle, altitude cruise, dash, and take-off conditions. Sea level and altitude ignition tests were also completed. Fuel fouling and carboning characteristics were established. Combustor operating parameters such as liner temperature, pattern factor, ignition fuel/air ratio, lean blow out fuel/air ratio, and exhaust emissions were correlated to fuel properties. The effect of fuel properties on combustor and turbine hardware durability was assessed analytically.

Accession For	
NTIS GDA&I	<input checked="checked" type="checkbox"/>
DDC TAB	<input type="checkbox"/>
Unannounced	<input type="checkbox"/>
Justification	<input type="checkbox"/>
By _____	
Distribution/ _____	
Availability Codes	
Dist	Avail and/or Special
A	

PREFACE

The Air Force Aero-Propulsion Laboratory (AFAPL) is investigating the effect of limited fuel property variations on the performance of several classes of aircraft gas turbine combustion systems. This report covers work accomplished by the Detroit Diesel Allison (DDA), Division of General Motors, under contract to AFAPL (No. F33615-78-C-2006) to assess fuel property effects on current high-pressure ratio, can-type combustors. The work was performed under Project 3048, Task 05, Work Unit 95. Thomas A. Jackson was the government project engineer for this program.

Supplemental funding for this program and technical guidance in the measurement and correlation of gaseous emissions data were provided by the Environmental Sciences Branch of the Environics Division in the Research and Development Directorate of the HQ Air Force Engineering and Services Center, located at Tyndall Air Force Base, Florida. Formerly this organization has been referred to as CEEDO and as the Civil Engineering Center.

Test fuel analysis was supplied by AFAPL through its own fuels laboratory, under contract with Monsanto Research Laboratory, and through the cooperation of the Air Force Logistics Command Fuels Laboratory (SFQLA).

The assistance and cooperation of these organizations are appreciated.

TABLE OF CONTENTS

SECTION		PAGE
I	INTRODUCTION.....	1
II	SUMMARY.....	3
III	EXPERIMENTAL.....	5
	A. TF41 Engine and Combustion System Description.....	5
	B. Experimental System Description.....	11
	C. Experimental Fuels Description.....	20
	1. General Description.....	20
	2. Physical and Chemical Description.....	22
	D. General Test Plan.....	30
	1. Operating Conditions.....	32
	2. Fuel Fouling Test Detail Plan.....	36
IV	RESULTS AND DISCUSSION.....	45
	A. Test Condition Summary	45
	B. Performance Analysis.	47
	1. CO and UHC Emissions.....	48
	2. NO _x Emissions.....	49
	3. Smoke Emissions.....	49
	4. Liner Wall Temperature.....	50
	5. Carbon Deposition.....	54
	6. Combustor Pattern Factor and Exit Profile.....	57
	7. Altitude Ignition and LBO.....	58
	8. Sea-Level Starting and Stability.....	61
	C. Single-Variable Linear Regression Analysis.....	62
	1. Combustion Efficiency--SLTO and Idle.....	64
	2. CO Emissions--SLTO and Idle.....	67
	3. UHC Emissions--SLTO and Idle.....	69

TABLE OF CONTENTS (Concluded)

SECTION	PAGE
4. NO _x Emissions--SLTO	70
5. Smoke Emissions--SLTO.....	71
6. Liner Wall Temperature.....	74
7. Pattern Factor and Exit Profile.....	78
8. Carbon Deposition and Fuel Nozzle Fouling.....	78
9. Sea-Level Starting.....	79
10. Altitude Ignition and LBO.....	80
11. Flame Stability.....	83
D. Multiple-Variable Linear Regression Analysis.....	87
E. Life Analysis Results.....	92
1. Combustor Life Analysis.....	100
2. HPT-1 Vane Life Analysis.....	101
3. HPT-1 Blade Life Analysis.....	104
V CONCLUSIONS AND RECOMMENDATIONS.....	107
A. Conclusions.....	107
B. Recommendations.....	108
REFERENCES.....	109
APPENDIX A--GENERAL DATA SUMMARY.....	111
APPENDIX B--COMBUSTOR OUTLET TEMPERATURE PATTERNS.....	127
APPENDIX C--CARBONING DATA SUMMARY.....	133
APPENDIX D--STRESS LIFE ANALYSIS.....	145

LIST OF ILLUSTRATIONS

FIGURE		PAGE
1	TF41 Engine Cross Section.....	5
2	TF41 Combustion System.....	7
3	TF41 Combustion Liner Details.....	8
4	TF41 Fuel Injection System.....	9
5	Airflow Distribution for TF41 Combustor at SLTO.....	11
6	Combustor Rig Cross Section.....	12
7	Principal Instrumentation for TF41 Experimental Fuels Test...	14
8	Emission Instrument System Arrangement (EPA Aircraft System).....	17
9	Smoke Sampling System.....	17
10	TF41 Combustor Liner Thermocouple Locations.....	18
11	TF41 Discharge Nozzle Thermocouple Axial Locations.....	19
12	TF41 Discharge Nozzle Thermocouple Locations.....	20
13	TF41 Combustor Rig Fuel Nozzle Body and Instrumentation.....	21
14	Detailed Test Plan Sequence and Test Points.....	32
15	Key Test Plan Events.....	33
16	Relative Fuel Fouling Rates.....	37
17	TF41 Engine Power Versus Speed.....	38
18	TF41 Engine Fuel Injector.....	39
19	Typical Calculated Fuel Injector Temperatures.....	40
20	Effect of Fuel Flow Rate and Fuel Inlet Temperature on Nozzle Feedarm Pilot Interface Temperature (Standard Nozzle).....	42
21	Slotted Fuel Nozzle Configurations.....	43
22	Effect of Fuel Flow Rate and Nozzle Slot Depth on Nozzle Feedarm Pilot Interface Temperature.....	44
23	Fuel System Schematic for Fuel Fouling Test.....	44
24	Effect of Operating Conditions on CO Emission Levels.....	51
25	Effect of Operating Conditions on UHC Emission Levels.....	51
26	Effect of Operating Conditions on Combustion Efficiency Levels.....	51
27	Effect of Operating Conditions on NO _x Emission Levels.....	51

LIST OF ILLUSTRATIONS (Continued)

FIGURE		PAGE
28	Effect of Operating Conditions on Smoke Emission Levels.....	52
29	Effect of Operating Conditions on Maximum Liner Wall Temperatures.....	52
30	Effect of Operating Conditions on Maximum Barrel Wall Temperatures.....	53
31	Effect of Operating Conditions on Average Barrel Wall Temperatures.....	53
32	Dome and Fuel Nozzle Carbon Deposition--JP-4 Fuel.....	55
33	Dome and Fuel Nozzle Carbon Deposition--JP-8 Fuel.....	56
34	SLTO Outlet Temperature Patterns.....	57
35	Effect of Operating Conditions on Combustor Temperature Pattern Factor.....	58
36	Effect of Operating Conditions on Combustor Exit Radial Temperature Profile.....	58
37	Effect of Altitude on Combustor θ Parameter.....	60
38	Altitude Relight Envelope Limits--JP-4 and JP-8 Fuels.....	60
39	Effect of Inlet Temperature on Sea Level Ignition and LBO....	61
40	Effect of Combustor θ Parameter on LBO F/A Ratio.....	62
41	Effect of Fuel Hydrogen Content on SLTO Combustion Efficiency.....	66
42	Effect of Fuel Total Aromatic Content on SLTO Combustion Efficiency.....	66
43	Effect of Fuel Smoke Point on SLTO Combustion Efficiency.....	67
44	Effect of Fuel Hydrogen Content on SLTO CO Emissions.....	68
45	Effect of Fuel Total Aromatic Content on SLTO CO Emissions...	69
46	Effect of Fuel Smoke Point on SLTO CO Emissions.....	69
47	Effect of Fuel Droplet Size (SMD) on Idle CO Emissions.....	69
48	Effect of Fuel Surface Tension on SLTO NO _x Emissions.....	72
49	Effect of Fuel Hydrogen Content on SLTO Smoke Emissions.....	73
50	Effect of Fuel Total Aromatic Content on SLTO Smoke Emissions.....	73

LIST OF ILLUSTRATIONS (Continued)

FIGURE		PAGE
51	Effect of Fuel Hydrogen Content on SLTO Maximum Liner Metal Temperature.....	75
52	Effect of Total Aromatic Content on SLTO Maximum Liner Wall Temperature.....	75
53	Effect of Fuel Hydrogen Content on SLTO Maximum Barrel Wall Temperature.....	76
54	Effect of Fuel Multi-Ring Aromatic Content on SLTO Maximum Barrel Wall Temperature.....	76
55	Effect of Fuel Hydrogen Content on Liner Temperature Parameter at Cruise Operating Conditions.....	77
56	Effect of Fuel Multi-Ring Aromatic Content on SLTO Average Barrel Wall Temperature.....	77
57	Effect of Fuel Viscosity on SL Ambient Inlet Ignition F/A Ratio.....	81
58	Effect of Fuel Hydrogen Content on Maximum Ignition Altitude.....	82
59	Effect of Fuel Total Aromatic Content on Maximum Ignition Altitude.....	82
60	Effect of Fuel Single-Ring Aromatic Content on Maximum Ignition Altitude.....	83
61	Effect of Fuel Surface Tension on 3-km Altitude LBO F/A Ratio.....	84
62	Effect of Fuel Vapor Pressure on 3-km Altitude LBO F/A Ratio.....	84
63	Effect of Fuel 10% Distillation Point on 10-km Altitude LBO F/A Ratio.....	84
64	Effect of Fuel Viscosity on 10-km LBO F/A Ratio.....	85
65	Effect of Fuel Vapor Pressure on 10-km Altitude LBO F/A Ratio.....	85
66	Effect of Fuel End Point Temperature on Cruise Condition LBO F/A Ratio.....	87

LIST OF ILLUSTRATIONS (Continued)

FIGURE		PAGE
67	Multiple Fuel Property Effect on SLTO Combustion Efficiency..	93
68	Multiple Fuel Property Effect on Idle Combustion Efficiency..	93
69	Multiple Fuel Property Effect on SLTO CO Emissions.....	94
70	Multiple Fuel Property Effect on Idle CO Emissions.....	94
71	Multiple Fuel Property Effect on SLTO UHC Emissions.....	95
72	Multiple Fuel Property Effect on Idle UHC Emissions.....	95
73	Multiple Fuel Property Effect on SLTO NO _x Emission.....	96
74	Multiple Fuel Property Effect on SLTO Smoke Emissions.....	96
75	Multiple Fuel Property Effect on SLTO Maximum Liner Wall Temperatures.....	96
76	Multiple Fuel Property Effect on SLTO Maximum Barrel Wall Temperatures.....	97
77	Multiple Fuel Property Effect on SLTO Average Barrel Wall Temperatures.....	97
78	Multiple Fuel Property Effect on SLTO Pattern Factor Levels..	98
79	Multiple Fuel Property Effect on Idle LBO F/A Ratio.....	98
80	Multiple Fuel Property Effect on Idle Ignition F/A Ratio.....	98
81	Multiple Fuel Property Effect on SL Ambient Inlet Ignition F/A Ratio.....	99
82	Multiple Fuel Property Effect on Maximum Ignition Altitude...	99
83	Mean Section of HPT-1 Vane.....	102
84	Mean Section of HPT-1 Blade.....	105
85	Effect of Fuel Multi-Ring Aromatic Content on Relative HPT-1 Blade Life.....	106
A-1	TF41 Combustor Liner Thermocouple Locations.....	112
B-1	SLTO Combustor Outlet Temperature Patterns--Fuels 2 through 6.....	128
B-2	SLTO Combustor Outlet Temperature Patterns--Fuels 8 through 12.....	130
C-1	Posttest Photograph of Carbon Deposition--Fuel 2.....	134
C-2	Posttest Photograph of Carbon Deposition--Fuel 3.....	135
C-3	Posttest Photograph of Carbon Deposition--Fuel 4.....	136

LIST OF ILLUSTRATIONS (Concluded)

FIGURE		PAGE
C-4	Posttest Photograph of Carbon Deposition--Fuel 5.....	137
C-5	Posttest Photograph of Carbon Deposition--Fuel 6.....	138
C-6	Posttest Photograph of Carbon Deposition--Fuel 8.....	139
C-7	Posttest Photograph of Carbon Deposition--Fuel 9.....	140
C-8	Posttest Photograph of Carbon Deposition--Fuel 10.....	141
C-9	Posttest Photograph of Carbon Deposition--Fuel 11.....	142
C-10	Posttest Photograph of Carbon Deposition--Fuel 12.....	143
D-1	Strength Versus Temperature--N263 Material.....	145
D-2	Computer-Simulated Discharge Nozzle Inner Surface (STRATA Model).....	147
D-3	Computer-Simulated Discharge Nozzle Outer Surface (STRATA Model).....	148

LIST OF TABLES

TABLE		PAGE
1	TF41 SITO Operating Conditions.....	6
2	Fuel Nozzle Flow Performance Limits.....	9
3	Airflow Distribution for TF41 Combustor.....	10
4	Rig Pressure and Temperature Instrumentation.....	15
5	Rig Flow and Exhaust Gas Instrumentation.....	15
6	On-line Exhaust Gas Measurement Instruments.....	16
7	Combustor Metal Temperature Thermocouple Locations.....	18
8	Fuels and Fuel Blends Tested.....	22
9	Principal Fuel Properties--High-Pressure Tests.....	23
10	Principal Fuel Properties--Low-Pressure Tests.....	24
11	Fuel Properties from High-Pressure Sample.....	25
12	Fuel Properties from Low-Pressure Sample.....	26
13	Fuel Property Correlation.....	27
14	Test Fuel Hydrocarbon Type Analyses--High-Pressure Fuel Sample.....	28
15	Test Fuel Hydrocarbon Type Analyses--Low-Pressure Fuel Sample.....	28
16	Test Fuel Gas Chromatographic Simulated Distillation-- High-Pressure Fuel Sample.....	29
17	Test Fuel Gas Chromatographic Simulated Distillation-- Low-Pressure Fuel Sample.....	29
18	Test Fuel Conventional Inspection Data--High-Pressure Fuel Sample.....	30
19	Fuel Property Effects on Combustor Performance.....	31
20	Combustion Rig Test Conditions.....	34
21	Summary of Condition Scaling.....	35
22	Estimated Mission-Mode Breakdown.....	38
23	Fuel Fouling Rates (Analytical).....	40
24	Fuel Fouling (Analytical).....	41
25	Comparison of Idle Rig Test Conditions to Engine Conditions..	47
26	Comparison of Cruise Rig Test Conditions to Engine Conditions.....	48

LIST OF TABLES (Continued)

TABLE		PAGE
27	Comparison of Dash Rig Test Conditions to Engine Conditions..	49
28	Comparison of SLTO Rig Test Conditions to Engine Conditions..	50
29	Fouling and Carboning Summary.....	54
30	Nominal Start Conditions.....	59
31	Single-Variable Linear Regresscion Summary.....	64
32	Summary of Combustion Efficiency Test Results.....	65
33	Summary of CO Emission Test Results.....	68
34	Summary of UHC Emission Test Results.....	70
35	Summary of NO _x Emission Test Results.....	71
36	Summary of Smoke Emission Test Results.....	72
37	Summary of Wall Temperature Test Results.....	74
38	Summary of Barrel Temperature Test Results.....	76
39	Summary of Barrel Temperature Test Results.....	78
40	Summary of Pattern Factor Test Results.....	79
41	Fuel Nozzle Fouling Summary.....	80
42	Sea-Level Starting Test Summary.....	80
43	Altitude Ignition Summary.....	81
44	Flame Stability Data Summary.....	86
45	Independent Variable (Fuel Properties) Groupings.....	88
46	Parameters Used in Multi-Regression Analysis.....	89
47	Multiple Variable Linear Regression Analysis Summary.....	90
48	Comparison of Combustor LCF Life for Four Representative Test Fuels.....	102
49	Comparison of Oxidation Penetration on TF41 HPT-1 Vane for the 12 Test Fuels.....	103
50	Variation in Stress Rupture Life of TF41 HPT-1 Blade for the 12 Test Fuels.....	104
51	Turbine Life Regression Analysis.....	105
A-1	Idle Condition Performance Data.....	113
A-2	Cruise Condition Performance Data.....	114
A-3	SL Dash Condition Performance Data.....	115

LIST OF TABLES (Concluded)

TABLE		PAGE
A-4	SLTO Condition Performance Data.....	116
A-5	Ignition and Flame Stability Summary.....	119
A-6	SLTO Fouling and Carboning Data.....	125
A-7	Fuel Fouling Test Results--Fuel Deposit Investigation.....	126
D-1	Maximum Stresses in the Transition Section of the TF41 Combustor for Typical Test Fuels.....	146

NOMENCLATURE

SYMBOL

A	area, m ²
A _r	reference area, m ²
AR	2040 aromatic solvent fuel additive
A _R	area ratio
b	function of combustion equivalence ratio
BIP	burner (combustor) inlet pressure
BIT	burner (combustor) inlet temperature, K
BOT	burner (combustor) outlet temperature, K
C-A	chromel-alumel thermocouple junction
CO	carbon monoxide
EI	emission index, g pollutant/kg fuel
e	base of natural logarithms
F/A	fuel to air ratio, g fuel/kg air
FN	fuel injector flow number, $W_f / \sqrt{\Delta P_f}$ W_f = fuel flow rate, kg/hr ΔP_f = fuel nozzle differential pressure, MPa
h	combustor dome height, cm
H	hydrogen
I-C	iron-constantan thermocouple junction
HPT-1	high-pressure turbine, first stage
IBP	initial boiling point, K
IGN	ignition
JFTOT	jet fuel thermal oxidation temperature (breakpoint), K
k	constant for statistical analysis
LBO	lean blow out
LCF	low cycle fatigue
LHV	fuel lower heating value, MJ/kg
M _N	Mach number
MS	Gulf mineral seal oil, fuel additive
NO _x	oxides of nitrogen
P	pressure, MPa
PF	pattern factor

NOMENCLATURE (Concluded)

SYMBOL

PPR	platinum-platinum rhodium thermocouple junction
RPF	radial pattern factor
R^2	statistical coefficient of determination
SL	sea level
SLTO	sea level takeoff
SMD	Sauter mean diameter (pressure atomizing fuel nozzle)

$$SMD = \frac{23 \nu_f^{0.2} \sigma_f^{0.6} W_f^{0.25}}{\Delta P_f^{0.4}}$$

where: SMD = droplet size, microns

ν_f = fuel kinematic viscosity, centistokes

σ_f = fuel liquid surface tension, dynes/cm

W_f = fuel flow rate, lbm/hr

ΔP_f = fuel nozzle pressure drop, psi

SN	smoke number
T	temperature, K
TC	thermocouple
T_g	gas temperature, K
T_w	wall temperature, K
UHC	unburned hydrocarbons
W_a	airflow, kg/s
$W_A \sqrt{T/P}$	flow factor
a	hydrogen to carbon molar ratio
η	combustion efficiency
ϕ	equivalence ratio, (fuel/air ratio, local)/(fuel/air ratio, stoichiometric)
σ	standard deviation in statistical analysis
$\sigma_x, \sigma_y, \sigma_z$	stress in Cartesian space
θ	combustion reaction rate parameter

SECTION I

INTRODUCTION

Since 1973 the cost and availability of military aviation jet fuel have changed dramatically. Over that period the cost has more than quadrupled. At the same time, the Air Force has encountered difficulties in procuring annual quantities of aviation jet fuel, even though these desired fuel quantities are significantly lower than those procured prior to 1973.

A similar history of rising costs is associated with commercial aviation jet fuel grades. At the same time, to obtain desired fuel quantities, batches of fuel, which have not fully met the existing specifications, have been bought. Limits on aromatic content and the smoke point have occasionally been waived.

Numerous alternatives to petroleum-derived fuel have been considered as a means of obtaining price stability and ensuring adequate fuel quantities for both military and commercial users. The more exotic of these options (nuclear, hydrogen, etc) have been discarded in the near term in favor of continued reliance on liquid hydrocarbon fuels. In this regard, nonpetroleum sources of liquid hydrocarbons lie in shale oil, coal, and tar sands resources. Crudes derived from these sources will be appreciably different from petroleum crudes. To maximize the benefits of using these alternate crudes, the effort involved in refining them must be minimized.

Additionally, the Air Force has been considering switching from JP-4 to JP-8 (similar to commercial grade Jet A-1) as its operational fuel. Reduced combat vulnerability and commonality with NATO gas turbine fuels have stimulated this interest. Operational and performance penalties that may be associated with such a change need to be assessed.

With these objectives the Air Force, through the Air Force Aero-Propulsion Laboratory (AFAPL) and in conjunction with other agencies, has initiated efforts to quantify gas turbine engine performance, durability, and environmental impact as a function of selected fuel properties. The effort reported

herein concerns the fourth contracted investigation in a series of programs sponsored by AFAPL to evaluate fuel effects in existing and near-future military aircraft gas turbine engines. Preceeding efforts looked at fuel effects in a current low pressure ratio, can-type combustor (J79, Reference 1); and in a high-pressure-ratio, full-annular combustor (F101, Reference 2). This effort involves the TF41 engine representing high pressure-ratio, can-type combustion systems.

SECTION II

SUMMARY

The purpose of this program was to determine the effects of fuel property variations on the performance, exhaust emission, and durability characteristics of the TF41 (high-pressure ratio, cannular) turbofan engine combustion system. Performance and emission characteristics were determined by combustor rig tests and substantial data analyses. Pressure and airflow scaling was required on some high-pressure test points because of rig facility limitations. The operational thermal stability of the fuels was assessed in a series of short fuel nozzle fouling tests. Durability characteristics of the combustor and turbine were evaluated by integrating rig test results into computer durability simulations.

Twelve refined and blended fuels, which incorporated systematic variations in hydrogen content (nominally 12.0 to 14.5 weight percent), aromatic type (single or multi-ring), 10% distillation point (353 to 464 K by gas chromatograph), final boiling point (541 to 612 K by gas chromatograph), and viscosity (0.884 to 2.316 centistokes at 298 K), were evaluated in this program.

At high-power operating conditions, characterized by sea level takeoff, fuel properties such as hydrogen content, aromatic content, and aromatic type were found to significantly affect CO and NO_x formation, combustion efficiency, smoke emission, and liner wall temperature. NO_x formation was also influenced by the physical properties of the fuel (especially surface tension). UHC and pattern factor were not affected by fuel properties.

At idle operating conditions no significant correlation between combustor performance parameters and fuel property characteristics could be found.

At sea level start conditions, both ambient and cold inlet, the required ignition F/A ratio correlated with 10% boiling point and fuel viscosity.

At altitude relight conditions, the maximum attainable successful ignition altitude was severely limited by decreased fuel hydrogen content (increased aromatic content). Combustor and/or fuel nozzle design modifications would be required if lower hydrogen content fuel were specified for TF41 use.

A special one hour fouling/deposition test at modified SLTO conditions was run with each fuel. Very little fouling or carbon deposition occurred, and results did not correlate to fuel property characteristics. A modified rig test procedure or an engine test would be required to accurately study the fouling/deposition potential.

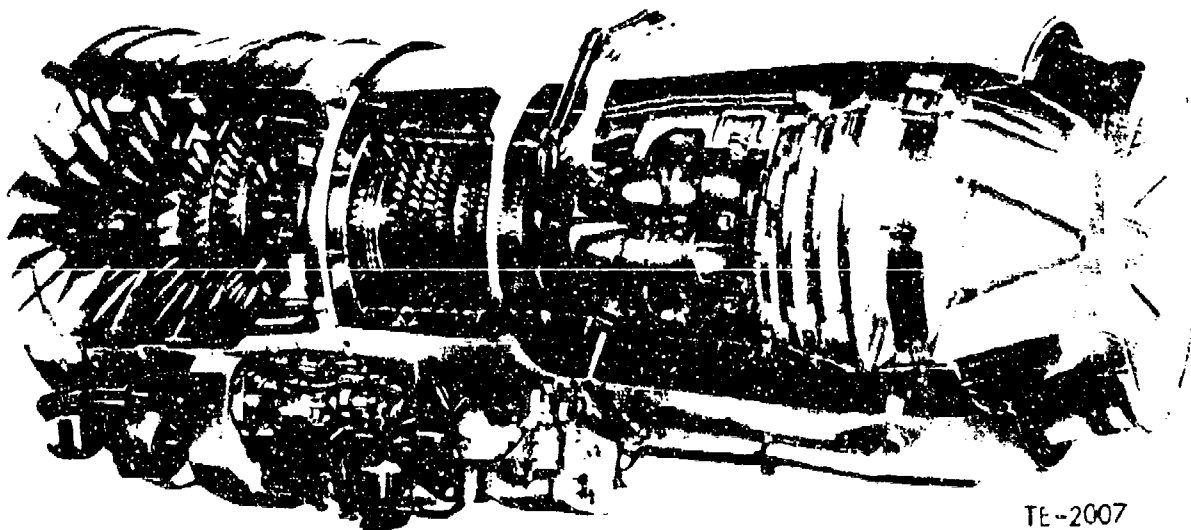
Computer projections of hot section hardware life were conducted incorporating rig data. Combustor life was not sensitive to fuel properties as the wall temperatures of the life limiting component, the discharge nozzle, were essentially unchanged by any fuel tested. Combustor barrel (section of the combustor between the dome and the discharge nozzle) temperatures did increase, however, as fuel hydrogen content was reduced. Turbine blading life (stator vane and rotor blade) did not correlate significantly to any fuel property.

SECTION III EXPERIMENTAL

A. TF41 ENGINE AND COMBUSTION SYSTEM DESCRIPTION

The TF41 turbofan engine shown in Figure 1 incorporates a twin-spool axial compressor-turbine configuration. The low-pressure system connects a three-stage, low-pressure fan and a two-stage, intermediate-pressure compressor to a two-stage, low-pressure turbine. The high-pressure section incorporates ten through-flow combustion chambers assembled in an annular chamber with a twelve-stage, high-pressure compressor directly coupled to a two-stage, air-cooled, high-pressure (gasifier) turbine.

The TF41 engine currently powers the LTV A-7D and A-7E military fighter/interceptor aircraft. First introduced in the mid-1960s, the TF41 is used by over 1100 U.S. and allied forces aircraft. TF41 engine production and service operation are projected well into the 1980s.



TE-2007

Figure 1. - TF41 Engine Cross Section.

The currently produced TF41-A-2 engine is rated at 64500 N thrust (minimum) at a nominal pressure ratio of 22:1 and an inlet airflow of 119 kg/sec at SLTO conditions. The nominal burner outlet temperature at this point is 1502 K. An abbreviated summary of the combustor operating conditions at SLTO is presented in Table 1.

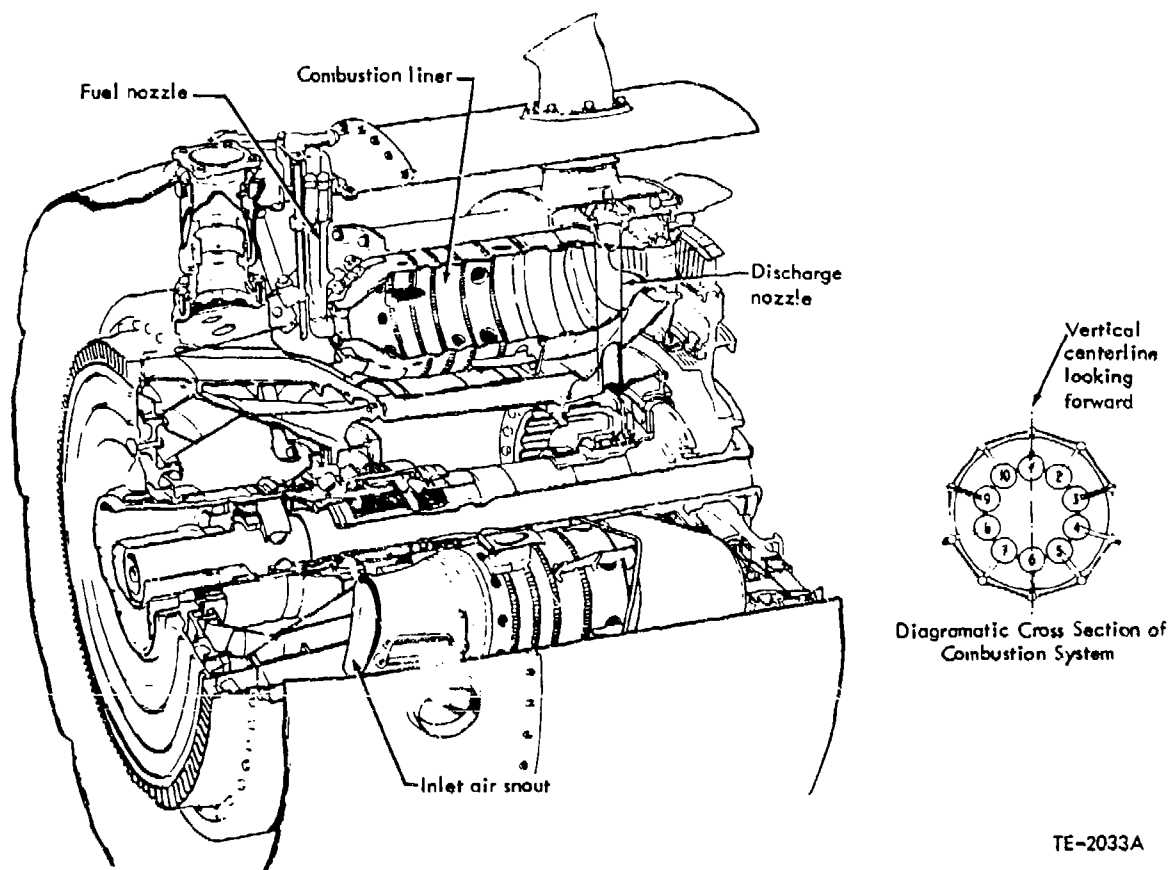
TABLE 1
TF41 SLTO OPERATING CONDITIONS

Combustor inlet pressure, kPa	2198.7
Combustor inlet temperature, K	765
Combustor airflow, kg/s	63.0
Fuel air ratio, g/kg	21.6
Combustor outlet temperature, K	1502

The TF41 combustion system shown in Figure 2 is a compact cannular design incorporating ten combustion liners in an air chamber formed between the outer combustor case and the turbine cooling air heat shield. Each combustor assembly is composed of the following four separate units:

- o Inlet air snout--distributes compressor discharge air to swirler and dome flares
- o Combustion liner--stabilizes combustion and establishes fuel and air distribution (this is often referred to as the barrel)
- o Fuel nozzle--provides fuel distribution for good ignition and low-smoke generation
- o Discharge nozzle--provides transition for passage of combustion air to turbine vane row

Inlet air snouts are employed to direct airflow into and around the combustor domes. The combustion liners are mounted and fixed on the snouts and allowed to expand on a slip joint at the turbine. The combustors are interconnected for cross firing by short crossover tubes. These have a fixed flange on one end and a sliding flange on the other to accommodate thermal growth. Ignition is accomplished with spark igniters located in two combustors.



TE-2033A

Figure 2. - TF41 Combustion System.

The combustion liner shown in Figure 3 is a welded assembly of formed sheet metal and machined forging details.

The dome consists of three concentric flare sections forming a hemisphere. At each flare junction, cooling air is injected through a splash cooling strip to protect the flare immediately downstream. The most forward flare is protected by swirler airflow.

Liner wall cooling is accomplished by film cooling air through five wigggle-strip corrugations, which connect the conical wall sections comprising the liner body. The discharge nozzle walls (not shown in Figure 3) are cooled by three rows of baffled cooling holes.

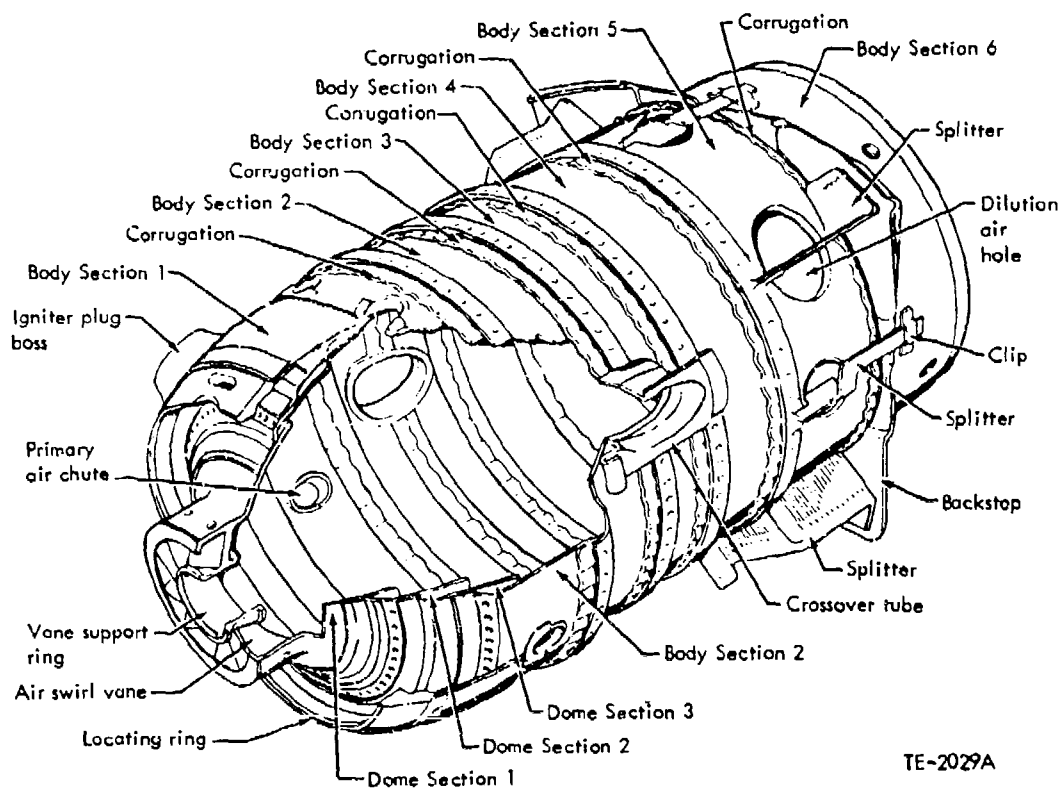


Figure 3. - TF41 Combustion Liner Details.

Primary holes are chuted to improve primary zone mixing and flow distribution. A backstop and splitters are fitted to the dilution zone holes to ensure consistent, uniform airflow into the liner.

The TF41 fuel nozzles are inserted through the inlet snout and into the combustor dome. The production fuel nozzle is a pressure-atomizing dual-orifice design (main and pilot) and incorporates a "four bar" pilot spray tip configuration. The function of the "four bar" pilot spray tip is to provide double spray cone angles with the wider angle providing fuel for ignition at the igniter plug and the narrower angle providing fuel in the primary combustion zone recirculating flow path. Fuel is injected through primary and main pressure atomizers having tangential swirl slots and concentric swirl chambers.

Spray tip design flow numbers (FN)* are 0.36 for the pilot and 8.10 for the main. The dual orifice fuel system provides precise fuel metering to meet variable engine operating conditions and good fuel distribution for cold starting and altitude relight.

Fuel injector and fuel system details for the TF41 engine are shown in Figure 4. Fuel injector flow performance limits are listed in Table 2.

TABLE 2
FUEL NOZZLE FLOW PERFORMANCE LIMITS

Combined flow rate (3.5 MPa), kg/hr	484-499
Pilot spray angle	
inner cone, deg	55-65
outer cone, deg	75-85
Main spray angle, deg	96-103

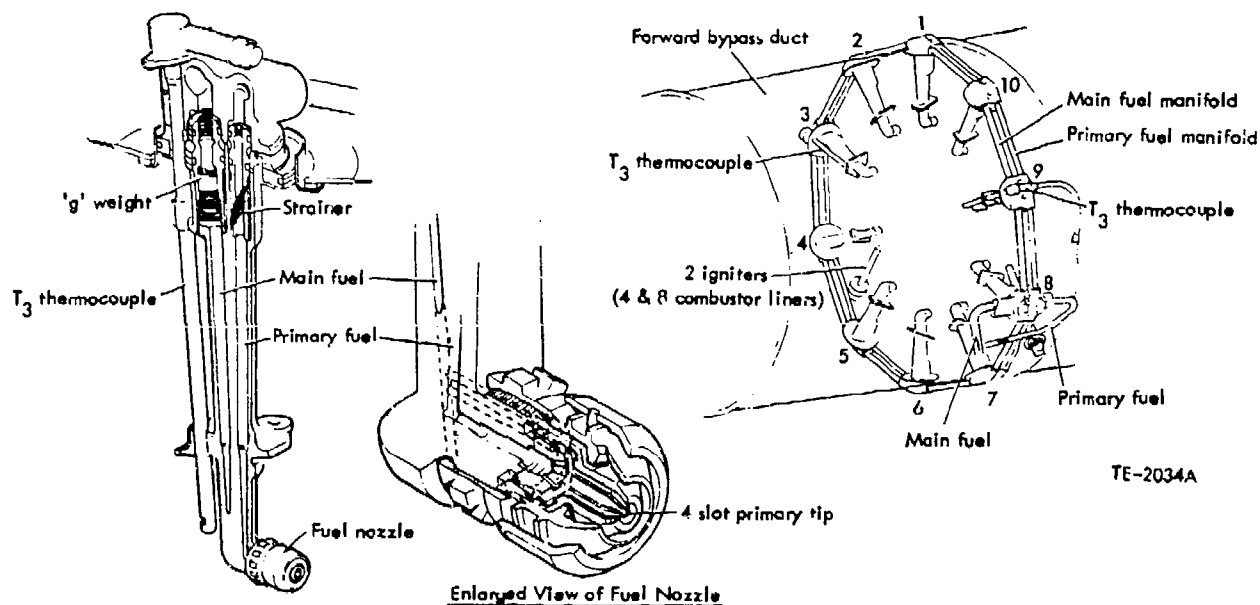


Figure 4. - TF41 Fuel Injection System.

*Flow number is defined as $(\text{fuel flow rate})/(\text{fuel nozzle differential pressure})^{1/2}$

The fuel injector pilot and main operating pressures are controlled independently in the TF41 engine. Pilot system pressure levels are maintained at a relatively high value (approx 2.1 MPa at starting and idle to approx 5.5 MPa at SLTO power) to provide good fuel atomization.

Ignition is accomplished by high energy (12 J), surface discharge ignitor plugs located in two combustion liners operating at a spark rate of one spark per second at cranking speed. The flame is propagated through the crossover tubes to achieve light-around.

The TF41 combustor sea level takeoff airflow distribution, based on analysis and flow tests, is shown in Table 3 and Figure 5.

TABLE 3
AIRFLOW DISTRIBUTION FOR TF41 COMBUSTOR

	<u>Percent of total combustor airflow</u>
Swirler	10.7
Primary holes	15.2
Dome flare (3 rings)	9.5
Wigglestrips (5)	22.6
Discharge nozzle (3 rows)	7.0
Leakages	1.1
Dilution holes	33.9

Primary combustion air effectively includes flow through primary holes, swirler, and a major part of the dome flare. The interaction of the swirler air with the fuel spray results in significant quantities of the fuel flow reaching the dome surface, thus making the flare air injection a strong contributor to the combustion process. When considering this flow reaction, which has been observed experimentally, the primary zone equivalence ratio (ϕ) is 0.91 or on the lean reaction side.

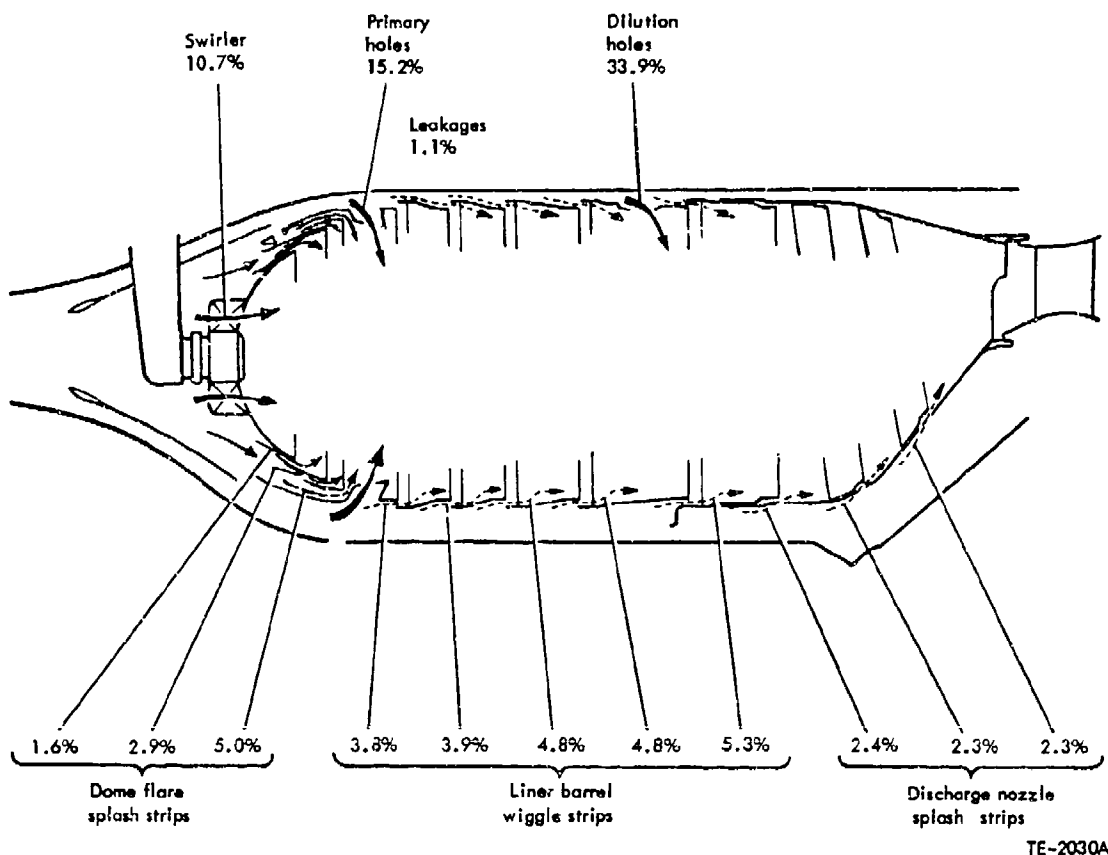


Figure 5. - Airflow Distribution for TF41 Combustor at SLT0.

B. EXPERIMENTAL SYSTEM DESCRIPTION

The effect of fuel property variation on TF41 combustion system performance was evaluated by testing the 12 experimental fuels in the TF41 single-can combustion rig. This rig, shown in Figure 6, simulates a 36-deg sector of the TF41 engine combustion system from diffuser inlet to turbine inlet. The combustor housing, inner heat shield, fuel nozzle arm and tip, inlet snout and diffuser section are actual engine hardware. An inlet bell and profile generator were used to simulate compressor discharge profile. The combustor exit plane wall geometry was fabricated to simulate the HP turbine inlet ramp.

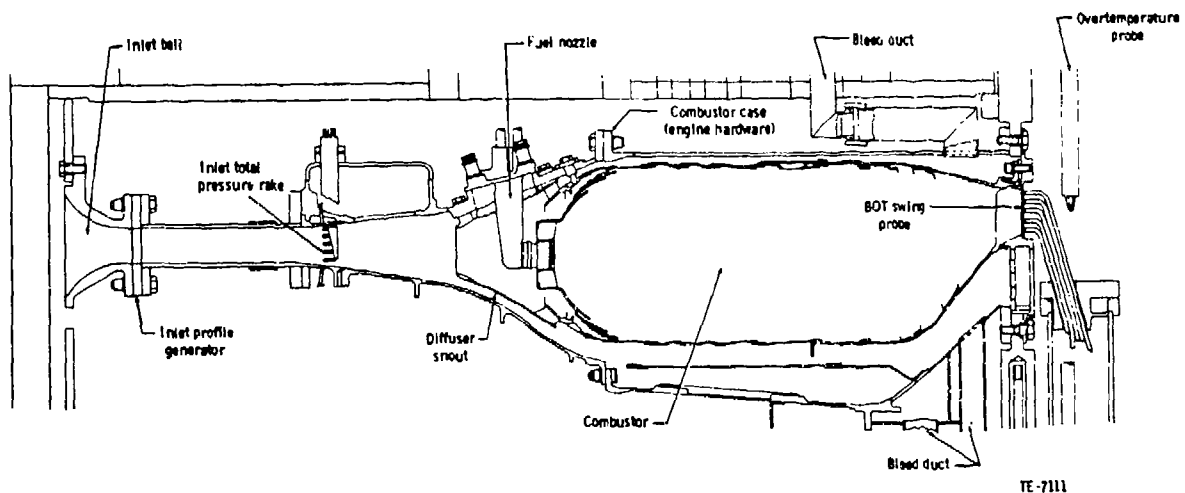


Figure 6. - Combustor Rig Cross Section.

The TF41 combustor rig has been used extensively in the TF41 CIP (component improvement program) to improve the combustor outlet temperature pattern (Reference 3). Numerous rig-to-engine performance examinations (on JP-4 fuel) have verified excellent rig-to-engine correlation on the following performance parameters:

- o Combustor inlet radial pressure profile
- o Combustor annulus circumferential pressure profile
- o Combustor system pressure drop
- o Combustor exit temperature pattern factor
- o Combustor exit radial and circumferential profiles of temperature and pressure
- o Combustor system bleed airflow rates and locations.

All combustor testing was conducted in Test Cell 823 at the DDA-Indianapolis facility.

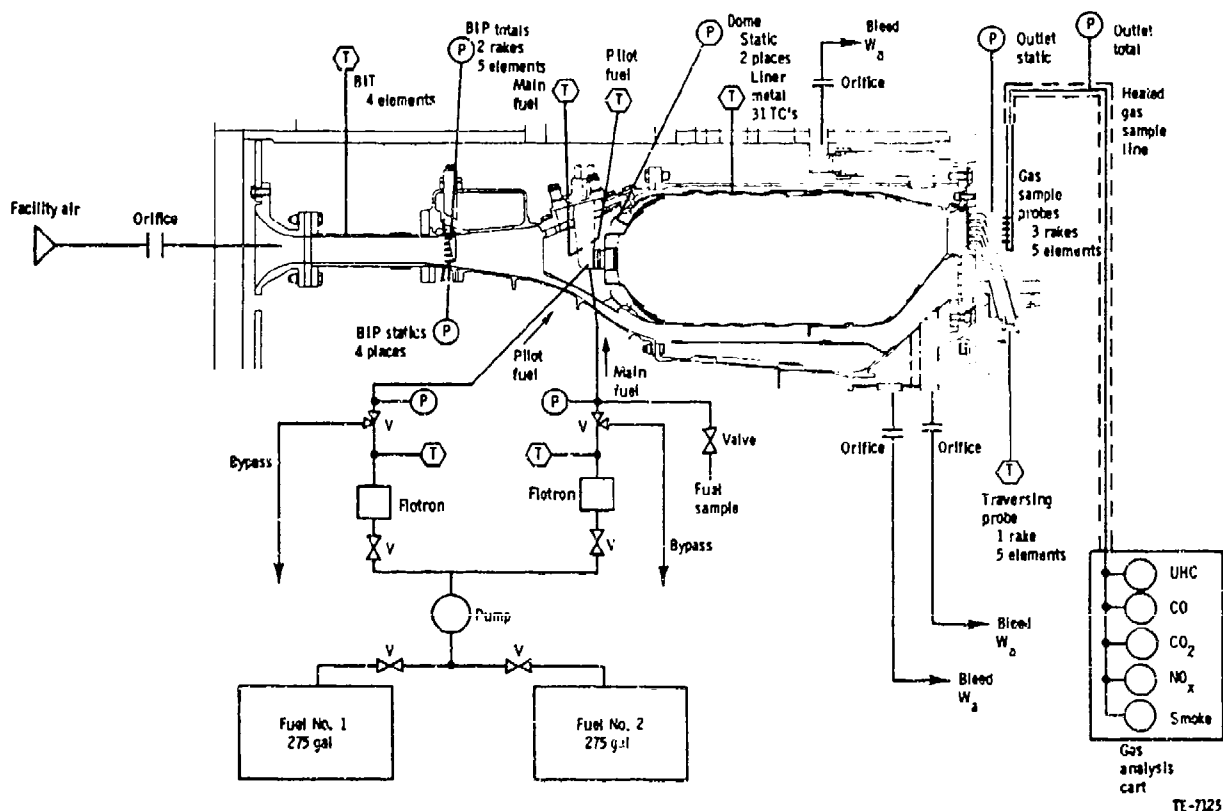
For high-pressure testing, nonvitiated air is supplied by a central air facility and heated by an oil-fired indirect heater located adjacent to the test

cell. Idle and cruise operating conditions can be exactly duplicated in the test rig facility. Dash and SLTO operating conditions of temperature, velocity and F/A ratio can be duplicated, but pressure and airflow rates must be reduced approximately 20% because of air facility limitations. Low-pressure test conditions (starting, altitude ignition) are achieved by evacuating the rig tailpipe section to obtain the required combustor inlet pressures. Test conditions are detailed in Section III-D - General Test Plan.

Airflow for all test conditions was metered with a standard ASME orifice. Fuel flow rates were measured with calibrated turbine flowmeters corrected for each fuel's density, viscosity and supply temperature. All high-pressure operation performance parameters (temperatures, pressures, flow rate) were linked to electronic data acquisition and processing equipment with direct visual feedback to the test stand operator. Ambient inlet pressure operation performance parameters were read on direct indicating instruments and recorded by the test stand operator.

Figure 7 is a schematic of the principal instrumentation that was employed to obtain the combustion system performance data. This instrumentation is further summarized in Tables 4, 5, and 6.

The exhaust gas sampling system consisted of three fixed, radial, five-element probes located just downstream of the exhaust temperature measuring plane. The probes were approximately equally spaced circumferentially in the 36-deg sector with the elements in each probe located in the same radial positions as the BOT thermocouples. The probes were water-cooled in the gas path and manifolded together to a common, electrically heated sample line. The gas analysis and smoke sampling systems are diagrammed in Figures 8 and 9. The gas sampling procedure conformed to Aerospace Recommended Practice (ARP), 1256, and exhaust smoke was determined as smoke number according to ARP 1179 procedure.



TE-7125

Figure 7. - Principal Instrumentation for TF41 Experimental Fuels Test.

The combustor instrumentation consisted of two wall static pressures in the liner primary zone plus 31 C-A thermocouples to measure combustor wall temperatures. Based upon the indicated metal temperature results from previous thermally sensitive paint tests and upon the requirements for temperature distributions and thermal gradients for the combustor life analyses, the 31 thermocouples were located as shown in Table 7 and illustrated in Figures 10, 11, and 12. On the combustor liner, two axial rows of ten thermocouples were located as shown to record the axial temperature distribution along the length of the liner. The circumferential temperature distribution for the TF41 combustor liner is quite uniform, thus the axial distribution provides the most meaningful data for the life analyses. By providing two identical rows of

TABLE 4
RIG PRESSURE AND TEMPERATURE INSTRUMENTATION

<u>Measurement</u>	<u>No. of rakes</u>	<u>Individual or elements/rake</u>	<u>Instrument</u>	<u>Accuracy</u>
Pressures				
Diffuser inlet total (BIP)	2	5	Transducer	<u>+0.25%</u>
Diffuser inlet static	-	4	Transducer	<u>+0.25%</u>
Combustor dome static (hot side)	-	2	Transducer	<u>+0.25%</u>
Main fuel manifold	-	1	Transducer	<u>+0.25%</u>
Pilot fuel manifold	-	1	Transducer	<u>+0.25%</u>
Temperatures				
Diffuser inlet (BIT)	-	4	I-C T/C	<u>+1.0%</u>
Combustor metal	-	31	C-A T/C	<u>+1.0%</u>
Combustor outlet (BOT)	1 (traversing)	5	PPR T/C	<u>+1.0%</u>
Main fuel inlet	-	1	C-A T/C	<u>+1.0%</u>
Pilot fuel inlet	-	1	C-A T/C	<u>+1.0%</u>
Main fuel nozzle fuel	-	1	C-A T/C	<u>+1.0%</u>
Pilot fuel nozzle fuel	-	1	C-A T/C	<u>+1.0%</u>

TABLE 5
RIG FLOW AND EXHAUST GAS INSTRUMENTATION

<u>Measurement</u>	<u>Instrument</u>	<u>Accuracy</u>
Flow		
Rig inlet air	Std thin plate orifice	<u>+1.0%</u>
Combustor bleed air	Std thin plate orifice (3)	<u>+1.0%</u>
Pilot fuel	Flotron	<u>+1.0%</u>
Main fuel	Turbine flowmeter	<u>+1.0%</u>
Exhaust Gas		
Carbon monoxide (CO)	Beckman Model 865-NDIR	} See Table 6
Unburned hydrocarbons (UHC)	Beckman Model 402-heated FID	
Total nitrogen oxides (NO _x)	TECO Model 10A-CV	
Carbon dioxide (CO ₂)	Beckman Model 864-NDIR	
Smoke	ARP 1179 procedure	

TABLE 6
ON-LINE EXHAUST GAS MEASUREMENT INSTRUMENTS

Unburned Hydrocarbons: Heated FID--Beckman Model 402

<u>Ranges, ppm</u>	<u>Accuracies, %</u>
0 to 10	+ 1 (full scale)
0 to 50	+ 1 (full scale)
0 to 100	+ 1 (full scale)
0 to 500	+ 1 (full scale)
0 to 1000	+ 1 (full scale)

Carbon dioxide: NDIR--Beckman Model 864

0 to 2	+ 1 (full scale)
0 to 5	+ 1 (full scale)
0 to 15	+ 1 (full scale)

Carbon monoxide: NDIR--Beckman Model 865

0 to 100	+ 2 (full scale)
0 to 500	+ 1 (full scale)
0 to 2500	+ 1 (full scale)

Oxides of nitrogen: CL-TECO Model 10A

0 to 2.5	+ 1 (full scale)
0 to 10	+ 1 (full scale)
0 to 25	+ 1 (full scale)
0 to 100	+ 1 (full scale)
0 to 500	+ 1 (full scale)
0 to 1000	+ 1 (full scale)

Range, SN

Accuracy, SN

Smoke: ARP 1179 Procedure

0 - 85

+ 3

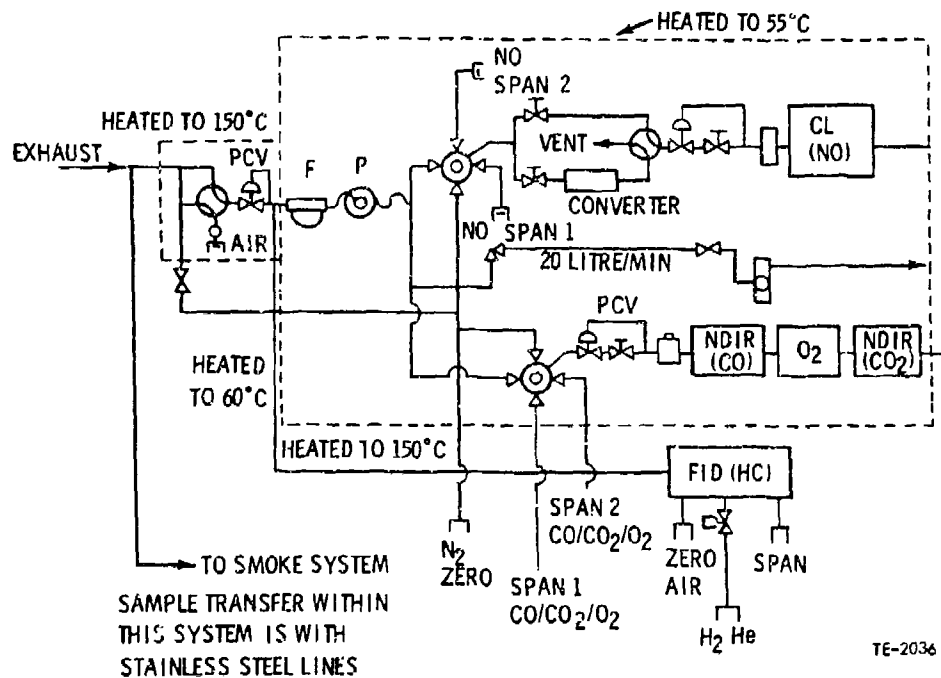


Figure 8. - Emission System Arrangement (EPA Aircraft System).

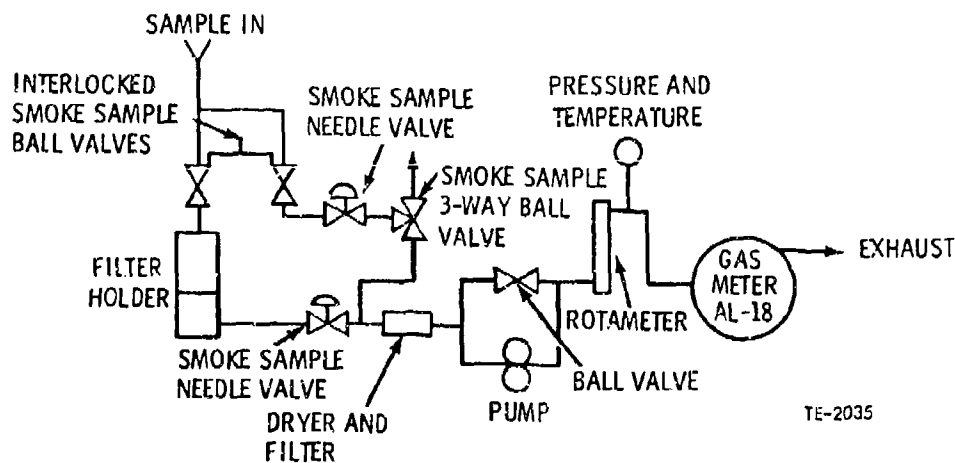
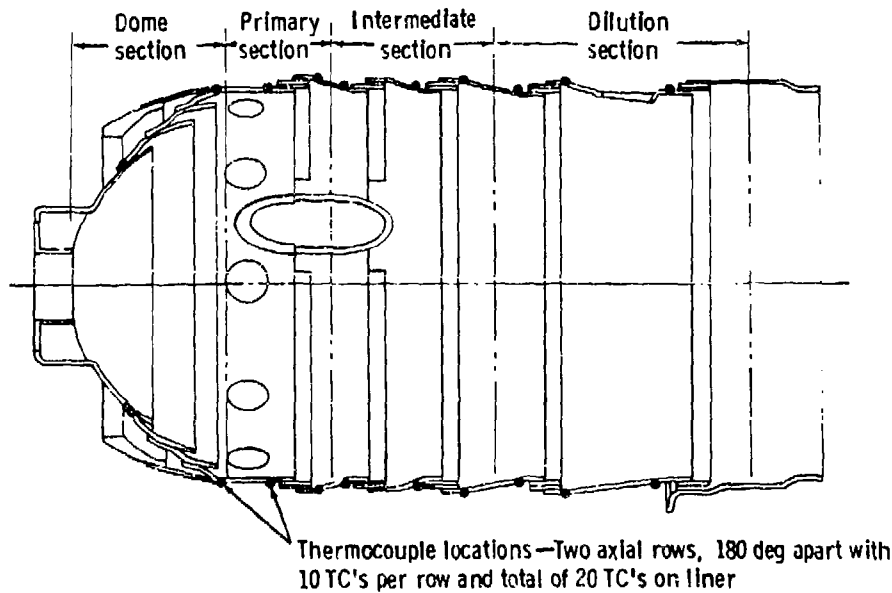


Figure 9. - Smoke Sampling System.

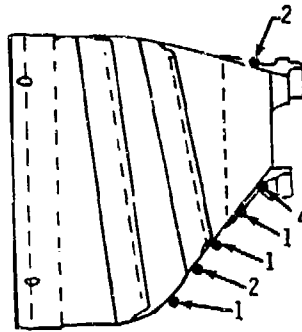
TABLE 7
COMBUSTOR METAL TEMPERATURE THERMOCOUPLE LOCATIONS

<u>Location</u>	<u>Total No. of TC's</u>	<u>No. of spare TC's</u>
Combustor liner		
Dome	4	2
Primary zone	4	2
Intermediate zone	6	3
Dilution zone	<u>6</u>	<u>3</u>
Liner total	20	10
Transition	<u>11</u>	<u>4</u>
Combustor total	31	14



TE-7127

Figure 10. - TF41 Combustor Liner Thermocouple Locations.



Total of 11 TC's on transition

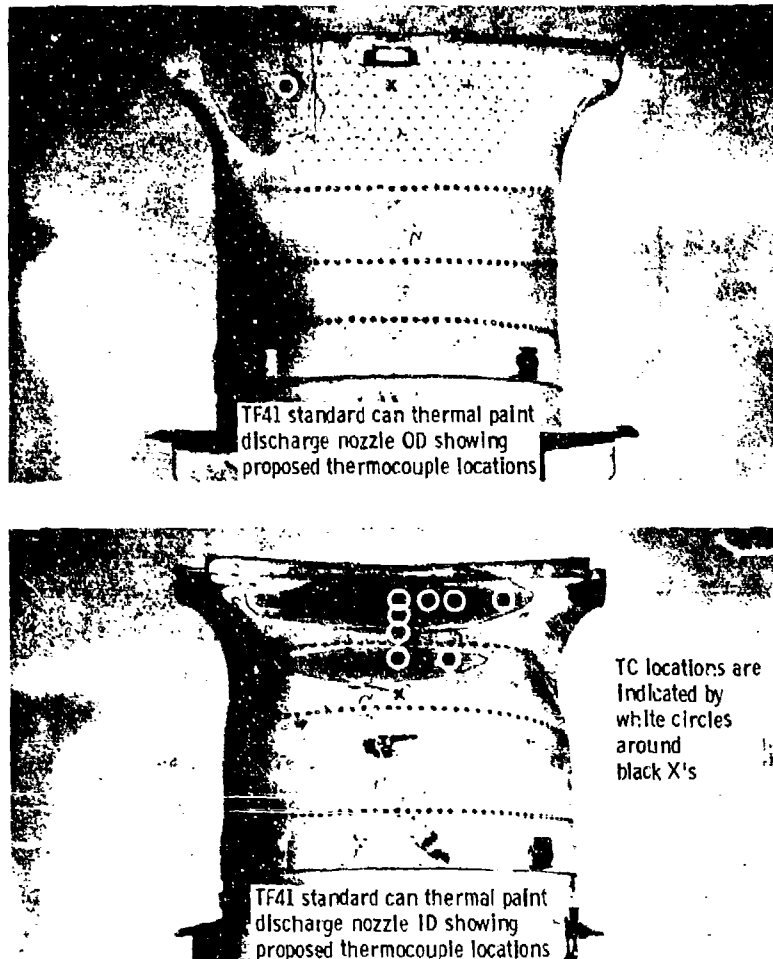
TE-7128

Figure 11. - TF41 Combustor Transition Thermocouple Axial Locations.

thermocouples, there is a one-for-one redundancy between the two rows. Each section of the liner (dome, primary, intermediate, and dilution) has either four or six thermocouples, providing ample documentation of the temperatures.

Since the combustor transition experiences the highest metal temperatures, 11 thermocouples were used in this section of the combustor to measure hot spot temperatures and the high thermal gradients. With this many thermocouples, four thermocouples were considered spares even though there were no truly redundant thermocouples.

The fuel nozzle instrumentation consisted of three thermocouples imbedded in the nozzle body as shown in Figure 13. These thermocouples were located not closer than 0.020 in. of the fuel passage walls and measured the metal temperature near the liquid-metal interface. These measured temperatures helped establish the fuel fouling characteristics of the test fuels.



TE-7126

Figure 12. - TF41 Combustor Transition Thermocouple Locations.

C. EXPERIMENTAL FUELS DESCRIPTION

1. General Description

Twelve test fuels were defined for combustion system evaluation in this program. The fuels included a baseline JP-4, JP-8*, five blends of JP-4, and five blends of JP-8.

*Waived specification on freeze point.

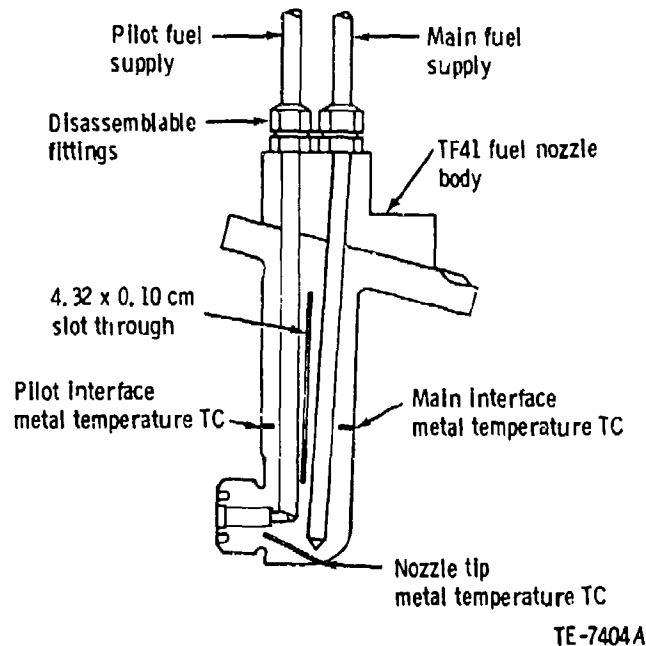


Figure 13. - TF41 Combustor Rig Fuel Nozzle Body and Instrumentation.

All fuel quantities were furnished by AFAPL and blended at DDA-Indianapolis. The baseline JP-4 fuel came from a special fuel batch that was used in similar AFAPL fuel character effects programs (listed in References 1 and 2). Two different types of aromatic components were systematically blended into the base fuels to reduce hydrogen content and to vary aromatic content: a single ring aromatic (xylene bottoms) and a multi-ring aromatic described as "2040 solvent" (a naphthalene concentrate). The final boiling point of two fuel blends was increased by the addition of mineral seal oil (a paraffinic white oil similar to cooking oil). This high boiling-point material increased distillation end point by approximately 25 to 70°C.

The fuel blends tested and their principal fuel properties (intended hydrogen content, aromatic content, and distillation end point) are summarized in Table 8.

Fuel blending and sampling procedures utilized by DDA during this contract are described in Section III-D.

TABLE 8
FUELS AND FUEL BLENDS TESTED

Fuel No.	Proportions for 750 gal of blend		Intended hydrogen content, wt %	Aromatic content, vol %	End point, °K
	Fuel	Volume, gal			
1	JP-4 special	750	14.5	10.3	541
2	JP-4 special 2040 solvent	486 264	12.0	41.9	587
3	JP-4 special 2040 solvent	598 152	13.0	29.4	567
4	JP-4 special Xylene bottoms	358 392	12.0	56.6	559
5	JP-4 special Xylene bottoms	522 228	13.0	36.8	557
6	JP-4 special Xylene bottoms Gulf mineral seal oil	595 65 90	14.0	18.2	612
7	JP-8	750	14.0	13.6	576
8	JP-8 2040 solvent	513 237	12.0	41.1	569
9	JP-8 2040 solvent	635 115	13.0	27.1	569
10	JP-8 Xylene bottoms	386 362	12.0	53.4	579
11	JP-8 Xylene bottoms	572 178	13.0	33.7	568
12	JP-8 Gulf mineral seal oil	660 90	14.0	13.7	604
Test method			D3701-K&M	ASTM D2789-71	ASTM D2887

2. Physical and Chemical Description

Detailed fuel property analyses for the 12 test fuels were determined by Monsanto Research Corporation under contract to the USAF. Post-test analysis of test fuel characteristics by Monsanto Research Corporation indicates that, despite rigorous precautions taken by DDA, fuel-to-fuel contamination of fuels used in low-pressure testing (starting, relight, and LEO) did occur. The contaminants have been identified as previously tested fuel blends, not foreign material. Therefore, two sets of fuel property data are presented where available and are designated as follows:

- o High-pressure fuel sample--includes all steady-state performance, emission, and durability testing (Fuel samples drawn throughout this test sequence show no appreciable change in properties from samples drawn at the time of blending.)
- o Low-pressure fuel sample--includes sea level starting (cold and ambient), altitude relight, and idle LBO testing

Major fuel property analysis results are presented in Tables 9, 10, 11, and 12.

TABLE 9
PRINCIPAL FUEL PROPERTIES--HIGH-PRESSURES TESTS

<u>Fuel No.</u>	<u>Description</u>	<u>Hydrogen, wt %</u>	<u>IBP, K</u>	<u>50% BP, K</u>	<u>EP, K</u>	<u>Smoke point, mm</u>	<u>Lower heating value, MJ/kg</u>
1	JP-4	14.4	294	416	541	38.0	43.54
2	JP-4 + 2040	12.0	308	482	587	12.0	42.13
3	JP-4 + 2040	12.9	296	451	567	14.0	42.70
4	JP-4 + Xyl	11.9	298	436	559	11.0	42.21
5	JP-4 + Xyl	13.6	308	448	557	14.0	42.73
6	JP-4 + Xyl + GM	13.9	292	441	612	23.0	43.31
7	JP-8	13.9	402	504	576	24.0	43.06
8	JP-8 + 2040	11.9	381	496	569	12.0	41.97
9	JP-8 + 2040	12.9	374	492	569	16.0	42.59
10	JP-8 + Xyl	12.0	393	462	579	12.0	42.15
11	JP-8 + Xyl	12.9	401	483	568	18.0	42.59
12	JP-8 + GM	13.9	402	500	604	25.0	43.16

In the blending process to vary fuel properties, no single property can be altered without affecting others. Fuel property characteristics are inter-related. Past examinations that have demonstrated these relationships between fuel properties may help explain how fuel property variations alter combustor performance behavior. In this program linear single regression techniques were employed to determine the interdependency of fuel properties, and the results later compared to combustor performance (see Sections IV-B and -C).

TABLE 10
PRINCIPAL FUEL PROPERTIES--LOW-PRESSURE TESTS

Fuel No.	Description	Hydrogen, wt %	IBP, K	50% BP, K	EP, K	Aromatics, vol %
1	JP-4	14.4	298	438	563	9.4
2	JP-4 + 2040	12.3	310	486	590	34.7
3	JP-4 + 2040	12.6	302	457	576	32.6
4*	JP-4 + Xyl	---	---	---	---	---
5	JP-4 + Xyl	13.1	306	466	590	26.9
6	JP-4 + Xyl + GM	14.0	282	427	592	15.1
7	JP-b	13.9	348	499	575	11.7
8	JP-8 + 2040	12.1	358	492	571	34.2
9	JP-8 + 2040	13.0	342	497	590	23.3
10	JP-8 + Xyl	12.3	304	452	560	42.0
11	JP-8 + Xyl	12.7	323	471	564	31.6
12	JP-8 + GM	13.2	330	484	610	24.3

*Fuel 4 sample destroyed in transit.

A coefficient of determination (R^2 --an indicator of linear curvefit, 1.0 equals a perfect fit) value ≥ 0.75 was arbitrarily chosen to suggest a "strong" dependency/relationship of one fuel property to another. An R^2 value ≥ 0.50 was chosen to suggest a "reasonable" correlation between fuel properties. Table 13 lists the fuel property correlations deemed as "strong" or "reasonable" and illustrates the expected relationships, i.e., hydrogen content and aromatic content, hydrogen content and smoke point, surface tension and vapor pressure, etc. All regression analysis was done with the high-pressure fuel sample properties.

Tables 14 and 15 show the hydrocarbon composition (by mass spectroscopy) of the test fuels.

Tables 16 and 17 list the gas chromatographic simulated distillation (ASTM D2887) data for the test fuels, high-pressure and low-pressure samples, respectively.

TABLE 11
FUEL PROPERTIES FROM HIGH-PRESSURE SAMPLE

Fuel No.	1	2	3	4	5	6	7	8	9	10	11	12
Base fuel	JP-4	JP-4	JP-4	JP-4	JP-4	JP-4	JP-8	JP-8	JP-8	JP-9	JP-8	JP-8
Additive fuel	AR	AR	AR	X	X	X+CM	AR	AR	AR	X	X	CM
Atomic content, vol %												
Total (D1319)*	11.4	42.2	31.0	59.1	40.1	21.0	19.0	48.2	33.1	58.5	40.6	17.6
Total (Monsanto)*	10.3	41.9	29.4	56.6	36.8	18.2	13.6	41.1	27.1	53.4	33.7	13.7
1-ting (Monsanto)*	9.7	17.1	14.3	56.2	36.3	17.6	11.6	17.4	14.6	32.4	32.1	11.7
2-ting (Monsanto)*	0.5	24.8	15.1	0.4	0.5	0.6	2.0	23.7	12.5	1.0	1.6	2.0
Density, g/cm ³ (D445)*												
0°C	0.7739	0.3483	0.8183	0.8326	0.8083	0.7928	0.8252	0.8755	0.8495	0.8515	0.8389	0.8564
21°C	0.7574	0.3322	0.8017	0.8153	0.7713	0.7763	0.8099	0.8600	0.8343	0.8352	0.8230	0.8113
38°C	0.7445	0.3193	0.7887	0.8021	0.7780	0.7636	0.7977	0.8480	0.8225	0.8222	0.8106	0.7994
Kin viscosity, cs (D455)*												
-18°C	1.854	2.582	2.208	1.705	1.742	2.342	6.068	5.916	5.841	2.796	3.900	7.075
25°C**	0.941	1.158	1.062	0.888	0.914	1.133	2.068	1.956	2.001	1.229	1.516	2.305
38°C	0.812	0.966	0.906	0.764	0.785	0.957	1.670	1.576	1.610	1.047	1.289	1.841
Surface tension, dynes/cm (capillary rise)*												
0°C	24.67	26.50	25.85	27.90	26.62	26.10	27.56	29.33	28.59	30.00	29.59	29.10
21°C	22.65	24.78	23.94	25.95	24.49	24.18	25.81	27.47	26.83	27.95	27.45	27.13
38°C	21.05	23.45	22.50	24.43	22.84	22.72	24.44	25.99	25.43	26.33	25.79	25.58
Vapor pressure, mm Hg (D551-71)*												
0°C	46.5	24.0	23.0	14.5	19.7	16.5	5.0	8.5	8.0	7.0	10.5	9.5
21°C**	86.0	42.0	63.5	42.2	50.5	66.0	14.7	16.5	14.0	12.0	11.6	15.2
38°C	160.0	91.5	98.0	80.5	88.0	77.0	11.0	17.0	16.5	21.5	25.5	16.5
JFTOT breakpoint, °C												
ΔTDR	282.	284.	269.	272.	272.	277.	319.	249.	290.	267.	313.	310.
Visual code	280.	289.	257.	286.	272.	277.	330.	301.	308.	312.	319.	320.
ΔP	275.	260.	285.	260.	260.	270.	320.	250.	320.	260.	330.	320.
Overall	275.	260.	267.	260.	260.	270.	319.	250.	290.	260.	313.	310.

*Test method in ().
**Values represent an average of three fuel samples taken during high-pressure testing.

TABLE 12
FUEL PROPERTIES FROM LOW-PRESSURE SAMPLES

Fuel No.	1	2	3	4**	5	6	7	8	9	10	11	12
Base fuel	JP-4	JP-4	JP-4	JP-4	JP-4	JP-4	JP-8	JP-8	JP-8	JP-8	JP-8	JP-8
Additive fuel	AR	AR	AR	X	X	X+CH	AR	AR	AR	X	X	GM
Aromatic content, vol %												
Total (D1319)*	12.1	42.4	38.6	---	33.8	20.3	17.4	45.1	31.5	49.8	39.9	31.6
Total (Monsanto)*	9.4	34.7	32.6	---	26.9	15.1	11.7	34.2	23.3	42.0	31.6	24.3
1-ring (Monsanto)*	9.0	19.7	23.8	---	22.5	14.6	10.3	15.9	13.6	37.6	26.5	22.6
2-ring (Monsanto)*	0.4	15.0	8.8	---	4.4	0.5	1.4	18.3	9.7	4.4	5.1	1.7
Density, g/cm ³ (D445)*												
0°C	0.7769	0.8449	0.8296	---	0.8230	0.7952	0.8214	0.8709	0.8443	0.8424	0.8395	0.8286
21°C	0.7603	0.8285	0.8130	---	0.8068	0.7795	0.8066	0.8552	0.8288	0.8261	0.8239	0.8128
38°C	0.7474	0.8154	0.8001	---	0.7941	0.7669	0.7946	0.8430	0.8166	0.8132	0.8112	0.8004
Kin viscosity, cs (D455)*												
-18°C	1.934	2.825	2.430	---	2.753	2.480	5.441	5.711	5.223	2.662	3.504	3.918
25°C	0.979	1.243	1.128	---	1.240	1.161	1.942	1.938	1.864	1.209	1.450	1.580
38°C	0.840	1.044	0.956	---	1.043	0.9854	1.571	1.560	1.510	1.018	1.203	1.303
Surface tension, dynes/cm (capillary rise)*												
0°C	25.81	28.09	27.38	---	27.98	26.61	25.91	30.47	29.50	28.70	29.09	28.78
21°C	23.67	26.28	25.93	---	25.52	24.67	26.89	28.53	27.33	26.50	27.00	26.75
38°C	22.01	24.86	24.08	---	24.35	23.17	25.31	27.02	25.63	25.35	25.38	25.18
Vapor pressure, mm Hg (D2551-71)*												
0°C	29.5	19.5	22.0	---	17.0	22.0	11.0	9.5	10.0	12.0	9.5	13.0
21°C	65.0	44.0	48.0	---	39.5	51.0	20.5	16.0	19.0	26.0	20.5	26.0
38°C	113.0	76.5	83.0	---	69.0	91.0	31.0	22.5	29.5	45.0	34.0	42.0

*Test method in ().

**Fuel sample lost in shipment.

TABLE 13
FUEL PROPERTY CORRELATION

<u>Fuel property</u>	<u>Curvefit correlation parameter, R^2</u>
These fuel property combinations exhibit a "strong" degree of dependence:	
Monsanto total aromatic content & D1319 aromatic content	0.982
Hydrogen content & Monsanto total aromatic content	0.902
Hydrogen content & D1319 total aromatic content	0.893
10% distillation point & kinematic viscosity	0.858
Hydrogen content & smoke point	0.818
Surface tension & vapor pressure	0.802
These fuel property combinations exhibit a "reasonable" degree of dependence:	
Monsanto total aromatic content & single ring aromatic content	0.741
10% distillation point & vapor pressure	0.730
Monsanto total aromatic & smoke point	0.720
D1319 total aromatic content & smoke point	0.676
Density & surface tension	0.662
D1319 total aromatic content & single ring aromatic content	0.656
10% distillation point & surface tension	0.653
Hydrogen content & density	0.592
Kinematic viscosity & vapor pressure	0.532
Density & smoke point	0.520
Density & vapor pressure	0.516

TABLE 14
TEST FUEL HYDROCARBON TYPE ANALYSES (MASS SPECTROSCOPY, ASTM METHOD 2789-71)---
HIGH-PRESSURE FUEL SAMPLE

<u>Compound type</u>	<u>1</u>	<u>2</u>	<u>3</u>	<u>4</u>	<u>5</u>	<u>6</u>	<u>7</u>	<u>8</u>	<u>9</u>	<u>10</u>	<u>11</u>	<u>12</u>
Liquid volume percent in fuel number												
Paraffine	62.2	37.6	45.6	30.6	44.4	55.3	42.3	29.1	35.9	22.8	33.0	43.9
Monocyclo-paraffins	24.1	20.5	25.0	10.4	15.1	25.4	41.0	28.0	34.4	20.5	30.2	39.1
Dicyclo-paraffins	3.4	---	---	2.4	3.7	1.1	3.1	1.9	2.6	2.3	3.1	3.3
Alkylbenzenes	8.4	12.6	11.0	55.6	35.3	16.2	7.5	11.3	9.4	52.4	30.3	7.6
Indane and tetralins	1.3	4.5	3.3	0.6	1.0	1.4	4.1	6.1	5.2	---	1.8	4.1
Napthalenes	0.6	24.8	15.1	0.4	0.5	0.6	2.0	23.7	12.5	1.0	1.6	2.0
Total aromatics	10.3	41.9	29.4	56.6	36.8	18.2	13.6	41.1	27.1	53.4	33.7	13.7

TABLE 15
TEST FUEL HYDROCARBON TYPE ANALYSES (MASS SPECTROSCOPY, ASTM METHOD 2789-71)---
LOW-PRESSURE FUEL SAMPLE

<u>Compound type</u>	<u>1</u>	<u>2</u>	<u>3</u>	<u>4*</u>	<u>5</u>	<u>6</u>	<u>7</u>	<u>8</u>	<u>9</u>	<u>10</u>	<u>11</u>	<u>12</u>
Liquid volume percent in fuel number												
Paraffine	63.8	40.1	42.0	---	43.5	58.1	45.1	33.4	39.8	32.9	37.8	41.5
Monocyclo-paraffins	22.0	25.2	25.4	---	29.6	21.3	41.4	30.8	33.4	24.8	30.8	33.4
Dicyclo-paraffins	4.8	---	---	---	---	5.5	1.8	1.6	1.5	0.3	0.8	0.8
Alkylbenzenes	7.7	16.6	22.1	---	21.0	12.2	7.0	10.7	9.5	37.3	24.7	20.9
Indane and tetralins	1.3	3.1	1.7	---	1.5	1.4	3.3	5.2	4.1	0.3	1.8	1.7
Napthalenes	0.4	15.0	8.8	---	4.4	0.5	1.4	18.3	9.7	4.4	5.1	1.7
Total aromatics	9.4	34.7	32.6	---	26.9	15.1	11.7	34.2	23.3	42.0	31.6	24.3

*Fuel sample lost in shipment.

Table 18 presents the conventional fuel data, generated by the Air Force Logistics Command Fuels Laboratory at WPAFB. These data may aid in assessing the variability and accuracy of test methods and for comparison to these fuels used in other investigations.

Some fuel property data shown in Table 18 duplicates data generated by Monsanto Corp. and was presented earlier in this subsection. Whenever fuel property tests were duplicated (for example aromatic content and distillation data), the Monsanto results were chosen to define the fuel properties.

TABLE 16
TEST FUEL GAS CHROMATOGRAPHIC SIMULATED DISTILLATION (ASTM METHOD D2887)--
HIGH-PRESSURE FUEL SAMPLE

Temperature (K) at percent recovered	Fuel number											
	<u>1</u>	<u>2</u>	<u>3</u>	<u>4</u>	<u>5</u>	<u>6</u>	<u>7</u>	<u>8</u>	<u>9</u>	<u>10</u>	<u>11</u>	<u>12</u>
0.5 (IBP)	294	308	296	298	308	299	402	381	374	393	401	402
1.0	295	317	300	308	318	308	425	401	397	412	411	416
5.0	334	359	339	355	358	343	451	437	436	420	425	442
10.0	353	377	362	364	375	364	464	452	450	428	433	456
20.0	368	403	384	397	402	390	479	465	464	438	439	470
30.0	384	426	399	416	419	401	488	476	475	440	454	481
40.0	399	456	423	428	437	425	497	485	484	446	471	490
50.0	416	482	451	436	448	441	504	496	492	462	483	500
60.0	441	496	473	440	453	460	513	500	500	481	439	508
70.0	463	516	490	445	464	485	520	507	507	495	504	520
80.0	483	521	505	463	489	509	533	521	519	510	516	539
90.0	503	540	523	498	516	546	545	533	531	529	531	554
95.0	518	554	531	517	530	578	554	542	541	543	543	575
99.0	536	577	557	548	551	604	570	563	560	568	560	598
99.5 (FBP)	541	587	567	559	557	612	576	569	569	579	568	604

TABLE 17
TEST FUEL CHROMATOGRAPHIC SIMULATED DISTILLATION (ASTM METHOD D2887)--
LOW-PRESSURE FUEL SAMPLE

Temperature (K) at percent recovered	Fuel number											
	<u>1</u>	<u>2</u>	<u>3</u>	<u>4*</u>	<u>5</u>	<u>6</u>	<u>7</u>	<u>8</u>	<u>9</u>	<u>10</u>	<u>11</u>	<u>12</u>
0.5 (IBP)	298	310	302	---	306	282	348	358	342	304	323	330
1.0	300	322	312	---	326	290	368	380	363	324	337	342
5.0	338	372	359	---	364	326	423	429	414	365	380	391
10.0	360	388	375	---	382	347	451	445	443	388	407	418
20.0	378	416	401	---	415	373	471	461	466	416	425	438
30.0	397	448	429	---	436	391	481	472	478	427	433	448
40.0	414	464	442	---	445	412	492	481	490	433	456	471
50.0	438	486	457	---	466	427	499	492	497	452	471	484
60.0	458	501	479	---	483	451	508	497	506	471	482	496
70.0	478	517	495	---	498	474	516	505	513	486	495	510
80.0	496	526	511	---	510	495	528	517	527	500	506	525
90.0	515	544	529	---	529	528	541	530	540	518	520	546
95.0	529	558	541	---	545	560	551	540	552	531	534	570
99.0	549	580	565	---	578	586	569	563	578	552	554	601
99.5 (FBP)	563	590	576	---	590	592	575	571	590	560	564	610

*Fuel sample lost in transit.

TABLE 18
TEST FUEL CONVENTIONAL INSPECTION DATA--HIGH-PRESSURE FUEL SAMPLE

Method		Fuel number											
		1	2	3	4	5	6	7	8	9	10	11	12
D187	Gravity, °API	54.0	37.9	44.1	41.1	46.3	49.7	42.2	32.1	37.1	36.8	39.4	42.0
D2386	Freezing point, K	<215	226	<213	205	208	241	228	226	225	220	224	244
D381	Existent gum, mg/100 ml	0.8	2.2	2.6	1.4	2.2	1.4	1.2	2.4	1.6	0.8	0.2	1.4
D1740	Luminometer number	76	24	34	22	34	53	50	16	30	19	26	48
D1266	Total sulphur, wt %	0.02	0.01	0.01	0.00	0.00	0.02	0.09	0.05	0.02	0.05	0.05	0.08
G1319	Aromatics, vol %	11.4	43.2	31.0	59.1	40.1	21.0	19.0	48.2	33.1	58.5	40.6	17.6
D1319	Olefins, vol %	0.8	0.7	0.3	0.4	0.8	0.8	1.9	2.3	2.6	1.8	2.2	1.7
D56	Flashpoint K	---	---	---	---	---	---	334	332	333	316	323	339
D86	Distillation												
	Initial boiling point, K	333	346	341	351	347	347	460	455	460	432	440	466
	10%	374	385	380	406	389	378	475	476	475	441	451	479
	20%	387	405	396	418	404	399	480	482	480	444	457	484
	50%	425	470	454	432	432	442	493	496	495	459	479	501
	90%	498	514	515	482	493	542	520	522	520	517	518	547
	Endpoint	---	347	551	524	524	560	538	545	542	538	538	576

D. GENERAL TEST PLAN

The twelve experimental fuels exhibit significant variations in fuel hydrogen content, aromatic content, aromatic type (single ring and multiple ring), distillation characteristics, and viscosity as shown in Section III-C. Table 19 summarizes some of the key combustor performance parameters that may be affected by these fuel property changes. To fully assess the fuel property effects, a comprehensive test program was generated to encompass essentially all important operating conditions. This overall test plan sequence is shown in Figure 14. High- and low-pressure test series were accomplished in the same DDA test facility. High-pressure tests include:

- o Performance tests
- o Fouling and carboning tests

Performance tests were accomplished at idle, altitude cruise, dash, and SLTO conditions. The fouling and carboning test is a separate test, performed at SLTO conditions. The low-pressure tests include:

- o Sea level start tests (ambient and cold days)
- o Altitude ignition tests
- o Idle LBO

TABLE 19
FUEL PROPERTY EFFECTS ON COMBUSTOR PERFORMANCE

<u>Key fuel properties</u>	<u>Process affected</u>	<u>Potential combustor performance effects</u>
Hydrogen/aromatic content	Fuel breakdown process (carbon formation)	1. Radiation (liner wall temperature) 2. Carbon deposition (dome, nozzle, liner) 3. Emission levels
Volatility (vapor pressure)	Initial vapor formation	Ignition performance (SL and alt)
Surface tension	Initial vapor formation	Ignition performance
Boiling range (10% boiling point, end point)	Reaction time	Combustion efficiency Exhaust temperature pattern
Fuel stability (JFTOT breakpoint)	Fuel breakdown/gumming tendency	Fuel nozzle coking/plugging in long-term service

The high-pressure tests were done first to use most of the fuel immediately after blending. The entire quantity of an experimental fuel was blended at one time. After blending, a one-drum sample was sent to WPAFB for analysis, and another two drums were set aside for low-pressure testing later. The bulk of the experimental fuel was burned in the high-pressure tests. Upon completion of all high-pressure tests, the low-pressure tests were run from the two-drum fuel quantities previously set aside. This operating sequence minimized fuel handling, storage, and safety problems. Figure 15 presents a milestone chart of key test plan events.

To ensure that fuel character was maintained, the entire system was drained after each test (high and low pressure) and was then air purged. After the purging, the system was filled with 30 gal (113.6 L) of the next fuel, circulated, and then drained and purged again. The system was then filled and circulated.

In addition to the aforementioned one-drum fuel sample, three other fuel samples were drawn during the test sequence. The rig fuel sample point was lo-

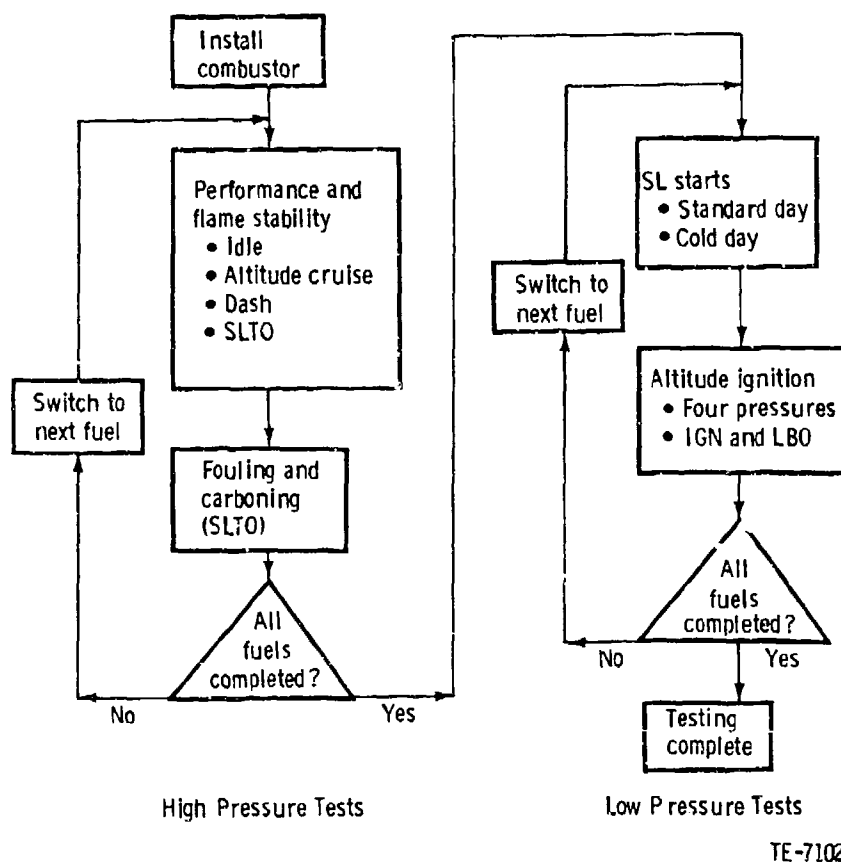


Figure 14. - Detailed Test Plan Sequence and Test Points.

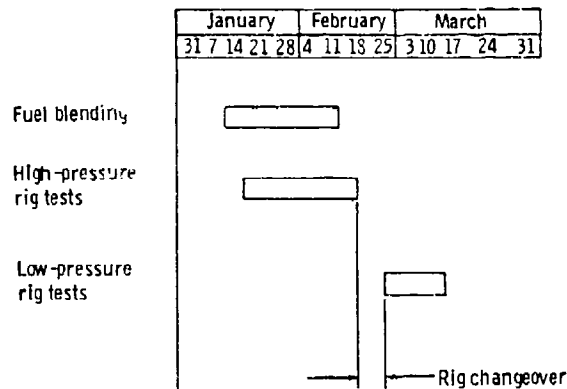
cated as close to the fuel nozzle as physically possible to ensure that the fuel to the combustor and the fuel withdrawn at the sample point were equivalent.

A 1-qt (0.9-L) sample of each fuel was withdrawn at the combustor at the start of the idle tests and at the start of the low-pressure tests. These samples were sent to AFAPL for analysis to verify integrity of the DDA fuel switching procedures. A 1-gal (3.8-L) sample of each fuel was withdrawn during the fuel fouling and carboning tests to document any changes in the fuels' thermal stability.

1. Operating Conditions

The combustor rig operating conditions for the Figure 14 test points are shown in Table 20. The condition scale is summarized in Table 21. The idle, alti-

CY 1979



TE80-300

Figure 15. - Key Test Plan Events.

tude cruise, and SL start conditions are at full engine scale. The dash and SLTO pressures and airflows are mildly scaled to approximately 85% of engine values as a result of the facility pressure limit. The altitude ignition points were run at pressures corresponding to nominal 3, 11, 12 and 15 km (0.6 flight M_N , 3 sec engine out). Ambient inlet temperature was used in these tests. This represents approximately 80% condition scaling on inlet temperature. Airflow was scaled to maintain flow factor ($W_A \sqrt{T/P}$). Since temperature is less than actual engine conditions and airflow is greater, conservative altitude ignition results were obtained.

The standard procedure for each fuel was to run a BOT survey at four sets of conditions: idle, cruise, dash, and SLTO. Airflow and inlet pressure were initially brought to near the required point, and the inlet temperature was then attained with thermal research heaters. The combustor was fired at the idle conditions, and the flame was maintained throughout all high-pressure testing. Stable emissions data determined the initiation of data acquisition. The emissions cart remained "on line" only during the time required to take manual data.

Immediately after the SLTO point, the fuel was heated to 366 K and run for 1 hr at takeoff conditions to investigate the nozzle fouling and liner carboning characteristics of the fuels. Upon shutdown, the flame was maintained until

TABLE 20
COMBUSTION RIG TEST CONDITIONS

	W_A , ** kg/sec	BIP, ** MPa	BIT, ** K	$W_A \sqrt{T/P}$	F/A *** K	BOT, K
I. Performance and flame stability						
Idle	1.06	0.293	422	74.2	13.9	964
Alt cruise (10.7 km)	1.70	0.511	577	79.9	15.2	1141
Dash (SL)*	5.49	1.950	740	76.6	18.9	1405
SLTO*	5.36	1.969	760	75.0	21.6	1504
II. Fouling and Carboning*						
o SLTO*	5.36	1.969	760	75.0	21.6	1504
III. Sea level starts and LBO						
o STD day	0.76	0.117	Amb	110.0	---	---
o Cold day	0.79	0.117	262	110.0	---	---
IV. Altitude ignition & LBO (3 sec out conditions)						
3,049 m, 0.6M _N	0.89	0.149	Amb	101.0	---	---
10,668 m, 0.6M _N	0.55	0.093	Amb	101.0	---	---
12,192 m, 0.6M _N	0.47	0.079	Amb	101.0	---	---
15,240 m, 0.6M _N	0.34	0.062	Amb	101.0	---	---

*Scaled condition, see Table 21

**Condition at diffuser inlet

***Condition at combustor inlet

TABLE 21
SUMMARY OF CONDITION SCALING

<u>Test point</u>	<u>Test scale</u>
I. Performance and Flame Stability	
Idle	100%
Alt cruise (10,668 m)	100%
Dash (SL)	87.0% on BIP, and W_A
SLTO	85.0% on BIP, and W_A
II. Fouling and carboning	
SLTO	85.0% on BIP and W_A Factor of 500 on fuel fouling rate
III. Sea level starts and LBO	
Std day	100% depending on T_{ambient}
Cold day	100%
IV. Altitude ignition and LBO (3 sec out conditions)	
3,048 m, 0.6 M_N	80% on BIT; W_A scaled to hold $W_A \sqrt{T/P}$
10,668 m, 0.6 M_N	
12,192 m, 0.6 M_N	
15,240 m, 0.6 M_N	

the outlet temperature was 533 K to minimize the thermal shock effects. After shutdown, the rig was opened up, and pictures of the liner interior were taken for carboning documentation. The fuel nozzle was then removed and flowed, and samples were weighed for fouling effects determination.

After the high-pressure testing of all fuels, the rig was set up for ignition work. Ambient temperature sea level and altitude points for each fuel were

run first with the rig set up for evacuation. The inlet air was then refrigerated to 272 K to attempt the SI cold ignition. This was followed by the high-pressure ignition and LEO for idle and cruise conditions. For all ignition testing, airflow and inlet temperature were set, and attempts to fire were made at small increases of fuel flow. Fuel flow was then decreased until the flame was extinguished. This process was repeated until the band narrowed.

2. Fuel Fouling Test Detail Plan

a. Introduction

Fuel nozzle fouling can result from fuel thermal decomposition and is generally a long-term problem. This can occur in the fuel nozzle feed arm, the nozzle tip, and the fuel injector face. The fouling tendency of the 12 experimental fuels was evaluated in a special 1-hr rig test (concurrent with the carboning test). The fuel temperature was increased and the fuel nozzle was modified to increase the potential fouling rate so that the special test would simulate long-term fouling. The selected fouling test strategy was based on an analysis of fuel fouling rate, TF41 engine duty cycle, and a fuel injector thermal analysis.

b. Fuel Fouling Rate

A number of experimental studies to determine the effect of fuel temperature on coking rates have been completed. Most of these employed standard procedures (ASTM D1660 and D3741). Data from an EXXON study (Reference 4) were used to estimate fuel fouling rates. Analysis of the data for standard JP-5 indicated a nearly linear Arrhenius plot over the range 215-350°C with a coking rate increase of 280. These results indicate an apparent activation energy of 24,000 calories per mole for fuel decomposition reactions. Based on these results, the relative fuel fouling rate as a function of temperature is shown in Figure 16.

c. TF41 Engine Duty Cycle

The TF41 duty cycle was determined from an analysis of typical shore-based mission profiles (Reference 5). These missions and mission mixes follow:

<u>Mission</u>	<u>Time, %</u>
Familiarization	8
Instrument	7
Navigation	26
Formation	10
Tactics	7
Ground attack	27
FCLP (Touch and Go)	<u>15</u>
Total	100

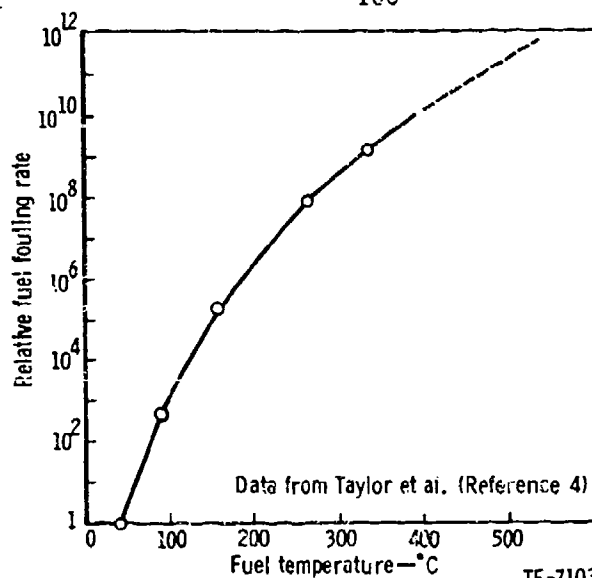


Figure 16. - Relative Fuel Fouling Rates.

The mission descriptions (time, altitude, engine rpm) allowed an approximate breakdown of each of the missions into the four engine performance modes of this program from a consideration of engine power versus engine rpm, as illustrated in Figure 17 for sea level. The results of this mode breakdown analysis are shown in Table 22. The overall duty cycle resulting from the mission mix follows:

SLTO	12%
Dash	22%
Cruise	37%
Idle	29%

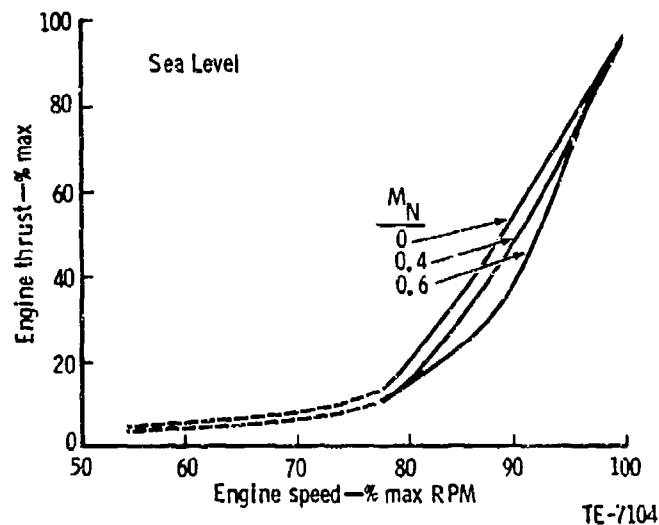


Figure 17. - TF41 Engine Power Versus Speed.

TABLE 22
ESTIMATED MISSION-MODE BREAKDOWN

<u>Mission</u>	<u>Mission time in mode, %</u>				<u>Mission mix, %</u>
	<u>SLTO</u>	<u>Dash</u>	<u>Cruise</u>	<u>Idle</u>	
Familiarization	20	6	47	27	8
Instrument	21	0	57	22	7
Navigation	1	64	13	22	26
Formation	20	0	44	36	10
Tactics	32	20	25	23	7
Ground attack	10	13	43	34	27
FCLP	13	0	5	35	<u>15</u>
					100

d. Fuel Injector Thermal Analysis

The TF41 fuel injector is shown in Figure 18. The feed arm has separate pilot and main fuel passages. The feed arm is exposed to high-temperature and -pressure air, especially in the core engine. This increases fuel interface temperature with potential fuel fouling. Feed arm fouling deposits can flow to the nozzle tip to block flow, especially in the pilot. Fuel nozzle fouling is also conceivable in the tip itself or on the fuel nozzle face as a result of the thermal breakdown.

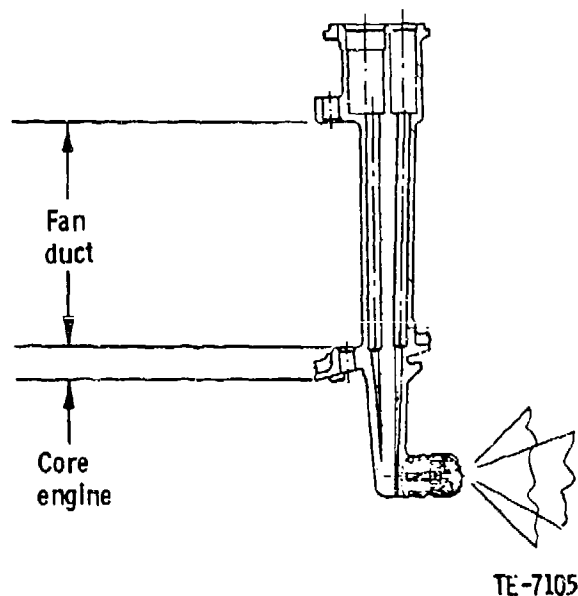


Figure 18. - TF41 Engine Fuel Injector.

The fuel nozzle feed arm temperatures were estimated at idle, cruise, dash, and SLTO by a finite-element convection/conduction heat transfer analysis considering the air heating and fuel cooling. Typical results (at SLTO) are shown in Figure 19 for ambient (27°C) fuel inlet temperature. The analysis indicates very high feed arm/fuel interface temperatures (up to 318°C). These high temperatures can cause fuel breakdown (fouling). The pilot and main peak interface temperatures, relative fuel breakdown rates (from Figure 16), and fuel fouling in each engine mode are summarized in Tables 23 and 24. The following conclusions are apparent:

1. As a result of the low pilot fuel flow, the most fuel fouling (by a factor of 6000) is expected in the pilot passage.
2. The pilot passage has a maximum fouling temperature (at SLTO) of 318°C.
3. The pilot passage has 49% of its fouling at SLTO.
4. The main passage has a peak fouling temperature (at SLTO) of 134°C.
5. The main passage has 27% of its fouling at SLTO.

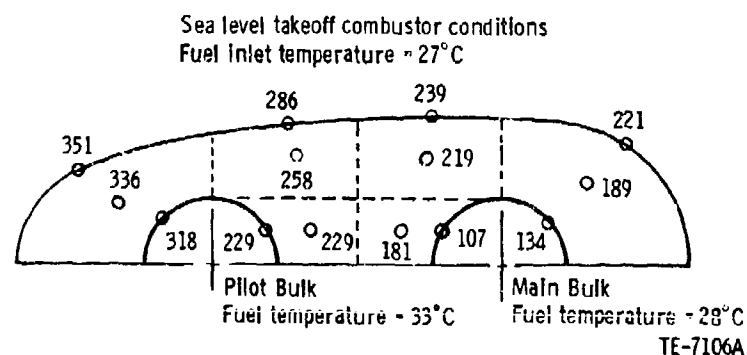


Figure 19. - Typical Calculated Fuel Injector Temperatures.

TABLE 23
FUEL FOULING RATES (ANALYTICAL)

Mode	Percent	Interface temperatures, °C		Fuel fouling rate (1 at 27°C)	
		Pilot	Main	Pilot	Main
SLTO	12	318	134	3.2×10^8	3×10^4
Dash	22	307	133	1.8×10^8	3×10^4
Cruise	37	179	118	5×10^5	1×10^4
Idle	29	88	69	1×10^3	200

TABLE 24
FUEL FOULING (ANALYTICAL)

Mode	Percent	Fuel fouling (rate x time)		Percent fuel fouling	
		Pilot	Main	Pilot	Main
SLTO	12	3.8×10^7	3.6×10^3	49	27
Dash	22	4.0×10^7	6.6×10^3	51	50
Cruise	37	0.02×10^7	2.9×10^3	--	22
Idle	29	---	0.1×10^3	--	1
Total		7.8×10^7	13.2×10^3	100	100

The fuel nozzle tip temperature was estimated as 149°C at SLTO. The temperature of this component is much less because this fuel injector part fits into a fuel injector ferrule and therefore does not experience much convective heating. With low tip temperatures, the tip will have a fouling rate 3000 times less than the feed arm pilot passage.

Fouling can also occur on the fuel nozzle face. The temperature of this item is influenced by interactions with the combustion zone that are not readily analyzed. The TF41 is not prone to this type of fouling on standard fuels, however.

With baseline conditions established, analysis was continued to define severe conditions (by fuel heating or other means) with the goal of obtaining, in the 1-hr SLTO fouling test, the fouling expected in 500 engine service hours. The analysis indicates that the pilot feed arm passage is expected to have the greatest fuel fouling. Mission analysis, as previously presented, indicates that 1 hr of SLTO operation is equivalent to 4.1 hr of mission operation. Therefore, a pilot fouling rate increase of 122 is required to duplicate 500 engine service hours. Figure 16 indicates that this requires an interface temperature increase from 318 to 477°C. However, experience with the TF41 combustion rig indicates that the fouling rate would be excessive at this temperature. For instance rig practice is to start fuel flow at SLTO hot conditions (487°C LIT). With this procedure, the pilot nozzle often plugs in-

stantly, indicating that the fouling rate at 477°C would be excessive, even with conventional fuel. In view of this consideration, an intermediate goal temperature of 393°C was used, providing a severe fouling test equivalent to approximately 75 service hours. A fouling rate increase was also imposed on the nozzle tip temperature from an estimated 149 to 204°C , providing a severe fouling test equivalent to 115 hr of mission operation for this component per previous considerations.

Heat transfer studies were done on requirements to elevate the nozzle arm pilot interface temperature from 320 to 393°C . The effect of fuel heating and pilot flow is shown in Figure 20. The pilot interface temperature does not respond sufficiently to these measures because of conduction to the main "sink." To overcome this problem, 50 and 100% depth fuel nozzle slots, to thermally isolate the pilot passage as illustrated in Figure 21, were studied. These results, shown in Figure 22, indicated that this approach could provide a reasonable solution. The nozzle was therefore completely slotted, and the pilot flow was reduced to 30% of normal flow to provide the severe

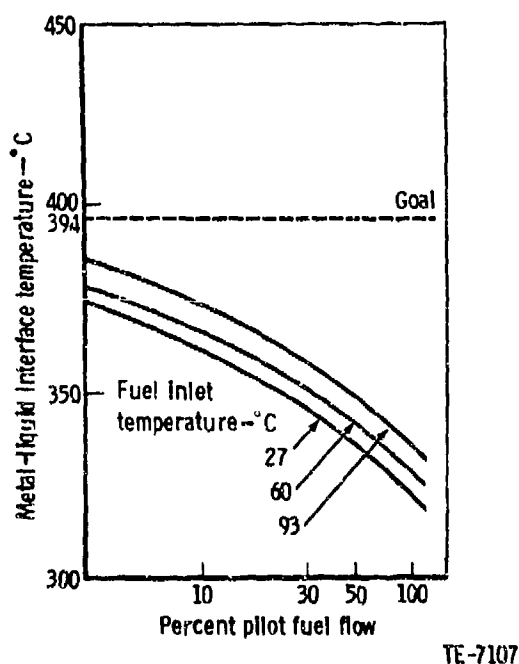
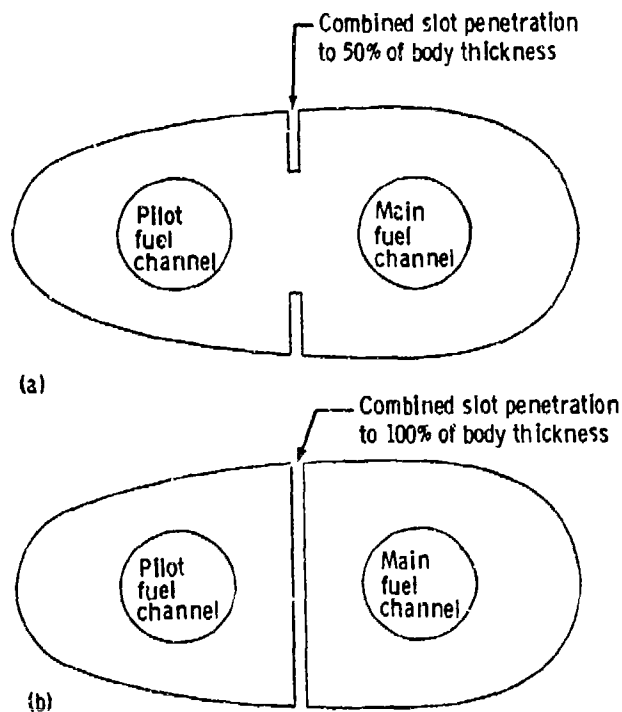


Figure 20. - Effect of Fuel Flow Rate and Fuel Inlet Temperature on Nozzle Feedarm Interface Temperature (Standard Nozzle).

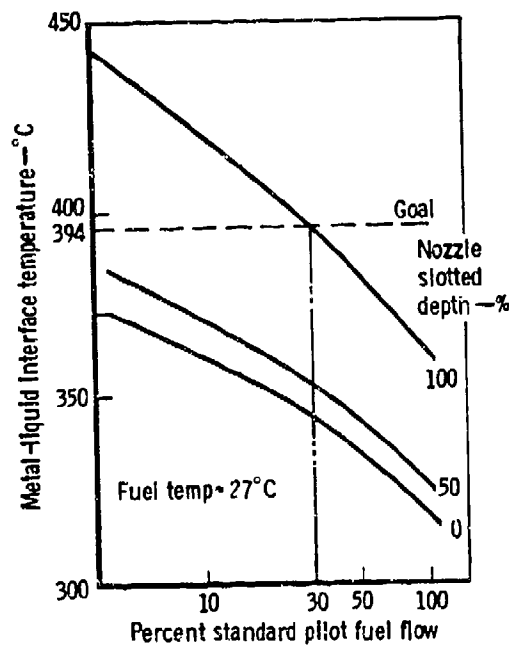


TE-7108

Figure 21. - Slotted Fuel Nozzle Configurations.

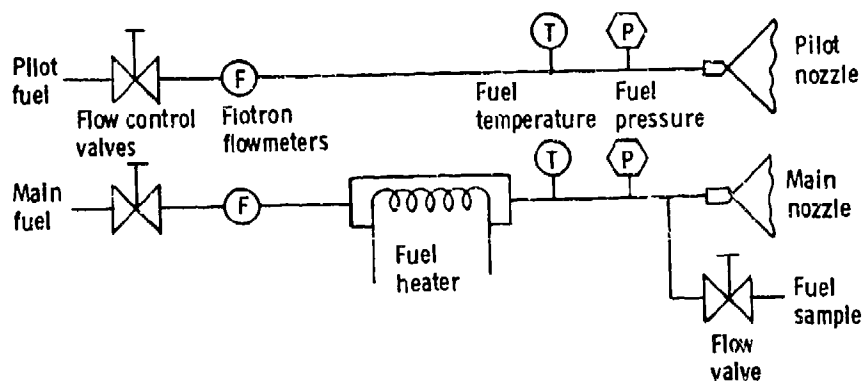
fouling conditions to simulate 75 service hours. The main fuel was heated in a steam heat exchanger to 93°C to provide a simulation of 115 hr service hours in the nozzle tip. This solution, although falling short of the original goal of 500 hr of service simulation, provides the most severe fouling conditions practical without major modification to the test rig or rig operating procedure.

The fuel system components applicable to the fouling test are shown in Figure 23. Pilot and main fuel flows were separately established and measured by individual Flo-tron mass flow meters and thermocouples.



TE-7109

Figure 22. - Effect of Fuel Flow Rate and Nozzle Slot Depth on Nozzle Feedarm Pilot Interface Temperature.



TE-7110

Figure 23. -- Fuel System Schematic for Fuel Fouling Test.

SECTION IV

RESULTS AND DISCUSSION

This section provides a summary of major results obtained from the test program. The first subsection (A) presents actual high-pressure test conditions and any correction/normalizing factors applied to the raw data prior to analysis. Detailed test results from all rig testing are tabulated in Appendix A. Results of the analyses of combustor performance with JP-4 and JP-8 at different power settings are discussed in Subsection B. Linear regression analyses of test results correlated with fuel properties are presented in Subsections C (single variable) and D (multiple variables). Projections of combustor and turbine hardware life based on this test program are discussed in Subsection E.

A. TEST CONDITION SUMMARY

Although great care was taken to reproduce test conditions for successive fuels, some variation in the setting of test parameters is unavoidable. Tables 25 through 28 present some of the important test parameters for the four high-pressure test points: idle, altitude cruise, sea-level dash, and sea-level takeoff. It can be seen that as inlet flow rate and pressure level increase (to simulate conditions from idle to SLTO) variability from set point is significantly reduced. In order to permit precise comparisons of the results, the emissions data for oxides of nitrogen (NO_x), carbon monoxide (CO), and unburned hydrocarbons (UHC), were corrected to respective full engine operating conditions for the four test points, described in Table 20. The NO_x emission indices were corrected for pressure, combustor inlet temperature, combustor exit temperature, and reference velocity. CO and UHC emission indices were corrected for pressure only. Smoke data are presented as measured at the rig operating conditions. The correlations used follow:

Oxides of Nitrogen

$$\text{NO}_x \text{ corr} = (\text{NO}_x \text{ meas}) \left(\frac{P_{T \text{ in corr}}}{P_{T \text{ in meas}}} \right)^{0.5} \left(\frac{V_{\text{ref meas}}}{V_{\text{ref corr}}} \right) \left(\frac{T_{\text{out corr}}}{T_{\text{out meas}}} \right) \exp \left(\frac{T_{\text{in corr}} - T_{\text{in meas}}}{288} \right)$$

(Reference 6)

No relative humidity measurements were taken during rig testing, therefore no humidity correction can be made. Relative humidity measurements made in simi-

lar DDA rigs at comparable test conditions indicate 14-20 grains of water vapor per kilogram of dry air.

Carbon Monoxide

$$CO \text{ corr} = (CO \text{ meas}) \left(\frac{P_{T \text{ in meas}}}{P_{T \text{ in corr}}} \right)$$

(Reference 7)

Unburned Hydrocarbons

$$UHC \text{ corr} = (UHC \text{ meas}) \left(\frac{P_{T \text{ in meas}}}{P_{T \text{ in corr}}} \right)$$

(Reference 7)

where: NO_x	= Emission level of oxides of nitrogen, Equivalent NO_2 , g/kg fuel
CO	= Emission level of carbon monoxide, g/kg fuel
UHC	= Emission level of unburned hydrocarbons, Equivalent CH_4 , g/kg fuel
$P_{T \text{ in}}$	= Combustor inlet total pressure, atm
T_{in}	= Combustor inlet total temperature, K
V_{ref}	= Reference velocity, m/s
T_{out}	= Combustor exit total temperature, K

and subscripts:

corr	= Relates to value at corrected (engine) condition
meas	= Relates to value at measured (rig) condition

TABLE 25
COMPARISON OF IDLE RIG TEST CONDITIONS TO ENGINE CONDITIONS

<u>Fuel No.</u>	<u>BIT, K*</u>	<u>BOT, K**</u>	<u>F/A req, g/kg***</u>	<u>F/A test, g/kg</u>
1	416	956	13.9	14.1
2	409	930	14.4	14.2
3	427	985	14.2	14.8
4	446	1029	14.3	15.5
5	429	959	14.2	14.2
6	437	1003	14.0	13.8
7	425	857	14.0	14.0
8	434	1025	14.4	15.0
9	438	1003	14.2	14.5
10	432	985	14.4	14.4
11	416	992	14.2	14.6
12	431	943	14.4	14.4

*TF41 idle BIT is 422 K.

**TF41 idle BOT is 964 K.

***F/A ratio required to achieve TF41 idle temperature rise of 542 K ($\eta = 100\%$).

B. PERFORMANCE ANALYSIS

The test program matrix was completed with no major problems in rig operation. Posttest fuel sample analysis indicated contamination in the ignition test fuel samples, which resulted in the need to use different fuel properties to correlate the ignition test results (refer to Section III-C). This subsection presents a comprehensive summary of general combustor performance characteristics over the specified range of simulated engine conditions (power level, altitude simulation, etc). JP-4 and JP-8 performance results are presented. DDA facility JP-4 test results are also presented wherever appli-

TABLE 26
COMPARISON OF CRUISE RIG TEST CONDITIONS TO ENGINE CONDITIONS

<u>Fuel No.</u>	<u>BIT, K*</u>	<u>BOT, K**</u>	<u>F/A req, g/kg***</u>	<u>F/A test, g/kg</u>
1	575	1063	15.2	15.2
2	585	1146	15.7	16.0
3	604	1137	15.5	15.1
4	577	1130	15.6	15.4
5	579	1107	15.5	15.3
6	582	1157	15.3	15.6
7	578	1038	15.3	15.1
8	570	1135	15.7	15.8
9	577	1128	15.6	15.5
10	583	1158	15.7	15.7
11	570	1130	15.5	15.4
12	575	1125	15.3	14.7

*TF41 cruise BIT is 577 K.

**TF41 cruise BOT is 1141 K.

***F/A ratio required to achieve TF41 cruise temperature rise of 564 K ($\eta = 100\%$).

cable. Single- and multiple-variable regression analyses in Sections IV-C and IV-D, respectively, document the effects of fuel property variation on the basic performance characteristics presented here.

1. CO and UHC Emissions

Carbon monoxide (CO) and unburned hydrocarbon (UHC) emissions are products of incomplete (i.e., inefficient) combustion and, therefore, are most prevalent during low-power operation (idle and cruise). Figure 24 shows the strong influence operating conditions have on CO formation. No effect of fuel variation (JP-4, JP-8) is evident. The same strong relationship to operating conditions can be seen for UHC in Figure 25. Combustion efficiency, calculated from gas emission data, is shown in Figure 26.

TABLE 27
COMPARISON OF DASH RIG TEST CONDITIONS TO ENGINE CONDITIONS

<u>Fuel No.</u>	<u>BIT, K*</u>	<u>BOT, K**</u>	<u>F/A req, g/kg***</u>	<u>F/A test, g/kg</u>
1	749	1344	18.9	18.6
2	744	1403	19.5	19.6
3	745	1407	19.3	19.2
4	744	1409	19.4	18.9
5	749	1396	19.3	19.0
6	744	1411	19.0	18.5
7	739	1370	19.1	18.7
8	744	1404	19.5	19.2
9	741	1377	19.3	19.1
10	746	1412	19.5	19.2
11	739	1407	19.3	19.3
12	743	1408	19.1	18.7

*TF41 dash BIT is 740 K.

**TF41 dash BOT is 1405 K.

***F/A ratio required to achieve TF41 dash temperature rise of 665 K ($\eta = 100\%$).

2. NO_x Emissions

Oxides of nitrogen (NO_x) are formed from oxidation of nitrogen, the sources being inlet airflow and fuel-bound nitrogen. "Thermal NO_x" is an equilibrium product of high-temperature combustion, and correspondingly is more evident at high-power operating conditions. Figure 27 shows the strong relationship between operating conditions and thermal NO_x formation. Again, little or no variation exists between JP-4 and JP-8 fuels.

3. Smoke Emissions

Like CO and UHC, smoke emission is a product of incomplete combustion. However, high-efficiency combustors can produce visible smoke plumes of soot particles. The TF41 engine produces a visible smoke trail at nearly all high-

TABLE 28
COMPARISON OF SLTO RIG TEST CONDITIONS TO ENGINE CONDITIONS

<u>Fuel No.</u>	<u>BIT, K*</u>	<u>BOT, K**</u>	<u>F/A req, g/kg***</u>	<u>F/A test, g/kg</u>
1	759	1492	21.6	21.2
2	756	1474	22.3	21.7
3	759	1495	22.0	21.9
4	761	1508	22.2	21.6
5	756	1475	22.0	21.5
6	760	1509	21.7	21.2
7	758	1470	21.8	21.4
8	760	1497	22.3	21.8
9	767	1477	22.1	21.9
10	762	1488	22.3	22.2
11	757	1488	22.0	21.7
12	762	1503	21.6	21.6

*TF41 SLTO BIT is 760 K.

**TF41 SLTO BOT is 1504 K.

***F/A ratio required to achieve TF41 SLTO temperature rise of 744 K ($\eta = 100\%$).

power operating points. Figure 28 shows smoke number as a function of operating level, with visible smoke in evidence over most of the engine operating range. JP-4 and JP-8 operations produce essentially the same smoke result.

4. Liner Wall Temperature

Liner and discharge nozzle wall temperatures were measured at 31 locations as described in Section III-B. Liner temperature is strongly influenced by flame radiation and therefore by operating power level. Figure 29 shows the highest liner metal temperature measured as a function of operating conditions.

Aerodynamic modeling of the TF41 combustion system suggests a substantial over-cooling of the liner barrel through the "wiggletstrip" cooling slots.

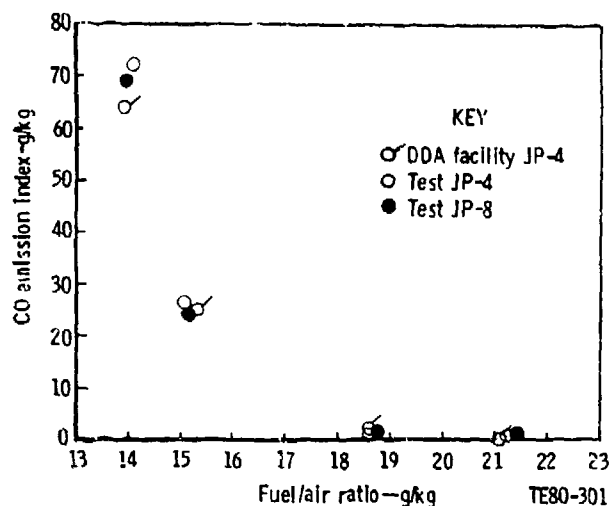


Figure 24. - Effect of Operating Conditions on CO Emission Levels.

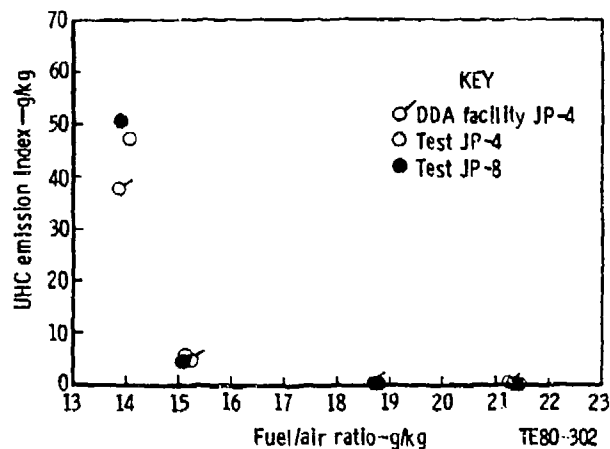


Figure 25. - Effect of Operating Conditions on UHC Emission Levels.

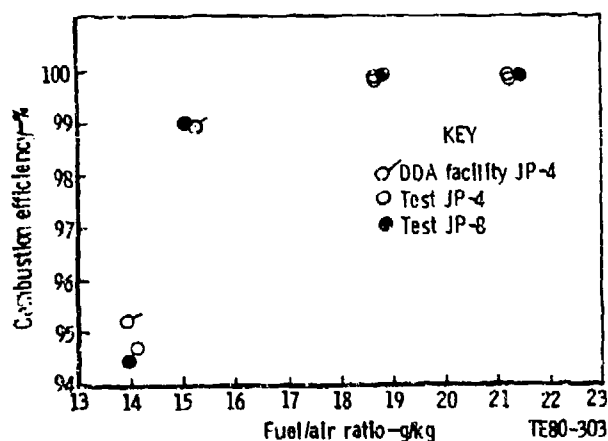


Figure 26. - Effect of Operating Conditions on Combustion Efficiency Levels.

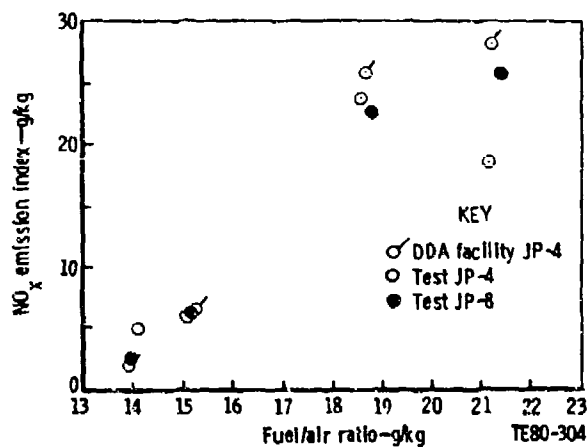


Figure 27. - Effect of Operating Conditions on NO_x Emission Levels.

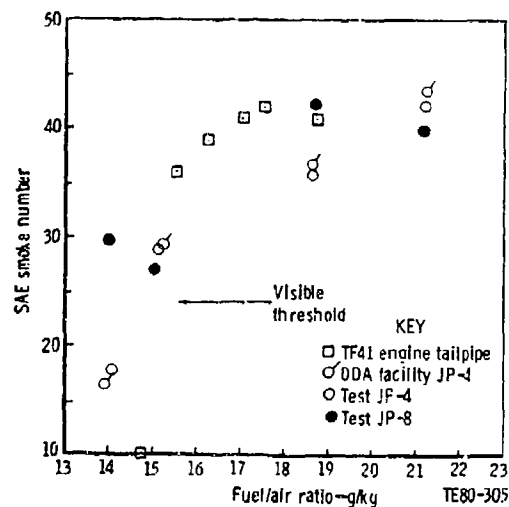


Figure 28. - Effect of Operating Conditions on Smoke Emission Levels.

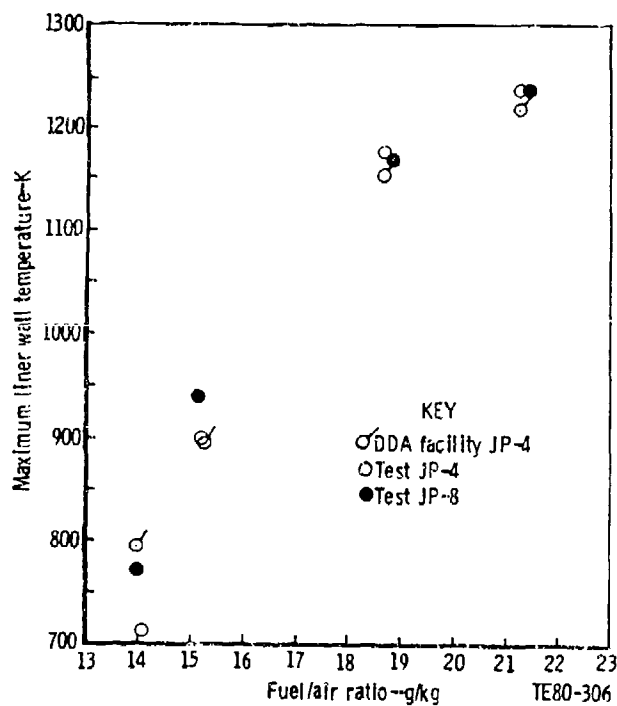


Figure 29. - Effect of Operating Conditions on Maximum Liner Wall Temperatures.

This is supported by service experience indicating nearly infinite liner life. The bolt-on discharge nozzle (transition section) however suffers heavy damage, particularly the inner wall ramp, in a relatively short service time. High combustor loading, radical geometry change, and combustor zonal burning characteristics are the suspected reasons for this condition. It is not surprising therefore that in all instances the maximum recorded wall temperature occurred on the discharge nozzle inner wall ramp.

In order to further study the effect of fuel properties on combustor durability, liner barrel wall temperatures (primary and intermediate zone thermocouples only) were analyzed independent of the discharge nozzle thermocouple data.

Figure 30 shows the maximum liner barrel temperature versus operating condition, and indicates a substantial temperature reduction from the levels of Figure 29. Figure 31 illustrates the average liner barrel temperature vs operating conditions. The strong influence of increased radiation from increased power level is evident.

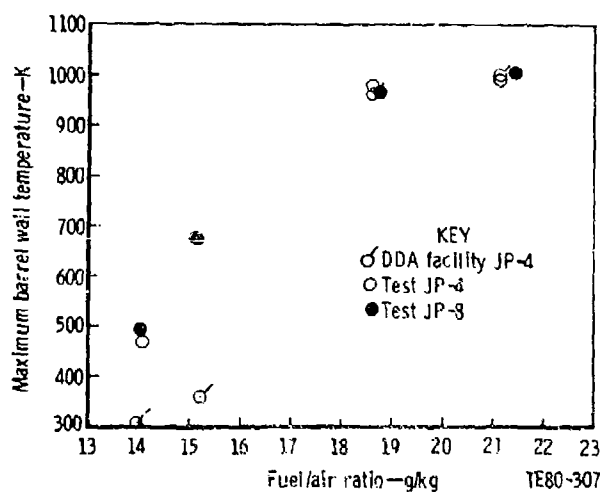


Figure 30. - Effect of Operating Conditions on Maximum Barrel Wall Temperatures.

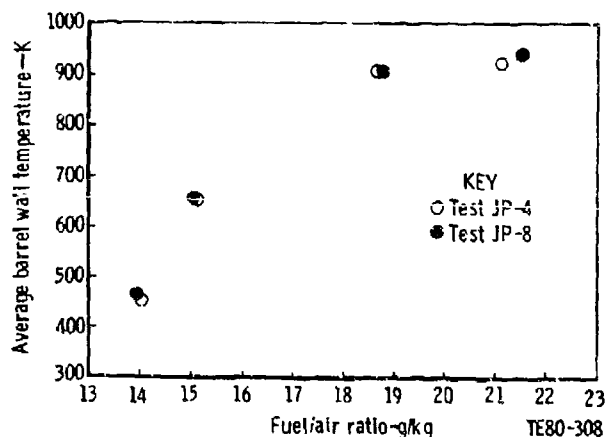


Figure 31. - Effect of Operating Conditions on Average Barrel Wall Temperatures.

5. Carbon Deposition

Fuel nozzle and combustor dome carboning characteristics were determined during a special 1-hr test at SLTO conditions, as described in Section III-D. Fuel nozzle flow numbers for JP-4 and JP-8 as recorded throughout the test are listed in Table 29 and show no appreciable clogging. Photographs of the fuel nozzle face and combustor dome posttest are shown in Figures 32 and 33 for JP-4 and JP-8 fuels. No significant carbon deposition was evident.

TABLE 29
FOULING AND CARBONING SUMMARY

Measured pilot nozzle flow nozzle

	Flow	<u>Rig test data using test fuels</u>					Flow
	bench	<u>Combustor rig operating time, min</u>					Bench
<u>Fuel</u>	<u>pretest*</u>	<u>0</u>	<u>15</u>	<u>30</u>	<u>45</u>	<u>60</u>	<u>posttest*</u>
JP-4	12.78	9.72	9.72	9.72	9.67	9.72	13.11
JP-8	12.89	11.14	11.14	11.14	11.14	11.09	12.07

Measured Main Nozzle Flow Number

	Flow	<u>Rig test data using test fuels</u>					Flow
	bench	<u>Combustor rig operating time, min</u>					Bench
<u>Fuel</u>	<u>pretest*</u>	<u>0</u>	<u>15</u>	<u>30</u>	<u>45</u>	<u>60</u>	<u>posttest*</u>
JP-4	276	241	243	240	240	240	275
JP-8	275	235	238	239	238	236	256

*Nonflammable test fluid used on flow bench, viscosity different from test fuels.

$$\text{Flow number units} = \frac{\text{kg/s fuel flow}}{\sqrt{\text{MPa fuel pressure differential}}}$$

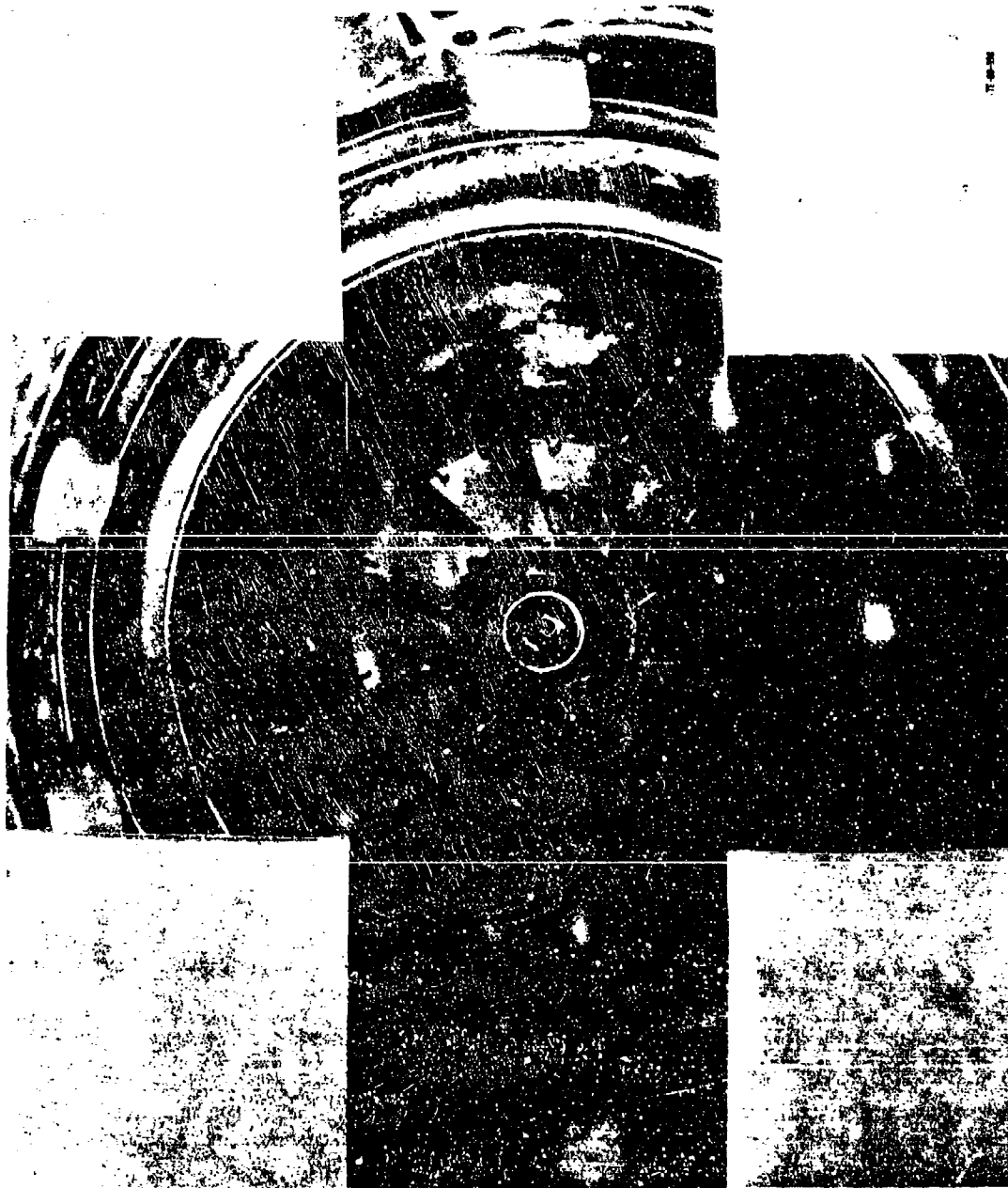
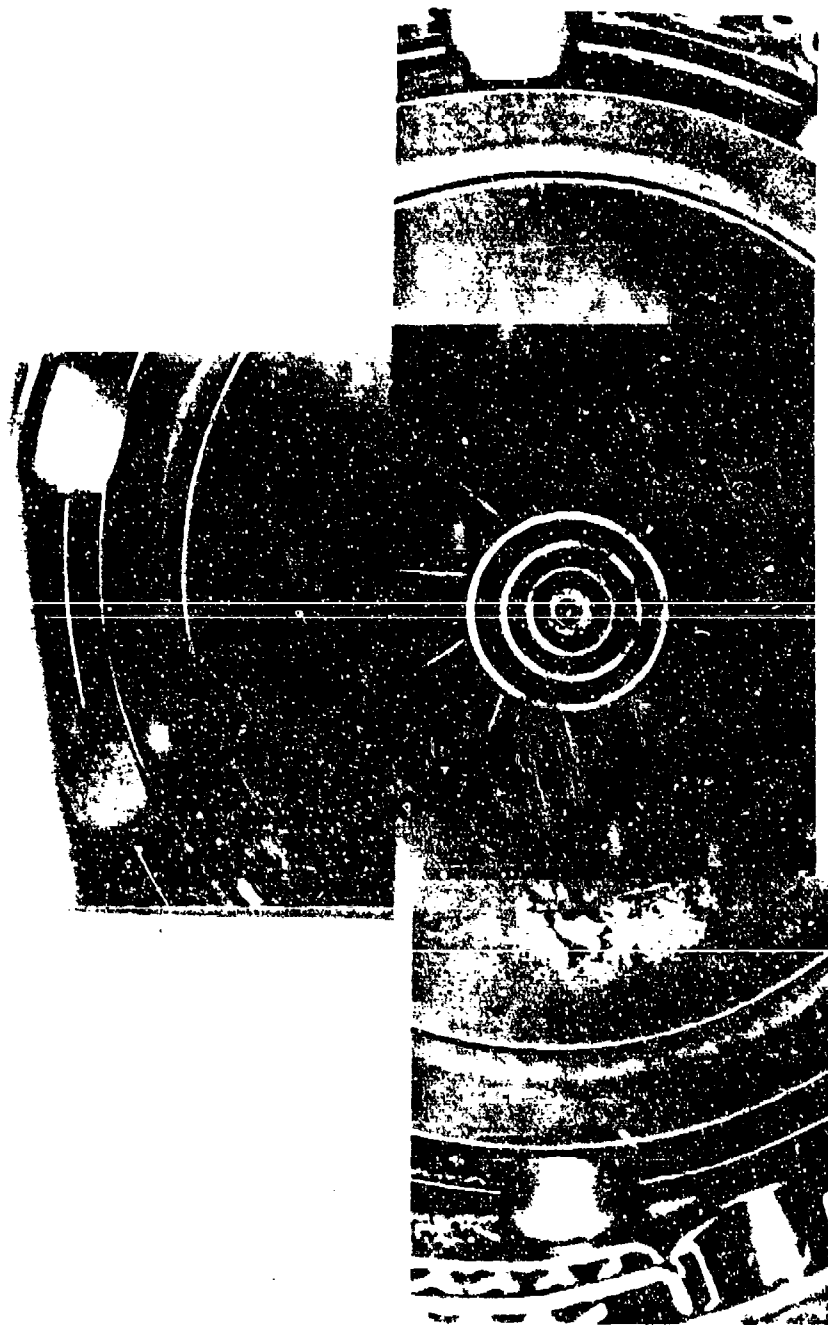


Figure 32. - Dome and Fuel Nozzle Carbon Deposition--JP-4 Fuel.



IT-40-299

Figure 33. - Dome and Fuel Nozzle Carbon Deposition--JP-8 Fuel.

6. Combustor Pattern Factor and Exit Profile

The combustor exit temperature distribution was measured with a five-element swing probe. Sample overall temperature distributions at SLTO for JP-4 and JP-8 fuels are shown in Figure 34. Peak temperatures generally occur in the upper left-hand quadrant (looking downstream) for all fuels.

The exit temperature pattern factor correlation to operating conditions is shown in Figure 35. Pattern factor is relatively constant at all off-idle operating power levels. Radial temperature profiles at the combustor exit are shown in Figure 36. As power level increases, the radial profile flattens

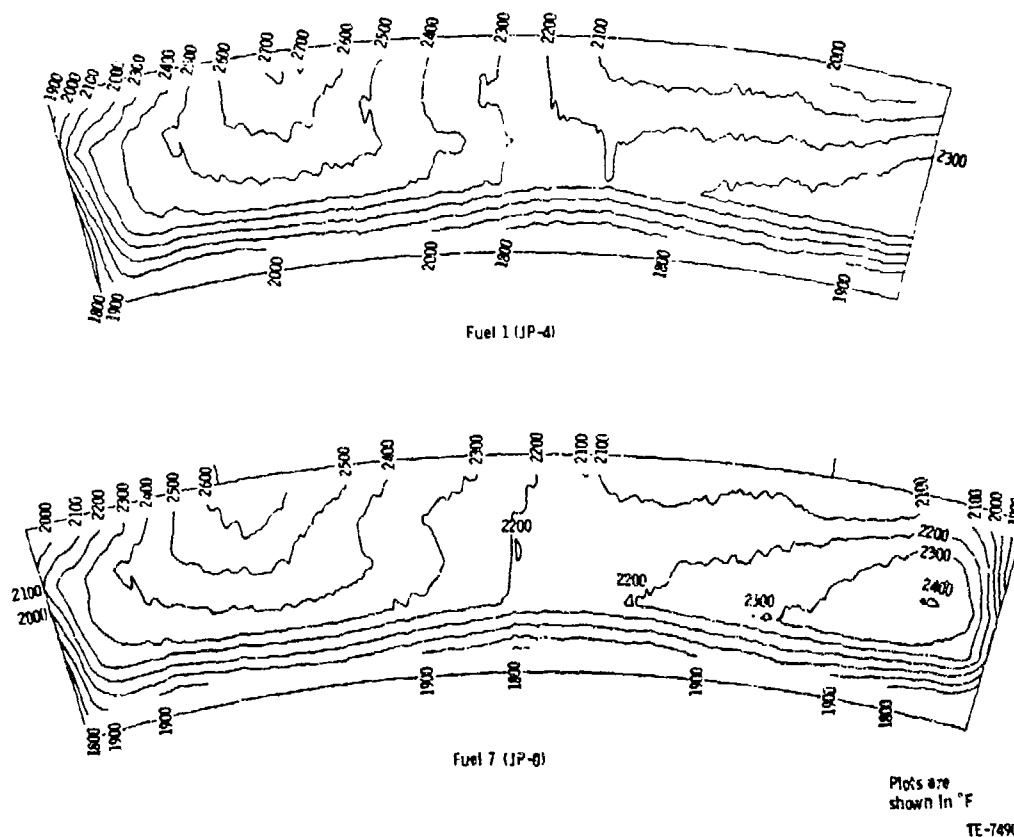


Figure 34. - SLTO Outlet Temperature Patterns.

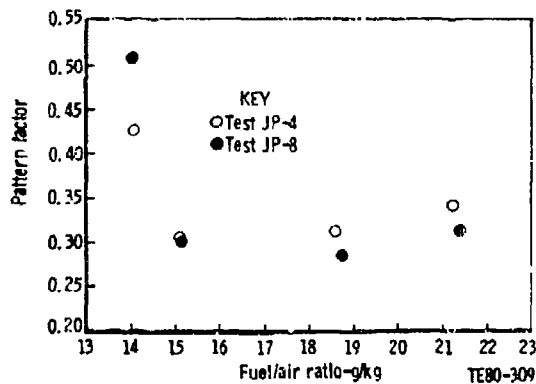


Figure 35. - Effect of Operating Conditions on Combustor Temperature Pattern factor.

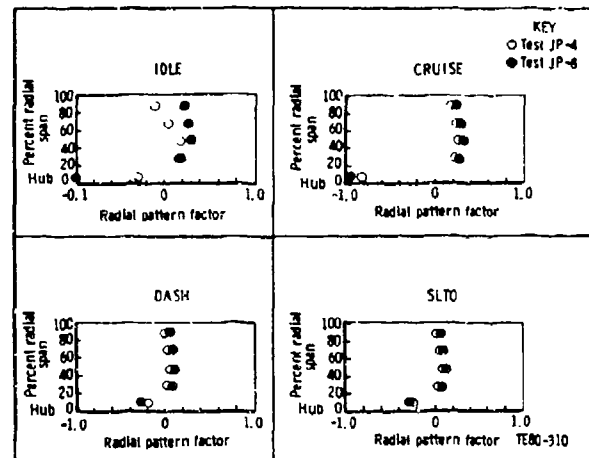


Figure 36. - Effect of Operating Conditions on Combustor Exit Radial Temperature profile.

appreciably. Very little difference between JP-4 and JP-8 pattern factor results can be noted.

7. Altitude Ignition and LBO

Altitude ignition tests were conducted to establish the approximate altitude ignition envelope and stability margin. The experimental work was conducted at $0.6 M_N$ flight conditions at 3 sec flame out. The nominal start conditions that were attempted in this program are listed in Table 30. A calculated parameter, θ (Reference 8), is used to quantify the severity of the combustor loading. Altitude ignition and LBO data are usefully correlated to the θ parameter, defined as follows:

$$\theta = \frac{p^{1.75} A_r h e^{T/b}}{W_c}$$

θ = combustor loading parameter
 P = combustor inlet pressure, kPa
 A_r = combustor reference area (cross section between combustor cases), m²
 h = combustor height or dia, m
 e = base of natural logarithms
 T = combustor inlet temperature, K
 b = function of reaction zone equivalence ratio, taken as 300 at stoichiometric conditions
 W_c = combustor airflow loading, kg/s

θ is basically the chemical reaction related to combustor loading, so that difficult combustion conditions are indicated by low θ values. Figure 37 is a plot of θ versus altitude for the TF41 at 0.6 M_N , 3 sec out windmill conditions. With increasing altitude, θ reduces drastically, indicating more difficult start conditions.

TABLE 30
 NOMINAL START CONDITIONS

Condition	W_A , kg/s	P , kPa	T , K	θ	F/A ratio, g/kg*** Pilot, max
Alt cruise	1.70	511	577	678.3	14.4
Idle	1.07	293	422	242.9	23.6
3.0 km windmill*	0.88	149	283	56.9	28.9
SL start**	0.79	117	283	41.5	32.6
10.7 km windmill	0.60	93	283	36.6	42.7
12.2 km windmill	0.52	79	283	31.7	49.9
15.2 km windmill	0.40	62	283	27.0	64.1

*All windmill conditions at 0.6 flight M_N , 3 sec out.

**Equivalent to 6.7 km windmill.

***Maximum PZ F/A ratio obtainable on pilot at 4.5 MPa fuel pressure differential.

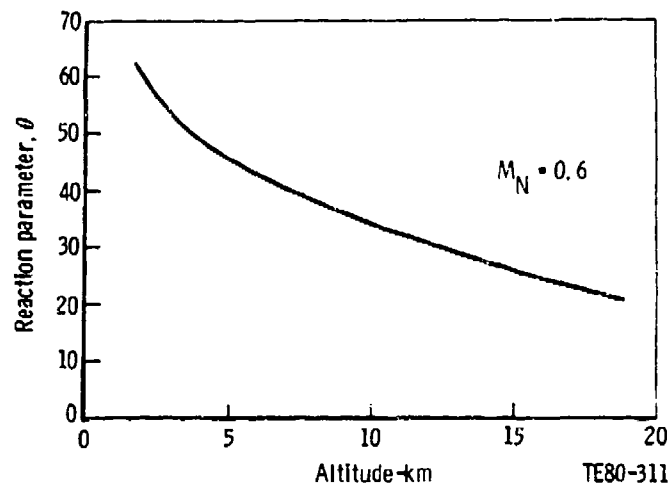


Figure 37. - Effect of Altitude on Combustor θ Parameter.

Figure 38 illustrates successful ignition results for JP-4 and JP-8 fuels. Rig ignition results on JP-4 exceed the engine specification, but rig results on JP-8 fall below the engine JP-4 spec.

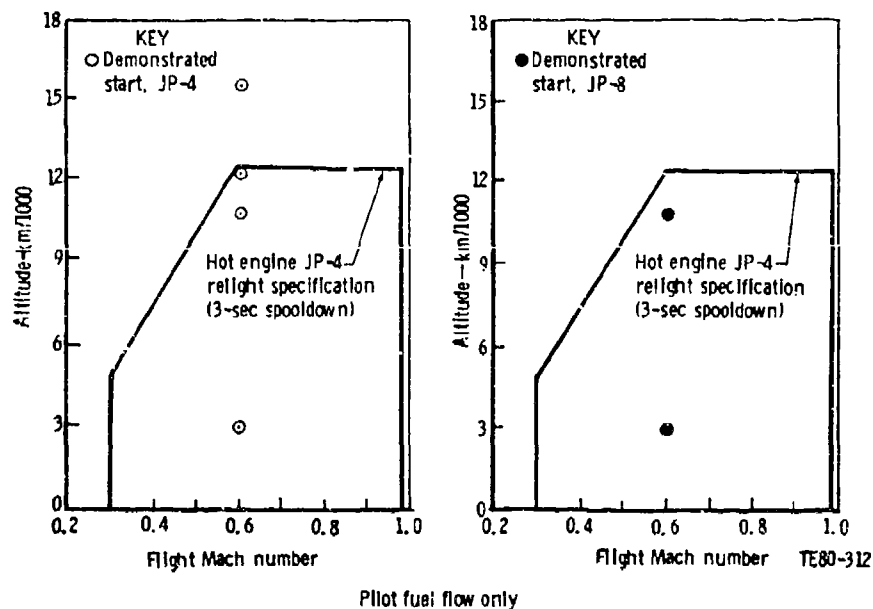


Figure 38. - Altitude Relight Envelope Limits--JP-4 and JP-8 Fuels.

8. Sea Level Starting and Stability

Sea level start and stability tests were conducted at ambient inlet (approximately 15°C) and cold inlet (approximately -2°C) temperature levels. The rig environment simulated engine ground idle operating conditions. The resultant ignition and LBO F/A ratios for JP-4 and JP-8 are shown in Figure 39. The data does not readily correlate with inlet air temperature as might be expected, but JP-8 fuel does indicate a higher F/A ratio requirement than JP-4 for ignition and LBO limit.

Generalized combustor stability, as described by F/A ratio at LBO versus the θ parameter, is detailed in Figure 40. As previously mentioned, low θ values indicate more severe starting and stability conditions. Again JP-8 fuel exhibits a more restricted LBO envelope than JP-4.

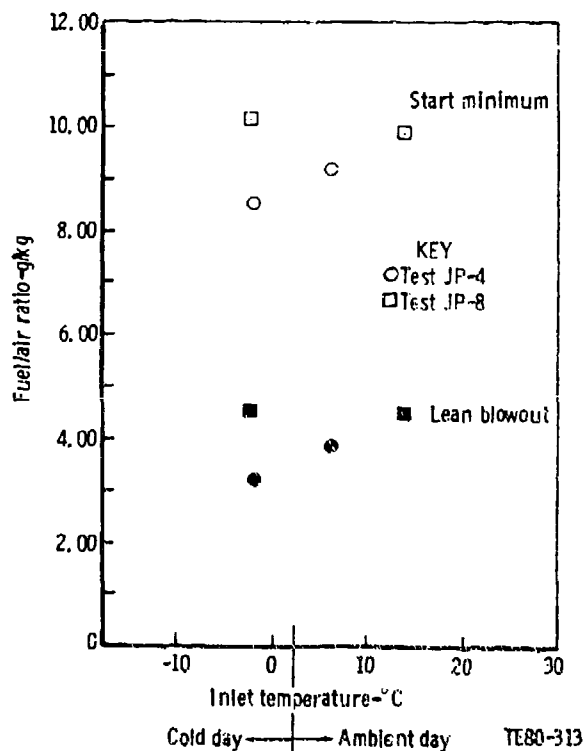


Figure 39. - Effect of Inlet Temperature on Sea Level Ignition and LBO.

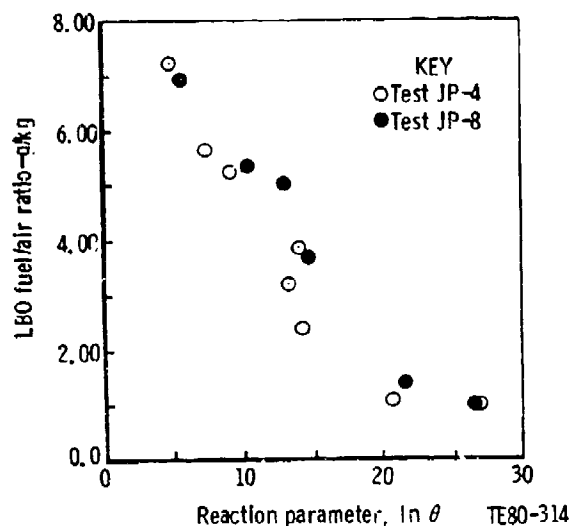


Figure 40. - Effect of Combustor θ Parameter on LBO F/A Ratio.

C. SINGLE-VARIABLE LINEAR REGRESSION ANALYSIS

The TF41 combustion system was tested in a single liner rig test with 12 different fuels consisting of basic JP-4 and JP-8 fuels and blends of these fuels with aromatic and paraffinic stocks to alter the basic fuel properties. In the process of blending fuels to vary specific properties, invariably other properties are affected. In this program fuel properties of interest were analyzed to determine which ones were statistically interrelated (refer to Table 13). The fuel properties were then grouped into two categories. Elements of each category have a significant statistical relationship to the other elements of that particular group.

The fuel properties used in the data analysis presented in this report can be grouped as follows:

o Group I

- Hydrogen content
- Aromatic content--total, single, and multiple ring
- Smoke point

o Group II*

- 10% boiling point distillation temperature
- End point distillation temperature
- Viscosity
- Surface tension
- Vapor pressure
- Breakpoint (JFTOT)

These individual fuel properties were used as the independent variables in a single-variable linear regression analysis technique to relate fuel property changes to changes in basic combustor performance parameters. These combustor performance parameters, detailed in Section IV-B, serve as the dependent variables in the regression analysis and include the following:

o SLTO conditions

- Combustor efficiency
- Emission levels--CO, UHC, NO_x and smoke number
- Pattern factor
- Liner metal temperature - maximum, average

o Idle conditions

- Combustor efficiency
- Emission levels--CO, UHC

o Low pressure conditions

- Idle ignition and LBO F/A
- Cruise LBO F/A
- SL ambient inlet ignition F/A
- SL cold inlet ignition F/A
- Maximum ignition altitude and LBO F/A

These regression analysis results were examined for cause/effect relationships. A good correlation, one which would indicate a significant cause/effect relation, was arbitrarily designated as any fuel property-combustor performance regression analysis result with a coefficient of determination (R^2 value) of ≥ 0.400 . A list of all correlation results

*This group contains many of the physical properties of fuels.

(R^2 values) from the regression analysis can be found in Table 31. The best-fit regression results (where $R^2 \geq 0.400$) are discussed in the following text.

TABLE 31
SINGLE-VARIABLE LINEAR REGRESSIONS SUMMARY

High-Pressure Fuel Sample

Fuel property	Coefficient of determination, R^2											
	Sea-level takeoff									Idle		
	CO emissions	UNC emissions	HU ₂ emissions	Combustion efficiency	Smoke emissions	Pattern factor	Liner max temp.	Barrel max temp.	Barrel avg temp.	CO emissions	UNC emissions	Combustion efficiency
Hydrogen content	0.655	0.219	0.364	0.655	0.490	0.183	0.498	0.400	0.377	0.004	0.232	0.169
Total aromatic content	0.523	0.197	0.230	0.524	0.471	0.258	0.421	0.190	0.198	0.024	0.321	0.243
Single-ring aromatic content	0.146	0.048	0.044	0.169	0.204	0.240	0.125	—	0.004	0.074	0.346	0.304
Multi-ring aromatic content	0.116	0.013	0.130	0.169	0.149	—	0.197	0.514	0.412	0.034	0.006	0.014
Smoke point	0.540	0.384	0.393	0.715	0.320	0.152	0.213	0.280	0.239	0.022	0.135	0.105
10% boiling dist point	0.340	0.058	0.120	0.025	0.001	0.034	0.010	0.156	0.134	0.016	0.005	0.015
Dist end point	0.001	0.102	0.247	0.021	0.148	0.284	0.106	0.007	0.007	0.017	0.174	0.042
Viscosity	0.004	0.094	0.103	0.007	—	0.078	—	0.185	0.138	0.026	—	0.006
Surface tension	0.197	—	0.405	0.303	0.120	0.019	0.012	0.295	0.261	0.073	0.201	0.248
Vapor pressure	0.235	0.007	0.395	0.267	0.040	—	0.092	0.193	0.152	0.182	0.041	0.079
JFTOT	0.227	0.371	—	0.791	0.232	0.201	0.014	—	—	0.035	0.125	0.084

— = value ≤ 0.000

Low-Pressure Fuel Sample

Fuel property	Coefficient of determination, R^2							
	Idle LBO F/A	Cruise LBO F/A	Idle ignition F/A	Cold start ignition F/A	Ambient start ignition F/A	Maximum ignition altitude	3.0-km altitude LBO F/A	10.6-km altitude LBO F/A
Hydrogen content	0.31	—	0.081	0.007	0.001	0.575	0.123	0.021
Total aromatic content	0.343	0.014	0.028	0.501	0.04	0.657	0.684	—
Single-ring aromatic content	0.342	0.081	0.011	0.025	0.185	0.563	0.049	0.010
Multi-ring aromatic content	0.046	0.029	0.194	0.030	0.039	0.223	0.039	0.019
Smoke point	No data available							
10% boiling dist point	0.015	0.115	0.106	0.137	0.375	0.013	0.203	0.658
Dist end point	0.077	0.498	0.269	0.010	0.012	0.006	0.074	0.008
Viscosity	0.010	0.119	0.136	0.342	0.494	0.021	0.345	0.584
Surface tension	0.293	0.072	0.018	0.231	0.248	0.058	0.455	0.342
Vapor pressure	0.201	0.020	0.144	0.268	0.141	0.003	0.442	0.447
JFTOT	No data available							

— = value ≤ 0.000

1. Combustor Efficiency--SLTO and Idle

Combustion efficiency values from the rig test program are summarized in Table 32. Although the total variation in combustion efficiency at SLTO is only $\approx 0.15\%$, there were definite correlations to fuel property variation substantiated by statistical analysis. Combustion efficiency increases with increasing hydrogen content, decreases with increasing total aromatic content, and increases with increasing fuel smoke point, as shown in Figures 41 through 43. Other fuel properties affected the SLTO efficiency but the correlations were not considered statistically significant.

At idle, combustion efficiency is substantially reduced as lower combustion reaction rates result from the lower inlet temperature and pressure conditions. No significant correlations between idle combustion efficiency and fuel property characteristics were found.

TABLE 32
SUMMARY OF COMBUSTION EFFICIENCY TEST RESULTS

Fuel No.	Combustion efficiency, %			
	Idle	Cruise	Dash	Takeoff
1	94.8	99.0	99.9	99.9
2	93.3	98.7	99.8	99.8
3	94.9	98.7	99.7	99.8
4	97.0	99.0	99.8	99.8
5	96.0	99.1	99.8	99.8
6	94.9	99.2	99.9	99.9
7	94.4	99.1	99.9	99.9
8	97.9	99.1	99.8	99.8
9	94.0	98.8	99.8	99.9
10	96.1	99.0	99.8	99.8
11	96.4	99.4	99.8	99.8
12	95.2	99.3	99.8	99.8

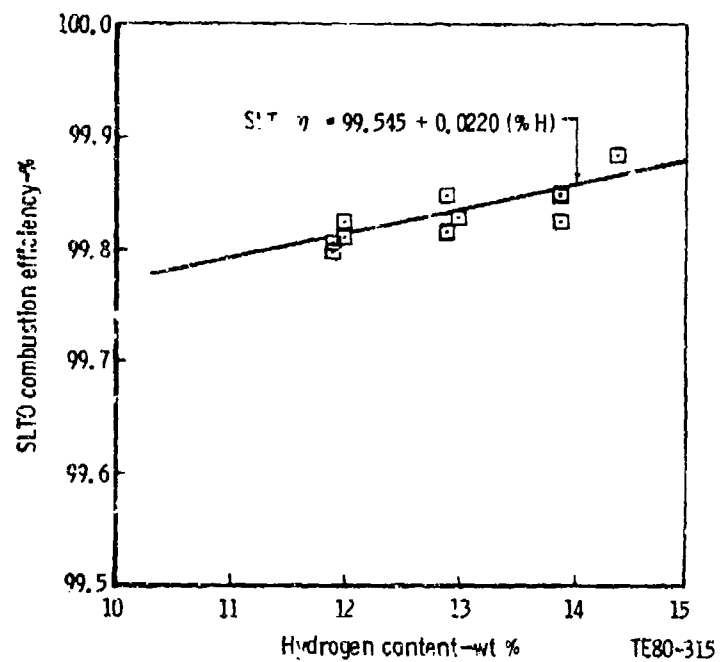


Figure 41. -- Effect of Fuel Hydrogen Content on SLTO Combustion Efficiency.

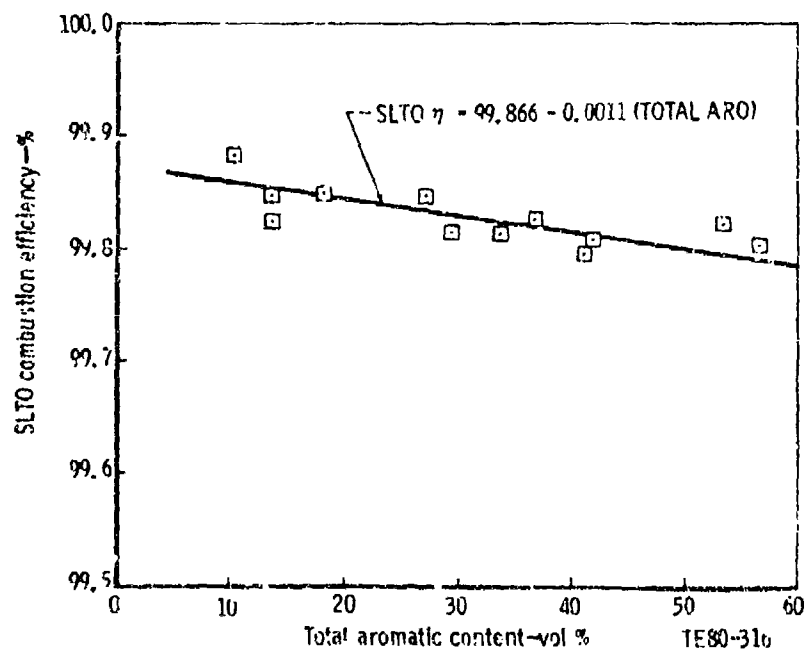


Figure 42 - Effect of Fuel Total Aromatic Content on SLTO Combustion Efficiency.

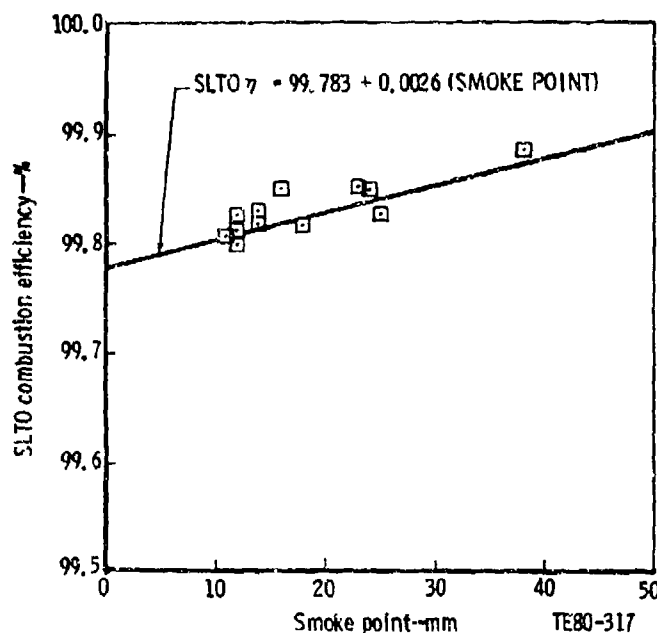


Figure 43. - Effect of Fuel Smoke Point on SLTO Combustion Efficiency.

2. CO Emissions--SLTO and Idle

CO formation (like UHC formation) is the result of incomplete combustion and is most prominent at low-power settings as demonstrated by Table 33. CO emission levels at SLTO are very small but do exhibit correlation to fuel properties very similar to combustion efficiency results; CO emissions decrease with increasing hydrogen content, increase with increasing total aromatic content, and decrease with fuel smoke point. These results are displayed in Figures 44 through 46. As shown, CO emission levels at idle were much higher than at SLTO but do not readily correlate to any measured fuel property. Fuel droplet sizes (SMD) were calculated and analyzed versus idle CO, but no significant correlation was found, as shown in Figure 47.

TABLE 33
SUMMARY OF CO EMISSION TEST RESULTS

Fuel No.	CO emission index, g/kg			
	Idle	Cruise	Dash	Takeoff
1	72.2	27.3	0.8	1.0
2	91.8	28.5	2.2	1.9
3	68.9	20.5	2.0	1.8
4	59.0	28.4	2.0	1.9
5	67.1	23.2	1.2	1.7
6	60.7	16.8	1.1	1.2
7	68.7	23.1	1.6	1.6
8	53.5	25.7	2.1	2.0
9	67.1	25.6	2.0	1.6
10	67.5	22.5	1.8	2.0
11	67.9	16.1	1.2	1.2
12	72.2	18.7	1.1	1.5

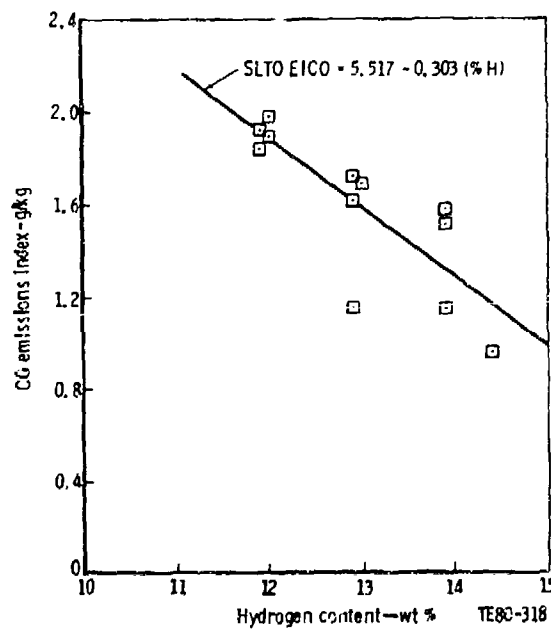


Figure 44. - Effect of Fuel Hydrogen Content on SLTO CO Emissions.

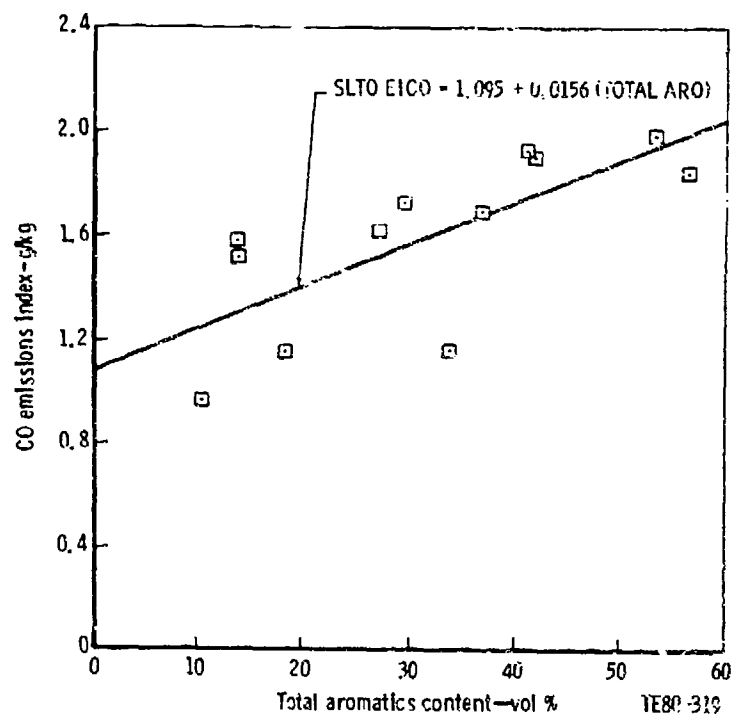


Figure 45. - Effect of Fuel Total Aromatic Content on SLTO CO Emissions.

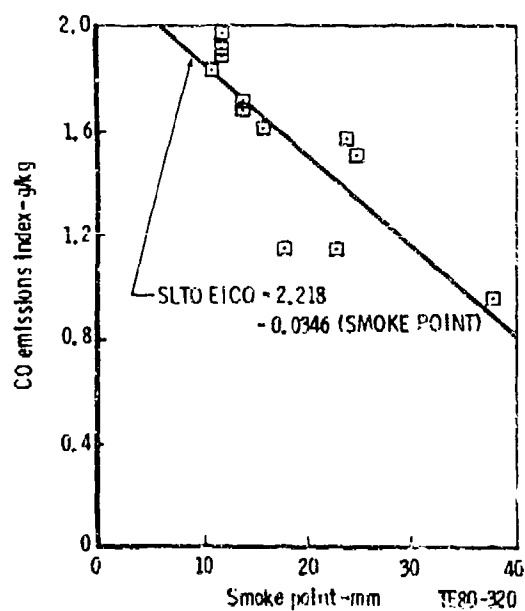


Figure 46. - Effect of Fuel Smoke Point on SLTO CO Emissions.

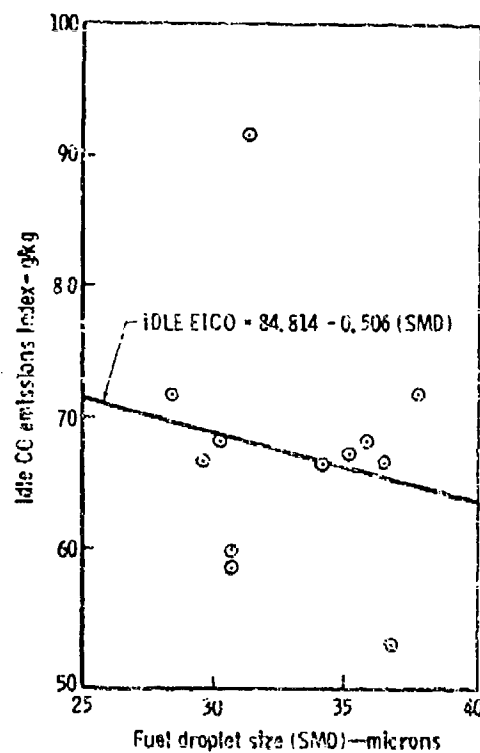


Figure 47. - Effect of Fuel Droplet Size (SMD) on Idle CO Emissions.

3. UHC Emissions--SLTO and Idle

UHC emissions are also the results of incomplete combustion, and therefore are much higher at low power settings. Rig tests of UHC levels are shown in Table 34. No substantial correlation between UHC emission levels and fuel properties exists at either SLTO or idle, but the regression analysis results may indicate a combination of fuel properties control UHC formation.

TABLE 34
SUMMARY OF UHC EMISSION TEST RESULTS

Fuel No.	UHC emission index, g/kg			
	Idle	Cruise	Dash	Takeoff
1	48.8	5.5	0.1	0.1
2	65.4	8.5	0.7	0.4
3	48.3	11.3	2.9	0.5
4	23.3	4.8	0.5	0.3
5	34.2	5.4	0.7	0.5
6	58.5	5.1	0.6	0.5
7	50.8	4.5	0.3	0.2
8	15.9	3.7	1.2	0.5
9	63.3	8.1	0.4	0.2
10	35.5	5.9	0.8	0.4
11	35.1	2.7	0.3	0.3
12	51.3	4.3	0.7	0.3

4. NO_x Emissions--SLTO

Thermal NO_x emissions are the product of high temperature combustion and thus are highest at high-power operating conditions. This is demonstrated in the TF41 results shown in Table 35. The strongest fuel property correlator is surface tension, with SLTO NO_x emission level increasing with increasing

surface tension, as shown in Figure 48. Other fuel properties showing a weaker correlation to SLTO NO_x levels are vapor pressure, smoke point, and hydrogen content.

TABLE 35
SUMMARY OF NO_x EMISSION TEST RESULTS

Fuel No.	NO _x emission index, g/kg			
	Idle	Cruise	Dash	Takeoff
1	5.1	5.3	22.2	17.5
2	3.5	6.6	26.8	27.6
3	1.3	6.2	23.4	26.4
4	3.1	6.9	27.9	29.1
5	2.5	6.2	20.7	20.2
6	2.7	6.8	26.2	28.1
7	2.1	6.0	21.4	24.3
8	3.5	7.2	26.7	30.1
9	1.9	5.4	22.9	25.2
10	2.9	7.1	26.5	27.4
11	3.1	7.6	28.8	29.3
12	3.2	7.3	24.1	28.0

5. Smoke Emission--SLTO

Smoke is also a product of incomplete combustion, but visible smoke may exist in an efficient combustor if soot particles are comparable with the visible light spectrum. All smoke data is shown in Table 36, with visible smoke in evidence (SN \geq 25) at nearly all off-idle operating conditions.

Smoke levels increase as fuel hydrogen level is decreased as shown in Figure 49. TF41 combustor smoke increased as total aromatic content increased, per Figure 50, but no correlation to aromatic type or fuel smoke point was noted.

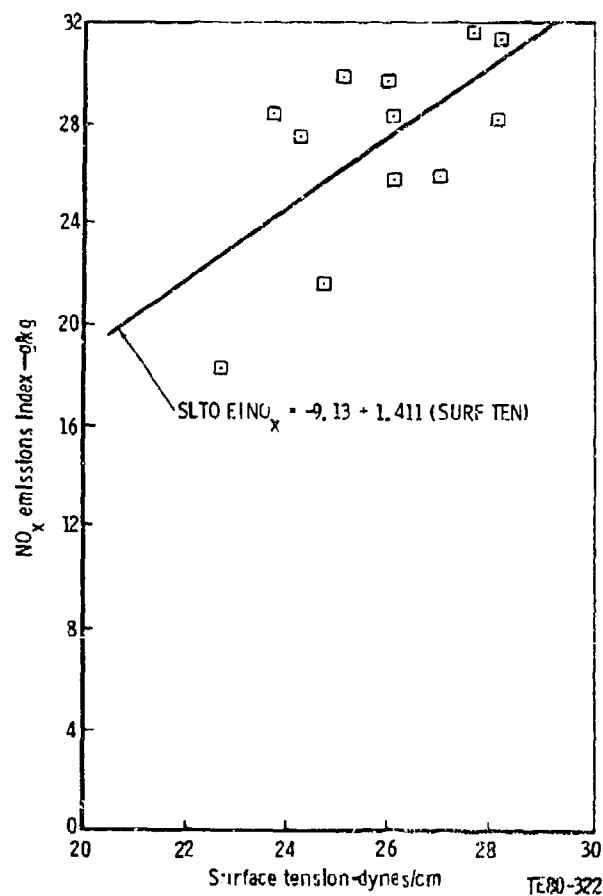


Figure 48. - Effect of Fuel Surface Tension on SLTO NO_x Emissions.

TABLE 36
SUMMARY OF SMOKE EMISSION TEST RESULTS

Fuel No.	Smoke number			
	Idle	Cruise	Dash	Takeoff
1	18	29	36	42
2	60	36	43	44
3	37	29	47	45
4	45	30	48	58
5	34	39	36	43
6	15	12	36	35
7	30	27	42	40
8	41	31	37	54
9	35	35	49	49
10	54	48	45	45
11	28	19	46	41
12	26	26	33	39

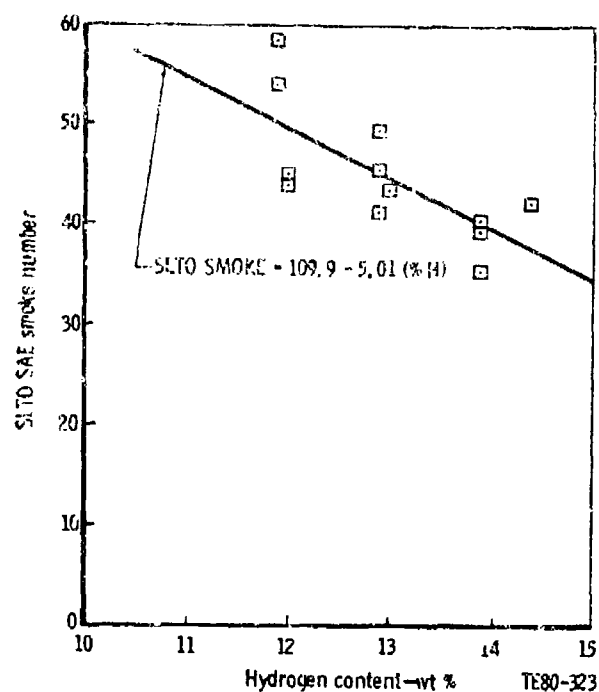


Figure 49. - Effect of Fuel Hydrogen Content on SLTO Smoke Emissions.

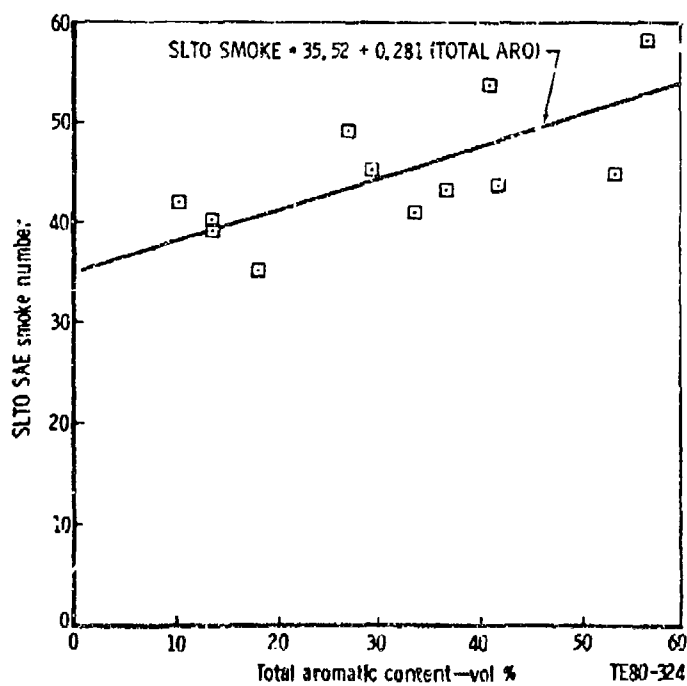


Figure 50. - Effect of Fuel Total Aromatic Content on SLTO Smoke Emissions.

6. Liner Wall Temperature

The presence of carbon particles in the combustion zone from incomplete combustion or poor fuel atomization may lead to increased liner wall temperature because of higher radiation. Poor fuel placement or inadequate fuel-air mixing in the primary zone could cause liquid fuel to reach the combustor walls and burn locally. It is believed that these conditions may exist in the TF41 combustor but that overcooling the liner wall through the corrugated "wobble strip" cooling slots minimizes the impact and masks the effects.

Wall temperature results at SLTO conditions were analyzed in three classifications for correlation to fuel properties.

- o Peak measured wall temperature is the maximum temperature reading recorded. It was stated earlier that all maximum temperature readings occurred on the discharge nozzle inner wall.
- o Peak barrel wall temperature is the peak temperature recorded in the primary and intermediate reaction zones only.
- o Average barrel wall temperature is the average temperature from the six thermocouples in the primary and intermediate reaction zones.

Peak measured wall temperature results are summarized in Table 37. Hydrogen content and total aromatic content are statistically significant correlations to the peak wall temperature, as shown in Figures 51 and 52, but the slopes are essentially zero.

TABLE 37
SUMMARY OF WALL TEMPERATURE TEST RESULTS

Fuel No.	Maximum liner wall temperature, K			
	Idle	Cruise	Dash	Takeoff
1	712	899	1175	1238
2	773	940	1204	1251
3	759	944	1184	1247
4	820	929	1183	1254
5	734	891	1166	1219
6	795	947	1159	1221
7	770	939	1166	1234
8	816	1145	1221	1244
9	777	957	1164	1236
10	746	941	1177	1249
11	742	910	1181	1235
12	800	896	1158	1218

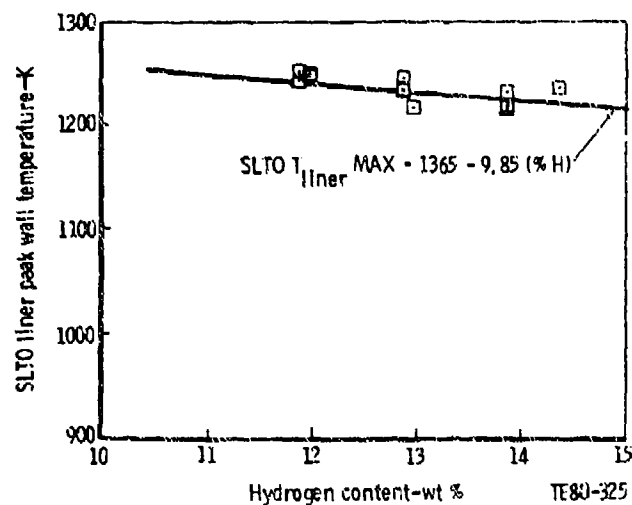


Figure 51. - Effect of Fuel Hydrogen Content on SLTO Maximum Liner Metal Temperature.

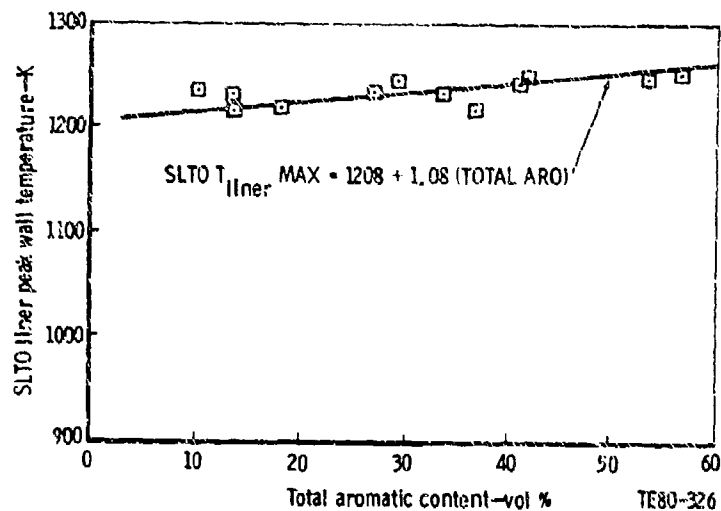


Figure 52. - Effect of Total Aromatic Content on SLTO Maximum Liner Wall Temperature.

Peak barrel wall temperatures are summarized in Table 38. Peak temperatures increase as hydrogen content is reduced, and increase as multiple-ring aromatic content is increased, as shown in Figures 53 and 54.

TABLE 38
SUMMARY OF BARREL TEMPERATURE TEST RESULTS

Fuel No.	Maximum barrel wall temperature, K*			
	Idle	Cruise	Dash	Takeoff
1	486	677	970	996
2	508	761	1019	1042
3	505	753	996	1030
4	538	728	1009	1045
5	493	687	996	1016
6	498	684	985	1019
7	490	679	965	1008
8	644	762	1164	1178
9	503	720	984	1088
10	513	724	1020	1050
11	481	716	992	1029
12	499	699	983	1014

*Primary and intermediate zones only, see Figure 10.

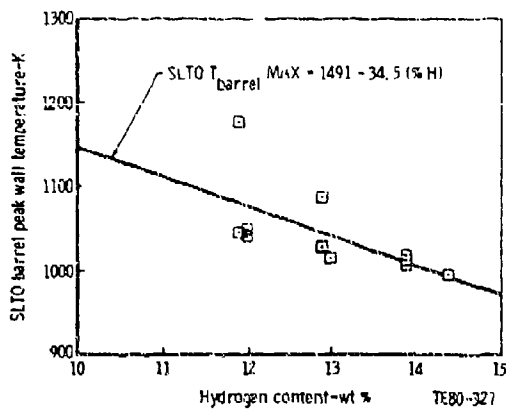


Figure 53. - Effect of Fuel Hydrogen Content on SLTO Maximum Barrel Wall Temperature.

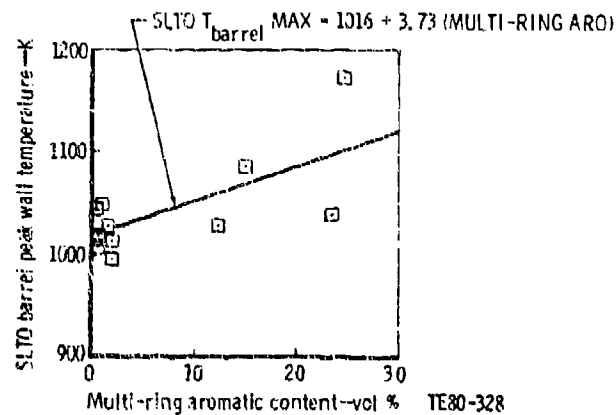


Figure 54. - Effect of Fuel Multi-Ring Aromatic Content on SLTO Maximum Barrel Wall Temperature.

A dimensionless liner temperature $(T_{L \text{ max}} - T_{L \text{ max, JP-4}})/(T_{L \text{ max, JP-4}} - T_3)$ was utilized to correlate a wide variety of data involving combustion systems with pressure atomizing fuel injection systems from different engine manufactures. TF41 data plotted over previously published data (References 1, 2, and 9) shows an increased sensitivity of TF41 barrel temperature to fuel hydrogen content, as illustrated in Figure 55.

Average barrel wall temperatures, which respond similarly to peak barrel wall temperatures, are shown in Table 39. Figure 56 shows the correlation between average barrel temperature and multi-ring (bicyclic) aromatic content. Peak barrel temperatures may be slightly more sensitive to hydrogen content than average barrel temperature, but both peak and average barrel temperature respond similarly to multi-ring aromatic content.

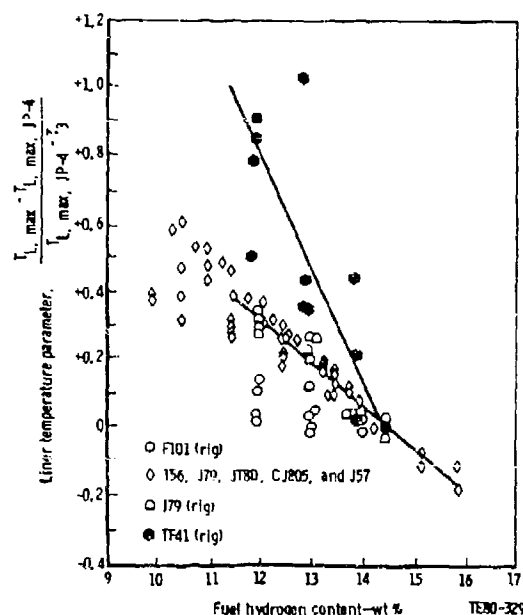


Figure 55. - Effect of Fuel Hydrogen Content on Liner Temperature Parameter at Cruise Operating Conditions.

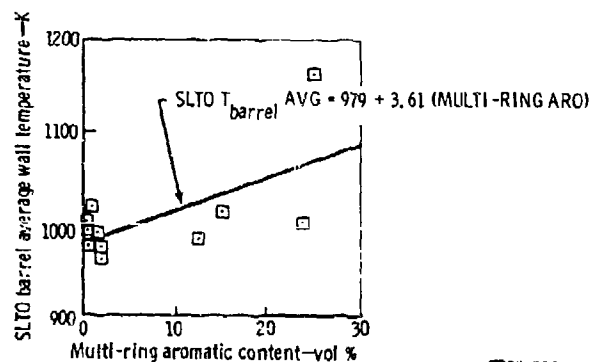


Figure 56. - Effect of Fuel Multi-Ring Aromatic Content on SLTO Average Barrel Wall Temperature.

TABLE 39
SUMMARY OF BARREL TEMPERATURE TEST RESULTS

Fuel No.	Average barrel wall temperature, K			
	Idle	Cruise	Dash	Takeoff
1	459	650	906	932
2	482	708	942	967
3	486	704	927	955
4	509	684	931	971
5	473	666	926	949
6	476	666	910	948
7	467	651	906	943
8	529	690	1123	1150
9	485	682	910	966
10	487	692	938	975
11	463	661	923	958
12	479	658	913	949

7. Pattern Factor and Exit Profile

The combustor exit temperature distribution was measured with a multi-element traversing probe as discussed in Section III-B. Pattern factor level and exit profile shape are dependent on operating conditions, as power level is increased pattern factor generally declined and the exit profile flattened. Pattern factor results are listed in Table 40. No significant correlation between SLTO pattern factor and fuel property characteristics was noted. Appendix B contains combustor exit isotherm plots for each of the test fuels.

8. Carbon Deposition and Fuel Nozzle Fouling

A special 1-hr test was conducted at SLTO operating conditions (with elevated fuel temperature) to accelerate carbon deposition and fuel nozzle fouling tendencies.

TABLE 40
SUMMARY OF PATTERN FACTOR TEST RESULTS

Fuel No.	Statistical pattern factor			
	<u>Idle</u>	<u>Cruise</u>	<u>Dash</u>	<u>Takeoff</u>
1	0.43	0.31	0.32	0.35
2	0.52	0.26	0.30	0.30
3	0.27	0.25	0.27	0.27
4	0.31	0.28	0.31	0.35
5	0.23	0.34	0.26	0.27
6	0.47	0.29	0.30	0.32
7	0.52	0.30	0.29	0.31
8	0.31	0.21	0.29	0.29
9	0.33	0.33	0.21	0.25
10	0.29	0.29	0.28	0.32
11	0.44	0.25	0.31	0.32
12	0.55	0.35	0.27	0.28

TF41 service experience shows that while the combustor dome remains essentially carbon-free (due in large part to the construction and cooling scheme), the pilot face of the fuel nozzle accumulates carbon in short running time. Photographs of the combustor dome and fuel nozzle face after each fuel test are presented in Appendix C. These photographs show no correlation between fuel properties and carbon deposition potential.

Fuel nozzle flow number and passage carbon deposition data, presented in Table 41, were subjected to statistical analysis versus fuel properties data. No significant correlation to fuel property was found.

9. Sea Level Starting

Sea-level ignition tests were conducted at engine cranking conditions at two inlet temperature levels, ambient inlet (284 K nominal) and cold inlet (272 K nominal). The fuel/air ratios required for ignition of the test fuels at these conditions are summarized in Table 42.

TABLE 41
FUEL NOZZLE FOULING SUMMARY

<u>Fuel</u>	<u>1</u>	<u>2</u>	<u>3</u>	<u>4</u>	<u>5</u>	<u>6</u>	<u>7</u>	<u>8</u>	<u>9</u>	<u>10</u>	<u>11</u>	<u>12</u>
<u>Pilot nozzle flow number:</u>												
Pretest	12.8	12.0	13.1	11.0	13.3	11.6	12.9	10.6	11.7	13.7	11.4	12.6
Posttest	13.1	11.9	13.2	11.4	11.0	11.9	12.1	10.5	10.3	11.5	11.5	13.1
Passage carbon, mg	1.0	0.4	1.3	0.3	4.0	5.8	0.3	0.4	0.2	4.5	3.1	2.1
<u>Main nozzle flow number</u>												
Pretest	276	258	275	258	277	258	275	258	256	280	257	276
Posttest	275	243	279	258	276	258	256	260	258	261	255	276
Passage carbon, mg	0.0	0.0	0.0	0.0	0.0	0.0	0.0	0.0	0.0	0.0	0.0	0.0

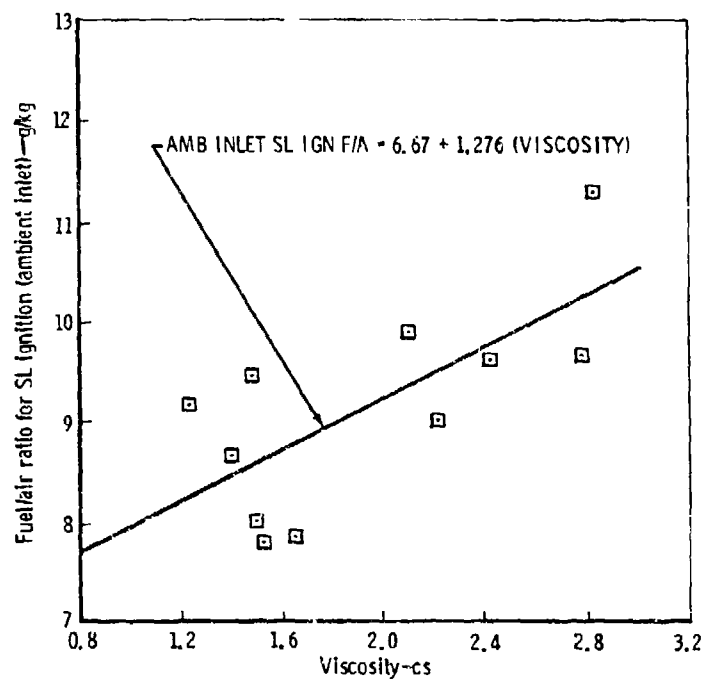
TABLE 42
SEA-LEVEL STARTING TEST SUMMARY

<u>Fuel</u>	<u>1</u>	<u>2</u>	<u>3</u>	<u>4</u>	<u>5</u>	<u>6</u>	<u>7</u>	<u>8</u>	<u>9</u>	<u>10</u>	<u>11</u>	<u>12</u>
<u>Ignition F/A, g/kg</u>												
Cold day (272 K nominal)	8.70	8.55	10.26	9.00	9.07	10.54	10.33	10.98	9.76	9.43	10.16	9.54
Ambient day (284 K nominal)	9.38	8.01	8.18	9.37	9.53	8.87	10.07	11.41	9.75	8.28	10.16	9.07

The F/A ratio required for ignition increased as the 10% distillation boiling point temperature increased, and also increased as the fuel viscosity increased as illustrated in Figure 57. The cold inlet ignition test results followed essentially the same correlation trends as the ambient inlet test results but were not nearly as strong statistically. No correlation was found to exist between sea-level starting performance and hydrogen or aromatic content.

10. Altitude Ignition and LBO

Altitude ignition and LBO testing were attempted at four altitude levels simulating 0.6 M_N , 3 sec out, engine windmilling conditions. Detailed test results are tabulated in Appendix A and are summarized in Table 43. The maximum ignition altitude and the F/A ratio required for ignition at a given altitude



TE80-331

Figure 57. - Effect of Fuel Viscosity on SL Ambient Inlet Ignition F/A Ratio.

TABLE 43
ALTITUDE IGNITION SUMMARY

	Fuel											
	<u>1</u>	<u>2</u>	<u>3</u>	<u>4</u>	<u>5</u>	<u>6</u>	<u>7</u>	<u>8</u>	<u>9</u>	<u>10</u>	<u>11</u>	<u>12</u>
3.0 km altitude, Ignition F/A	6.76	6.48	6.58	7.67	7.69	7.21	7.71	7.95	8.26	6.92	7.47	8.30
10.7 km altitude, Ignition F/A	10.98	No start	12.28	No start	12.10	11.97	12.38	11.93	6.76	No start	11.07	12.12
12.2 km altitude, Ignition F/A	9.66	No start	No start	No start	No start	10.43	16.14	No start	No start	No start	No start	No start
15.2 km altitude, Ignition F/A	11.16	No start	No start	No start	No start	11.69	No start	No start	No start	No start	No start	No start
F/A units = g/kg												

varied among the test fuels. Altitude ignition capability increased as hydrogen content increased, and decreased as total or single-ring aromatic content was increased, as shown in Figure 58 through 60.

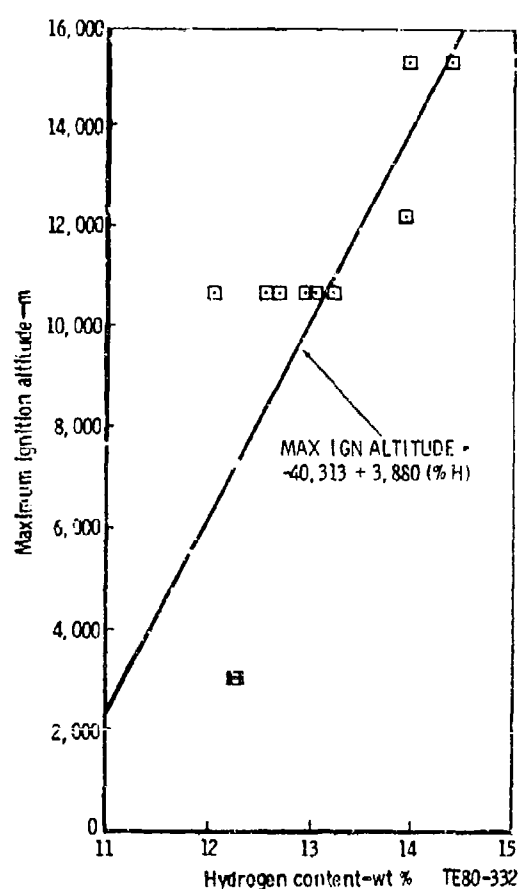


Figure 58. - Effect of Fuel Hydrogen Content on Maximum Ignition Altitude.

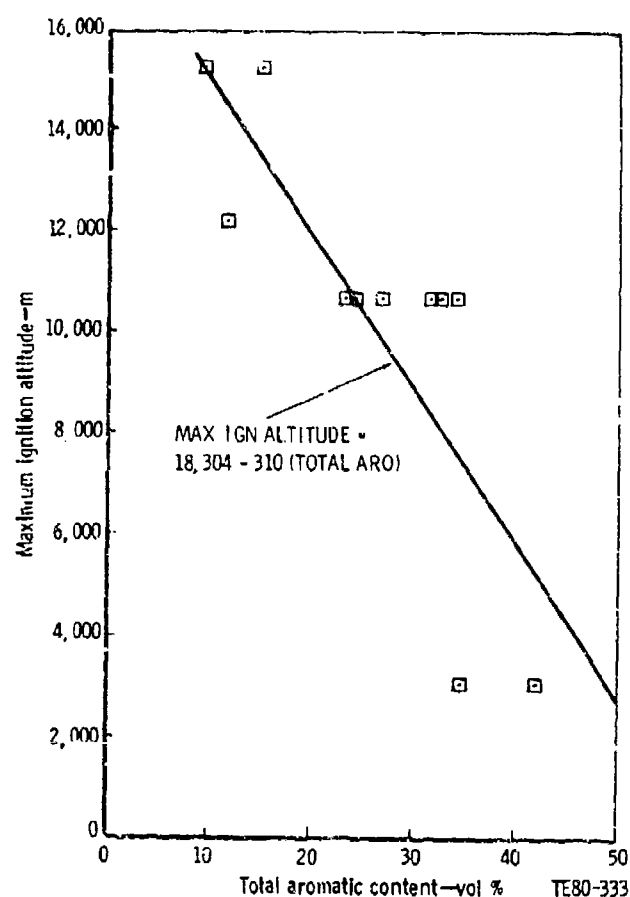


Figure 59. - Effect of Fuel Total Aromatic Content on Maximum Ignition Altitude.

Lean blow out (stability), once ignition was achieved, was strongly influenced by fuel properties affecting fuel preparation. The LBO F/A ratio at 3-km altitude increased with increasing surface tension and decrease with increasing vapor pressure as shown in Figures 61 and 62.

10-km altitude results follow the same trends as the LBO F/A ratio increasing with increasing 10% boiling point temperature and with increasing fuel viscosity, as shown in Figures 63 and 64. As before the LBO F/A ratio decreased with increasing fuel vapor pressure, shown in Figure 65.

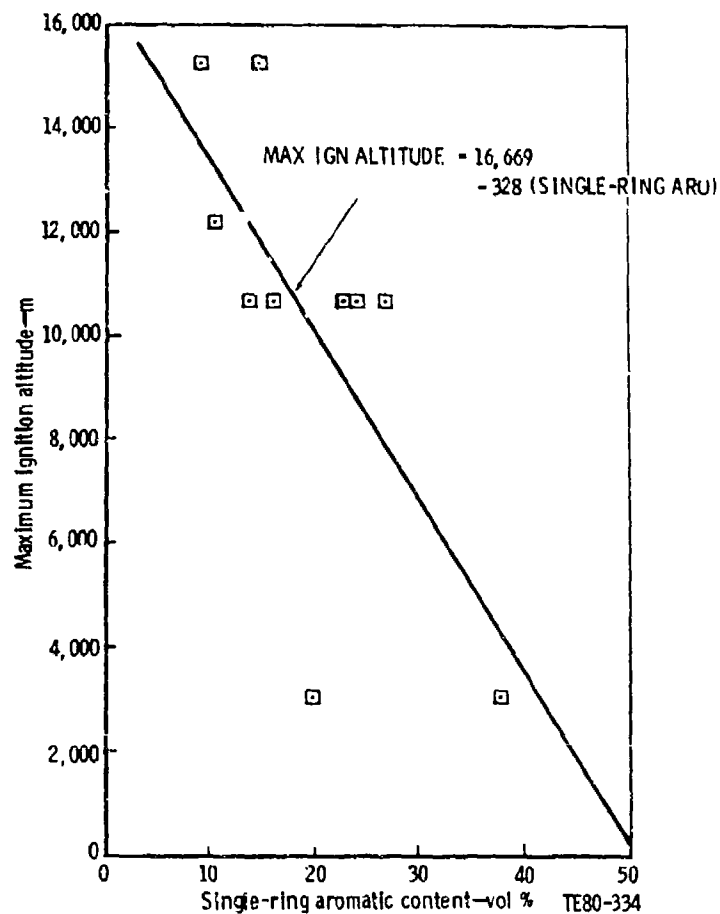


Figure 60. - Effect of Fuel Single-Ring Aromatic Content on Maximum Ignition Altitude.

11. Flame Stability

Flame stability can be represented by the difference between operating F/A ratios and LBO F/A ratios at low power conditions. Table 44 illustrates that the idle and cruise LBO F/A ratios vary widely: from 1.1 to 1.9 at idle and from 1.0 to 3 at the cruise condition. However flame stability is more than adequate as the engine operates at 14.0 F/A ratio at idle and at 15.2 F/A ratio at cruise.

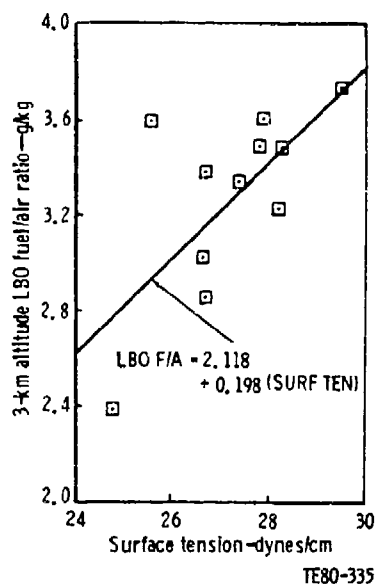


Figure 61. - Effect of Fuel Surface Tension on 3-km Altitude LBO F/A Ratio.

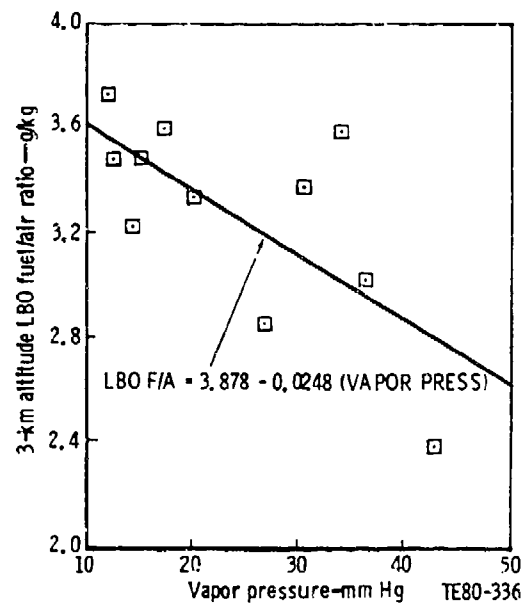


Figure 62. - Effect of Fuel Vapor Pressure on 3-km Altitude LBO F/A Ratio.

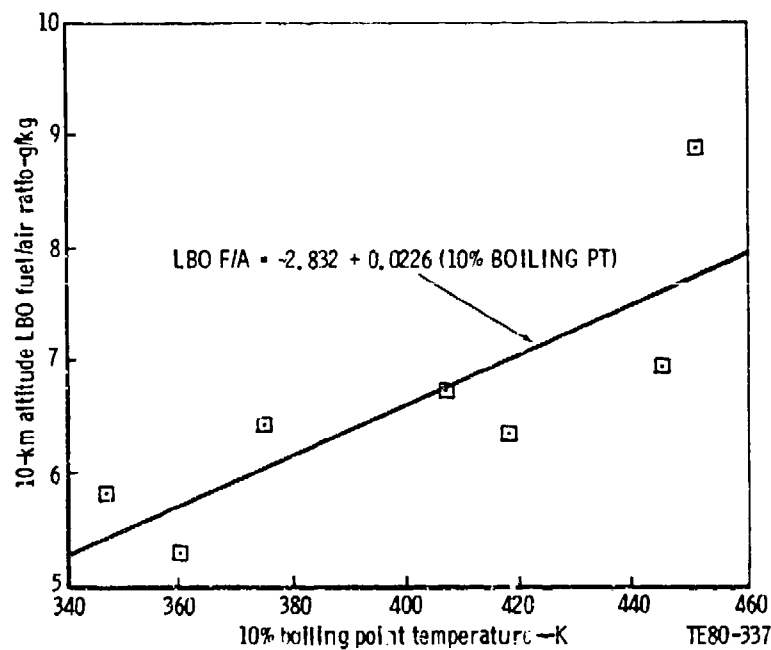


Figure 63. - Effect of Fuel 10% Distillation Point on 10-km Altitude LBO F/A Ratio.

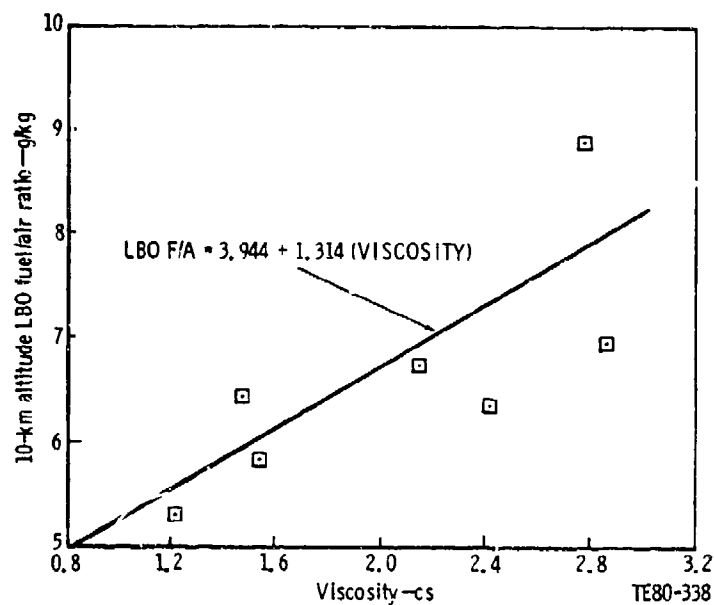


Figure 64. - Effect of Fuel Viscosity on 10-km LBO F/A Ratio.

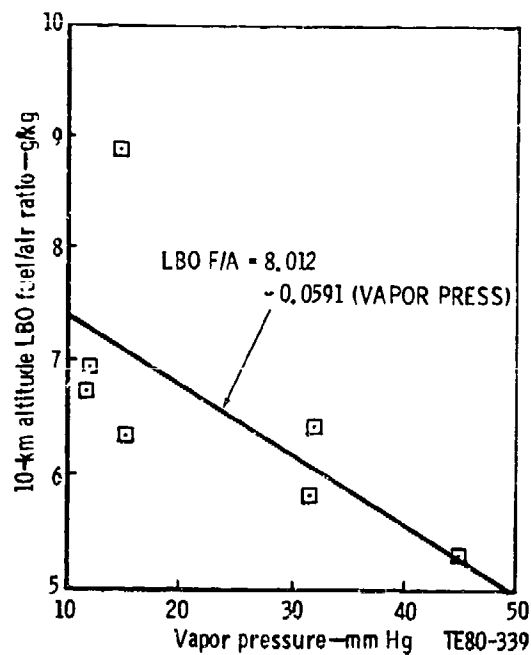


Figure 65. - Effect of Fuel Vapor Pressure on 10-km Altitude LBO F/A Ratio.

TABLE 44
FLAME STABILITY DATA SUMMARY

<u>Fuel</u>	Idle condition <u>LBO F/A, g/kg</u>	Cruise condition <u>LBO F/A, g/kg</u>
1	1.1	1.0
2	1.6	1.3
3	1.7	1.0
4	1.6	1.0
5	1.4	1.0
6	1.5	1.1
7	1.1	1.1
8	1.4	1.0
9	1.9	1.3
10	1.7	1.0
11	1.9	1.0
12	1.9	1.3
Engine operation F/A	14.0	15.2

None of the fuel property variables produced a reasonable correlation of idle LBO F/A ratio. There was a trend, however, to correlate idle LBO F/A to hydrogen, single ring aromatic, and total aromatic content.

Cruise condition LBO F/A ratios tended to correlate slightly to fuel physical properties, particularly to end point as shown in Figure 66. As fuel end point increased, the cruise LBO F/A ratio also increased, perhaps as a result of a decreased vaporization rate.

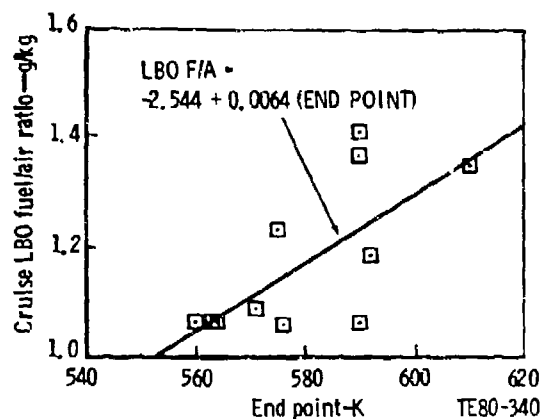


Figure 66. - Effect of End Point Temperature on Cruise LBO F/A Ratio.

D. MULTIPLE-VARIABLE LINEAR REGRESSION ANALYSIS

A multiple-variable linear regression analysis was conducted with the goal of identifying fuel property coefficients or exponents providing performance correlations not evident with single-property regression analysis.

In Section IV-C fuel properties were categorized into one of two groups by their interdependency. This list is re-established in Table 45, since only a maximum of one fuel property from each group can enter the multiple regression analysis and maintain the truly independent nature required of the independent variable.

It was anticipated that the multiple-regression analysis results would improve some cause-effect relationships between fuel properties and combustor performance. Nearly all areas of combustor performance that were analyzed by single-variable regression were subjected to multiple-variable regression. Only those performance parameters where no single-variable correlations were found were exempted from this effort. Table 46 lists the dependent performance parameters and the independent fuel properties used in the multiple-variable linear regression analysis. Independent variables were selected as those showing greatest relative strength from the single-variable regression analysis results.

TABLE 45
INDEPENDENT VARIABLE (FUEL PROPERTIES) GROUPINGS

I. Group I

Hydrogen content
Aromatic content - total
 - single ring*
 - multi-ring*
Smoke point

II. Group II

10% boiling point distillation temperature
End point distillation temperature
Viscosity
Vapor pressure
Surface tension
Breakpoint (JFTOT)

*Cannot be correlated to total aromatic content. May be used as separate independent variables.

Results from the multiple-variable regression analysis are summarized in Table 47 and the resulting correlations and equations are shown graphically in Figures 67 through 82. While some of the fuel property-to-performance correlations were strengthened with multiple independent-variable input, no significant improvement in correlations were noted. The multiple-variable regression analysis did not identify any new correlations between fuel properties and TF41 combustion system performance.

TABLE 46
PARAMETERS USED IN MULTIPLE-REGRESSION ANALYSIS

Dependent (performance) variable	Independent (fuel property) variables
Combustion efficiency - SLTO Idle	Smoke point, multi-ring aromatic content, Surface tension Single-ring aromatic content, surface tension
CO emissions - SLTO Idle	Smoke point, multi-ring aromatic content, vapor pressure, JFTOT Single-ring aromatic content, vapor pres- sure
UHC emissions - SLTO Idle	Smoke point, end point, JFTOT Single-ring aromatic content, surface tension, end point
NO _x emissions - SLTO	Smoke point, multi-ring aromatic content, surface tension, end point
Smoke Emissions - SLTO	Hydrogen content, multi-ring aromatic content, end point, JFTOT
Maximum liner wall temperature - SLTO	Hydrogen content, multi-ring aromatic content
Maximum barrel wall temperature - SLTO	Hydrogen content, multi-ring aromatic content, surface tension
Average barrel wall temperature - SLTO	Hydrogen content, multi-ring aromatic content, surface tension
Pattern factor - SLTO	Total aromatic content, end point, JFTOT
Ignition F/A ratio - Idle	Multi-ring aromatic content, end point
LBO F/A ratio - Idle	Total aromatic content, surface tension
Ignition F/A ratio - SL amb	Single ring aromatic content, 10% boiling point, viscosity
Maximum ignition altitude	Total aromatic content, surface tension

TABLE 47
MULTIPLE-VARIABLE LINEAR REGRESSION ANALYSIS SUMMARY

	Coefficient of determination, R^2	
	<u>Individual parameter</u>	<u>Cumulative multiple-variable</u>
<u>Idle combustion efficiency</u>		
Single-ring aromatics	0.304	0.304
Surface tension	0.248	<u>0.420</u>
<u>SLTO combustion efficiency</u>		
Smoke point	0.714	0.714
Surface tension	0.303	0.728
Multi-ring aromatics	0.169	<u>0.741</u>
<u>Idle CO emissions</u>		
Single-ring aromatics	0.074	0.074
Vapor pressure	0.082	<u>0.138</u>
<u>SLTO CO emissions</u>		
Smoke point	0.680	0.680
Multi-ring aromatics	0.216	0.701
Vapor pressure	0.235	0.710
JFTOT	0.227	<u>0.771</u>
<u>Idle UHC emissions</u>		
Single-ring aromatics	0.348	0.348
End point	0.179	0.448
Surface tension	0.201	<u>0.559</u>
<u>SLTO UHC emissions</u>		
Smoke point	0.384	0.384
JFTOT	0.371	0.516
End point	0.102	<u>0.667</u>

TABLE 47 (CONT)

	Coefficient of determination, R^2	
	<u>Individual parameter</u>	<u>Cumulative multiple-variable</u>
<u>SLTO NO_x emissions</u>		
Surface tension	0.405	0.405
End point	0.247	0.603
Smoke point	0.393	0.711
Multi-ring aromatics	0.130	<u>0.742</u>
<u>SLTO smoke emissions</u>		
Hydrogen content	0.490	0.490
End point	0.148	0.693
Multi-ring aromatics	0.149	0.694
JFTOT	0.232	<u>0.694</u>
<u>SLTO maximum liner wall temperature</u>		
Hydrogen content	0.498	0.498
Multi-ring aromatics	0.197	<u>0.514</u>
<u>SLTO maximum barrel wall temperature</u>		
Multi-ring aromatics	0.514	0.514
Surface tension	0.295	0.657
Hydrogen content	0.400	<u>0.664</u>
<u>SLTO average barrel wall temperature</u>		
Hydrogen content	0.377	0.377
Multi-ring aromatics	0.412	0.492
Surface tension	0.261	<u>0.576</u>

TABLE 47 (CONT)

	Coefficient of determination, R^2	
	<u>Individual parameter</u>	<u>Cumulative multiple-variable</u>
<u>SLTO pattern factor</u>		
Total aromatics	0.259	0.259
End point	0.284	0.343
JFTOT	0.201	<u>0.364</u>
<u>Idle ignition F/A ratio</u>		
End point	0.269	0.269
Multi-ring aromatics	0.194	<u>0.482</u>
<u>Idle LBO F/A ratio</u>		
Total aromatics	0.345	0.345
Surface tension	0.293	<u>0.408</u>
<u>SL Ambient ignition F/A ratio</u>		
Viscosity	0.494	0.494
Single-ring aromatics	0.186	0.558
10% Boiling point	0.375	<u>0.580</u>
<u>Maximum ignition altitude</u>		
Total aromatics	0.657	0.657
Surface tension	0.058	<u>0.675</u>

E. LIFE ANALYSIS RESULTS

Projected life calculations were computed for the combustor and for both the first-stage, high-pressure turbine vanes and blades. Data from combustor wall temperatures and exit temperatures were incorporated into the analyses. Details of the life analysis procedure used are found in References 9, 10, and 11.

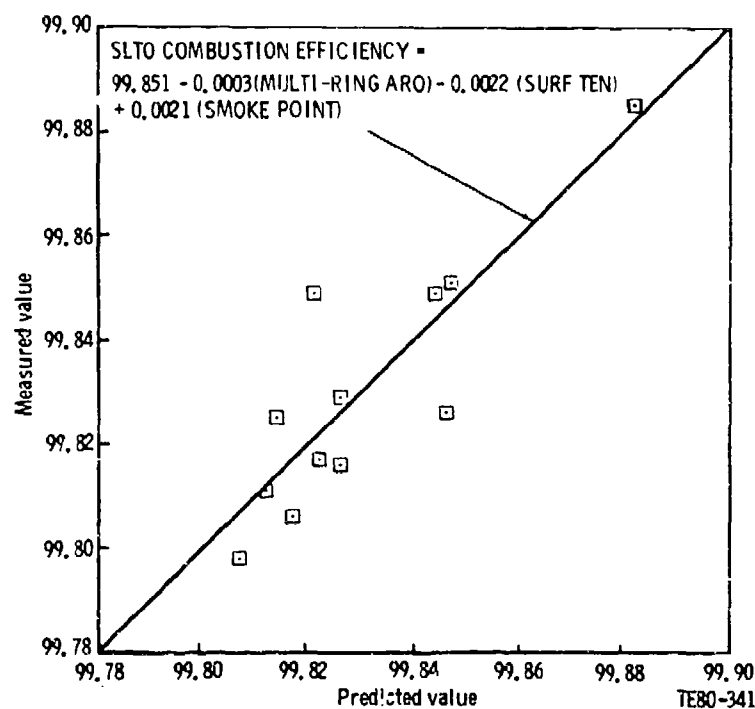


Figure 67. - Multiple Fuel Property Effect on SLTO Combustion Efficiency.

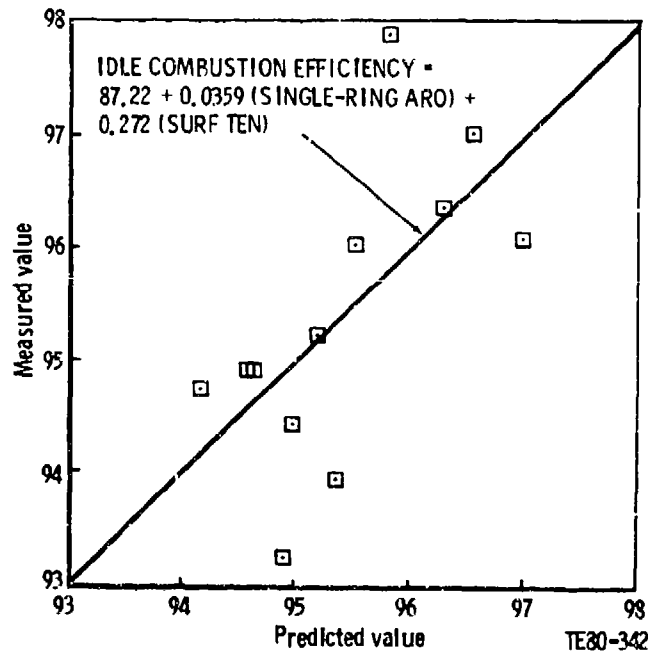


Figure 68. - Multiple Fuel Property Effect on Idle Combustion Efficiency.

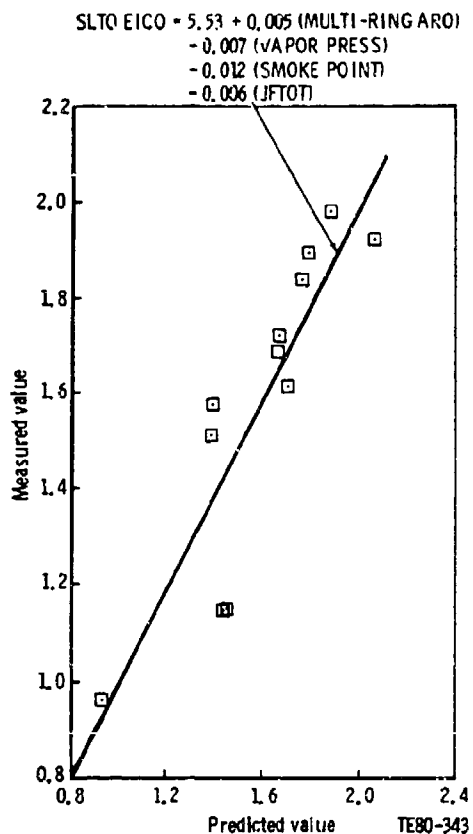
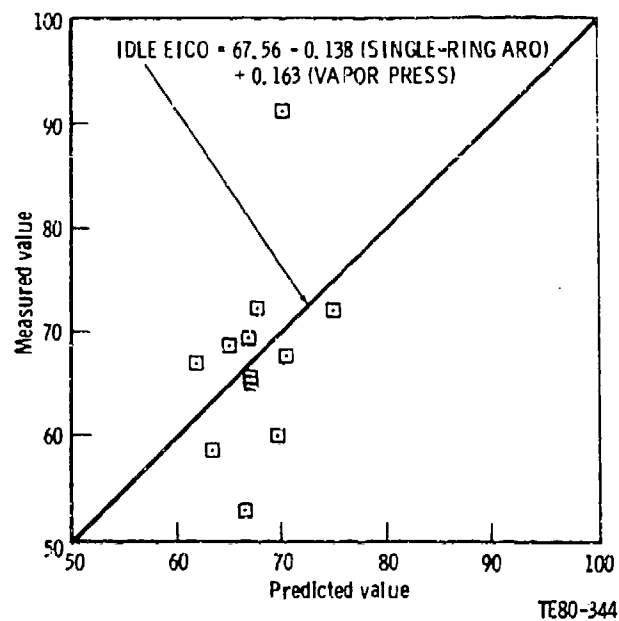


Figure 69. - Multiple Fuel Property
Effect on SLTO CO Emissions.

Figure 70. - Multiple Fuel Property
Effect on Idle CO Emissions.



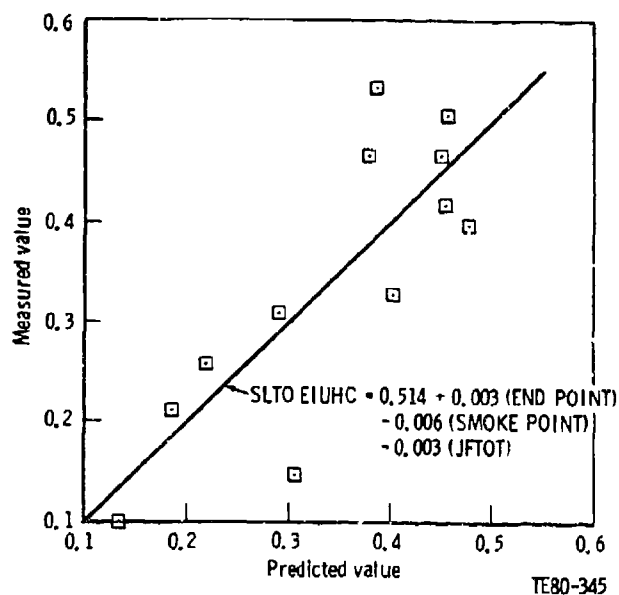


Figure 71. - Multiple Fuel Property Effect on SLTO UHC Emissions.

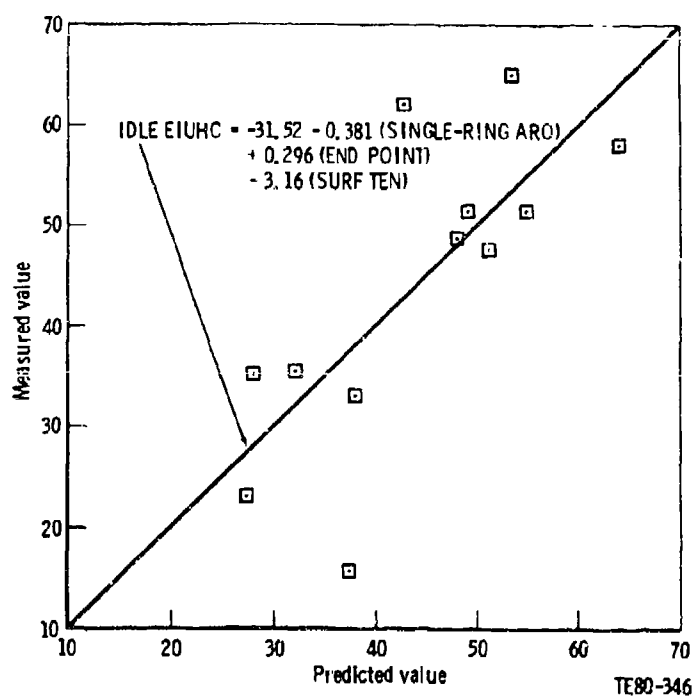


Figure 72. - Multiple Fuel Property Effect on Idle UHC Emissions.

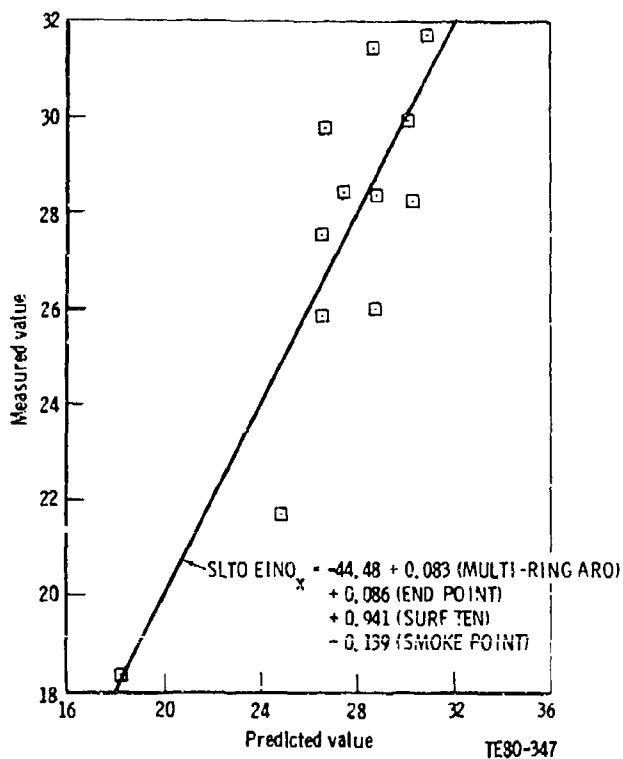


Figure 73. - Multiple Fuel Property
Effect on SLTO NO_x Emissions.

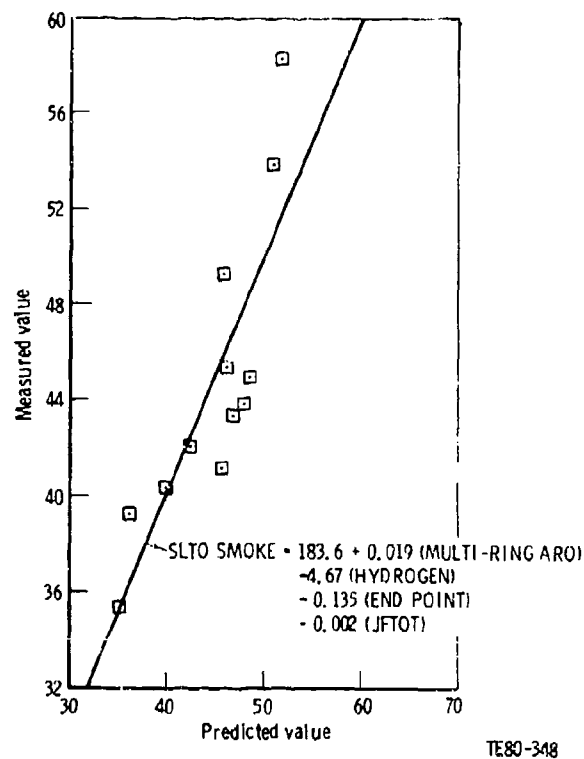


Figure 74. - Multiple Fuel Property
Effect on SLTO Smoke Emissions.

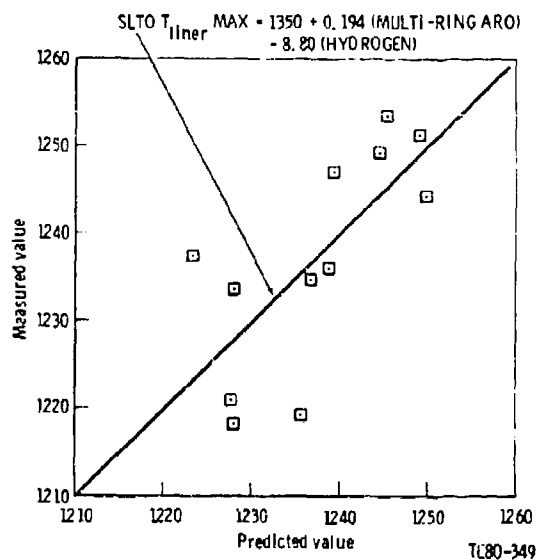


Figure 75. - Multiple Fuel Property Effect on SLTO Maximum Liner Wall
Temperatures.

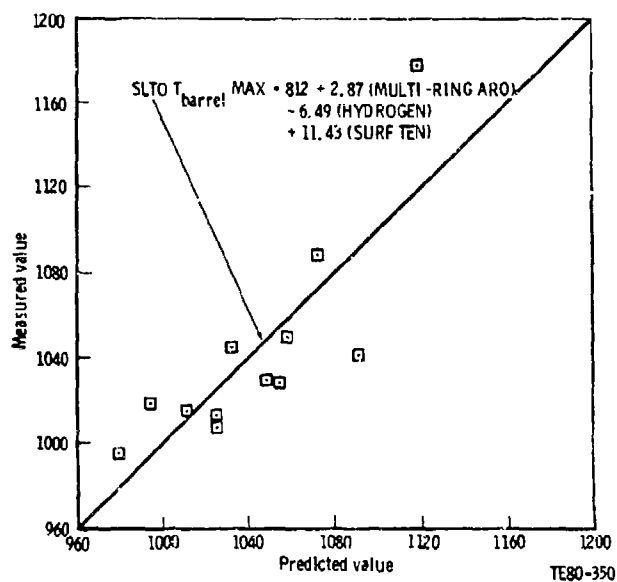
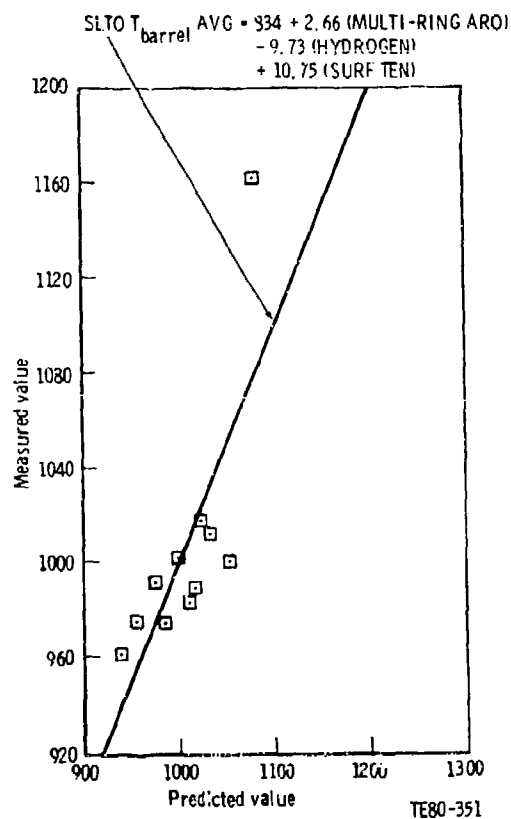


Figure 76. - Multiple Fuel Property Effect on SLTO Maximum Barrel Wall Temperatures.

Figure 77. - Multiple Fuel Property Effect on SLTO Average Barrel Wall Temperatures.



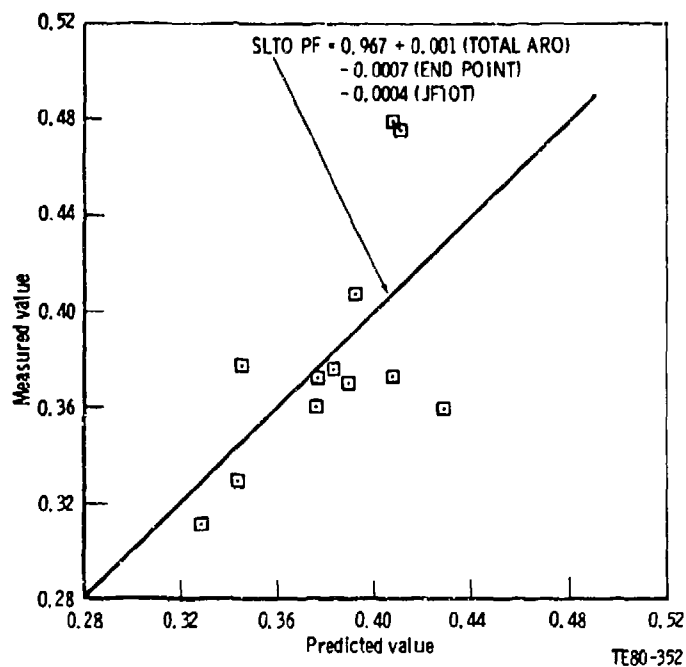


Figure 78. - Multiple Fuel Property Effect on SLTO Pattern Factor Levels.

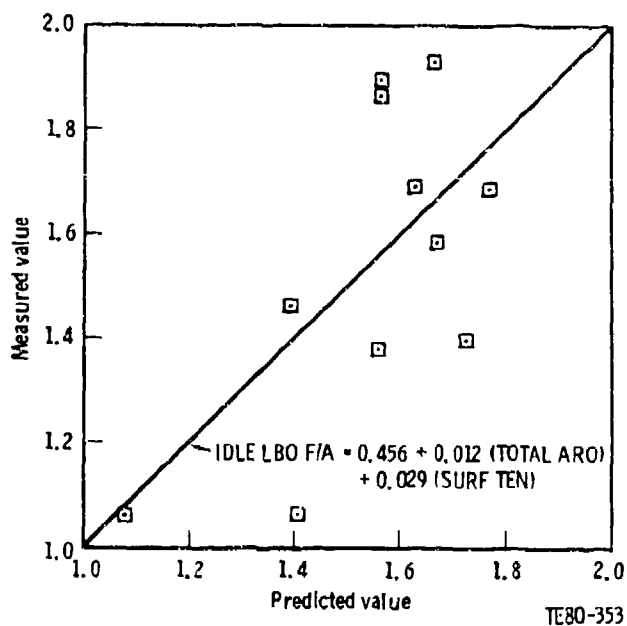


Figure 79. - Multiple Fuel Property Effect on Idle LBO F/A Ratio.

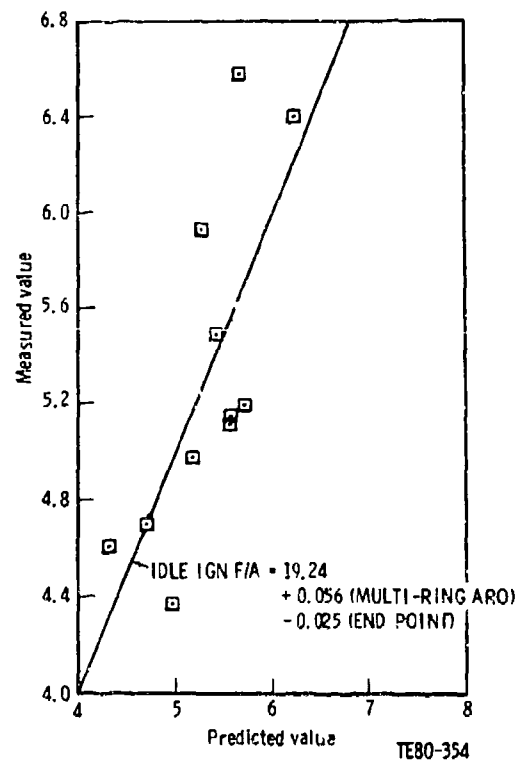


Figure 80. - Multiple Fuel Property Effect on Idle Ignition F/A Ratio.

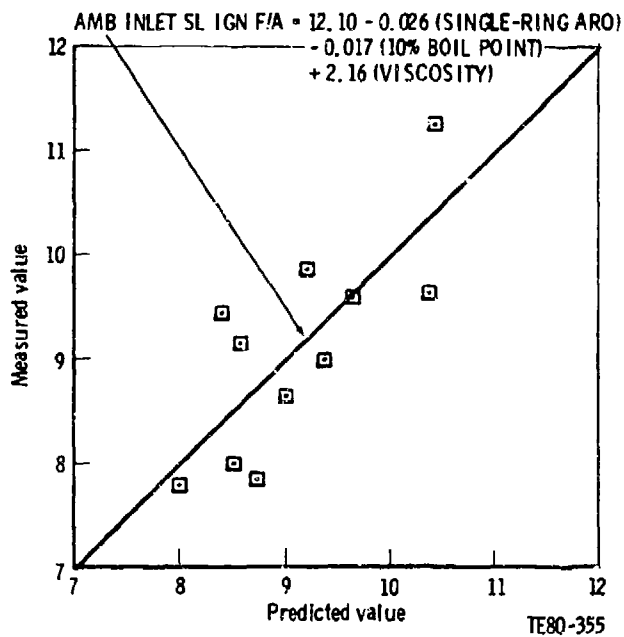
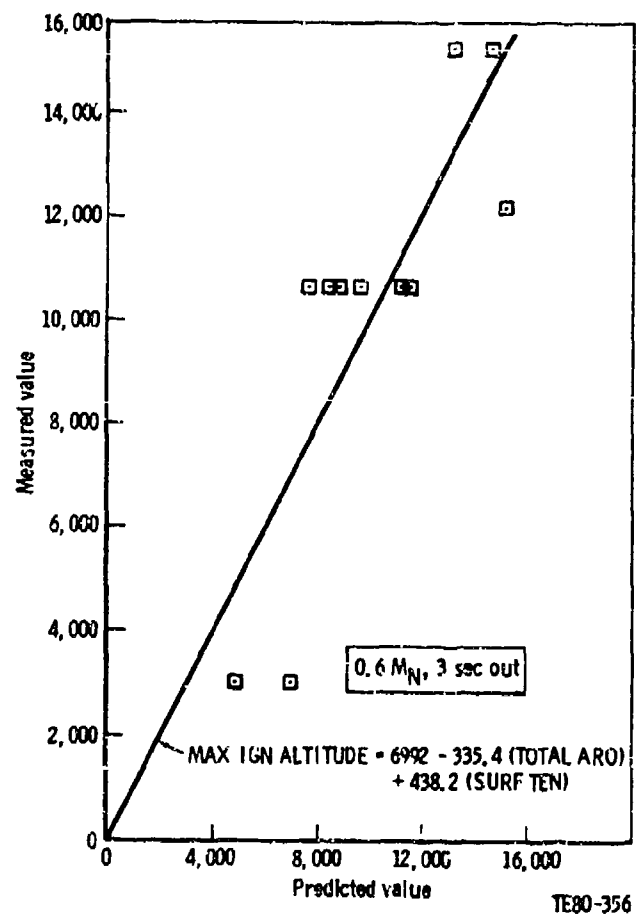


Figure 81. - Multiple Fuel Property
 Effect on SL Ambient Inlet Ignition
 F/A Ratio.

Figure 82. - Multiple Fuel Property
 Effect on Maximum Ignition Altitude.



The possible modes of failure in a combustor are:

- o Low cycle fatigue (LCF)
- o Oxidation/corrosion
- o Stress rupture
- o Buckling

The maximum combustor metal temperatures are not in the high oxidation-rate range. Stress rupture failure resulting from thermal stresses is not probable since, as the metal creeps, the stresses are relieved and redistributed. Buckling can be ruled out as a failure mode since the differential pressure is low and does not change with fuel type. A higher metal temperature decreases the buckling margin by weakening the wall material, but since the margin is high and the wall temperature change small, it was decided to base the life evaluation on LCF alone.

Experience with the TF41 engine has shown the mode of failure in the HP-1 vane to be oxidation. The peak metal temperature for each fuel was determined by heat transfer analysis, and the oxidation penetration rate was determined from available experimental data.

Experience has established the failure mode of the HPT-1 blade to be stress rupture. A study of temperature versus radial position on the blade and of average blade stress versus radial position indicated that the mean section was the most critical section.

1. Combustor Life Analysis

Metal temperatures were supplied from heat transfer analysis and from test thermocouple data. Since both the measured peak temperatures and the thermal gradients were larger in the transition section and since past durability history on this engine has shown the transition section to be the life limiting section, it was used to evaluate the effect of the various fuels on combustor life. The stress analysis was accomplished with the use of a finite-element computer program (see Appendix D). Because of the complexity of the mathematical model, the cost of analyzing each of the 12 fuels would have been

prohibitive. Eleven of the fuels produced wall temperatures in the transition section of the combustor that fell within a narrow band for both peak temperature and axial gradient. The remaining fuel (Fuel 8) had significantly higher temperatures but lower axial gradients across the cooling hole sections.

It was decided that a satisfactory evaluation could be made by analyzing the JP-4 baseline fuel (Fuel 1), and those producing the maximum and minimum thermal gradients, Fuels 10 and 7, respectively. Fuel 8, which generated substantially higher wall temperatures, was also evaluated.

The combustor LCF cyclic lives for the four fuels considered are shown in Table 48. Only the relative lives shown in the last column should be considered valid, because only high cycle fatigue, load-controlled data was available for the materials and the plastic line, and consequently the low life end of the LCF curve was of necessity based on a theoretical assumption. Since Fuels 7 and 10 represent the extremes of the 11 fuels that were closely grouped with regard to combustor wall temperature, these 11 fuels have combustor lives between 10,000 and 12,000 cycles. Fuel 8, which had higher wall temperatures but lower gradients, has an estimated combustor life of 26,000 cycles.

Based on the assumptions previously stated in the results, the use of alternate fuels has little effect upon combustor life. Eleven of the fuels resulted in a combustor LCF life between 100 and 120% of the baseline. The other fuel resulted in a higher life, 260% of the baseline.

2. HPT-1 Vane Life Analysis

Figure 83 shows an axial cross section of the HP-1 vane and a radial section of the mean section at which the peak temperature occurs. Table 49 shows the peak vane metal temperature (leading edge), the oxidation penetration in 100 hr at that temperature and the relative penetration rate compared with the baseline fuel. The temperature differences are quite small, but because of the slope of the oxidation penetration curve in this temperature range the penetration rate varies considerably from 0.16 cm in 100 hr to 0.61 cm in 100 hr.

TABLE 48
COMPARISON OF COMBUSTOR LCF LIFE FOR FOUR REPRESENTATIVE TEST FUELS

Test fuel	Stress range, MPa		Temp, K	Cyclic life	Percent of Baseline
	Min	Max			
1 (JP-4)	0	651	1127	10^4	100
7 (JP-8)	0	582	1102	1.2×10^4	120
8	0	418	1152	2.6×10^4	260
10	0	658	1153	10^4	100

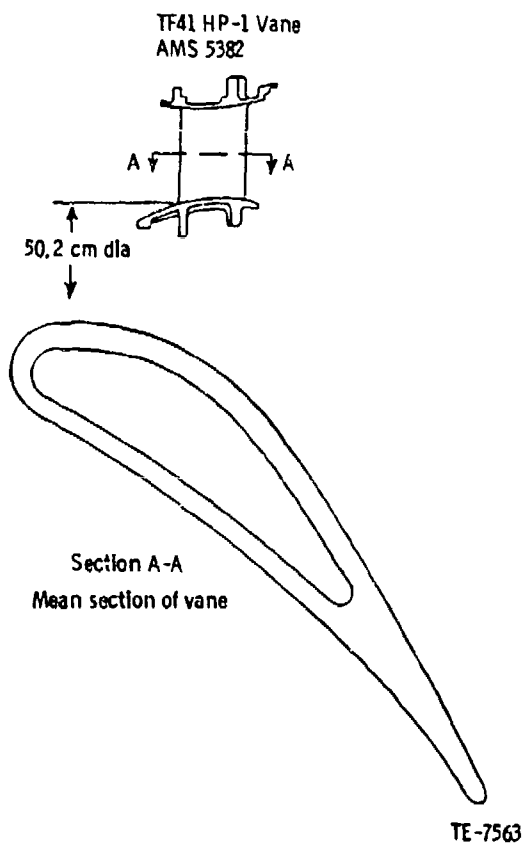


Figure 83. - Mean Section of HPT-1 Vane.

TABLE 49
COMPARISON OF OXIDATION PENETRATION ON TF41 HPT-1 VANE FOR THE 12 TEST FUELS

<u>Test</u> <u>fuel</u>	<u>Max metal</u> <u>temp (LE),</u> <u>K</u>	<u>Oxidation</u> <u>penetration</u> <u>in 100 hr,</u> <u>mm</u>	<u>Percent</u> <u>of baseline</u>
1 (baseline JP-4)	1412	2.59	100
2	1427	3.28	126
3	1409	2.41	93
4	1405	2.26	87
5	1428	3.33	128
6	1391	1.83	71
7 (JP-8)	1414	2.61	101
8	1410	2.43	94
9	1411	2.49	96
10	1459	6.09	235
11	1406	2.28	88
12	1382	1.60	62

Seven of the fuels resulted in HP-1 vane oxidation penetration rates lower than baseline, the lowest being 62% of baseline. Four of the fuels resulted in oxidation penetration rates higher than baseline. The highest was 235% of baseline.

Single-variable linear regression analysis results, which comprise Table 51, show no significant correlation between fuel properties and relative vane life. Subtle trends, however, may exist between relative vane life and hydrogen content, aromatic content and aromatic type. This would be expected since vane life is directly related to pattern factor, which also shows some correlations to these fuel properties.

3. HPT-1 Blade Life Analysis

A view of the HPT-1 blade and a radial section at the mean radius are shown in Figure 84. Table 50 lists the midspan blade temperature, typical stress rupture life, and relative life compared with the baseline, for each of the 12 fuels. The temperature variation is very small, from 6°C under the 1127 K baseline temperature to 12°C over the baseline. Because of the position on the stress rupture curve, however, the life ranges from 58% of baseline to 133% of baseline.

TABLE 50
VARIATION IN STRESS RUPTURE LIFE OF TF41 HPT-1 BLADE FOR THE 12 TEST FUELS

Test fuel	Midspan blade temp, <u>K</u>	-3 σ stress <u>rupture life, hr</u>	Percent <u>of baseline</u>
1 (Baseline JP-4)	1127	24000	100
2	1130	21000	83
3	1135	17000	71
4	1130	22000	92
5	1122	32000	133
6	1126	27000	113
7 (JP-8)	1127	25000	104
8	1132	20000	83
9	1139	14000	58
10	1123	30000	125
11	1124	28000	117
12	1127	24000	100

Six of the fuels resulted in HPT-1 blade stress rupture lives equal or higher than baseline. The highest was 133% of baseline. Five of the fuels resulted in a lower life, the lowest being 58% of baseline.

Single-variable linear regression analysis results, which comprise Table 51, show a statistical correlation between relative blade life and multi-ring aromatic content. The correlation plot shown in Figure 85, however, illustrates no conclusive relationship. Therefore it is felt that no correlation exists between fuel property and relative blade life for the TF41 combustion system.

TABLE 51
TURBINE LIFE REGRESSION ANALYSIS

Coefficient of determination for
relative life (JP-4 = 100%), R^2

<u>Fuel property</u>	<u>Vane</u>	<u>Blade</u>
Hydrogen content	0.196	0.049
Total aromatic content	0.287	--
Single-ring aromatic content	0.287	0.171
Multi-ring aromatic content	0.002	0.481
10% boiling point temperature	0.001	0.001
End point temperature	0.019	0.019
Viscosity	0.033	0.075
Surface tension	0.105	0.001
Vapor pressure	0.016	--
Smoke point	0.117	0.030
JFTOT	0.135	0.013

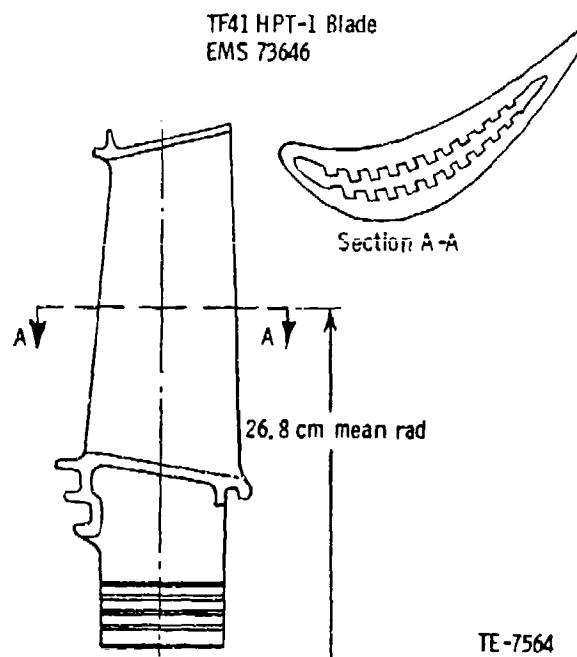


Figure 84. - Mean Section of HPT-1 Blade.

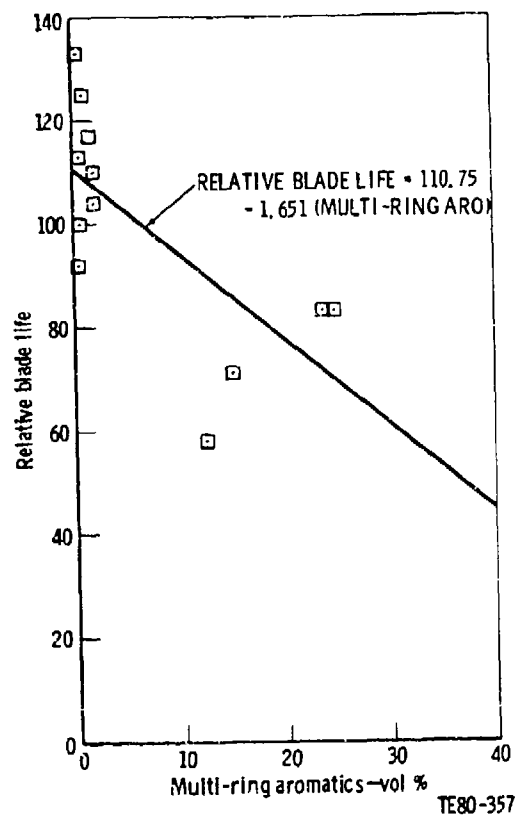


Figure 85. - Effect of Fuel Multi-Ring Aromatic Content on Relative HPT-1 Blade Life.

SECTION V
CONCLUSIONS AND RECOMMENDATIONS

Based on the TF41 combustion system experiments and analyses conducted in this program, the following conclusions and recommendations were offered:

A. CONCLUSIONS

1. Hydrogen content, total aromatic content, and multi-ring aromatic content strongly affect CO and smoke emissions, combustion efficiency, and liner wall temperatures at high power operation.
2. Fuel properties affecting atomization and vaporization such as surface tension and vapor pressure mildly influence NO_x formation but do not present strong correlation to any other performance parameter at high power. End point and surface tension properties affect sea-level ignition and LBO characteristics.
3. Statistical evidence indicates that the influence of multi-ring aromatic content on liner wall temperature is equal to, and sometimes greater than, the influence of hydrogen content.
4. None of the fuel property characteristics produced any measurable effect on combustor exit temperature distribution (pattern factor or radial profile), idle performance or emissions, or hot section hardware life.
5. Maximum achievable ignition altitude is most strongly influenced by total aromatic content and hydrogen content. Once ignition is achieved, combustor stability is controlled by 10% boiling point, viscosity, vapor pressure, and surface tension.

6. The fuel properties examined in this program can be classified into two groups. Elements of each group are properties that show a statistically significant relationship to other members of the group. In the multiple-variable regression analyses, these groups were useful in determining which fuel properties could be used in a single analysis. In general, two members of the same group could not be used in a single correlation.
7. The multiple-variable regression analyses did not accomplish any significant improvement in the correlations established in the single-variable analyses.

B. RECOMMENDATIONS

1. TF41-A-2 engine tests with selected fuels are recommended to verify trends and results obtained in this series of single-combustor rig tests.
2. Alternate fuel thermal stability (fouling/deposition) characteristics on long-term rig or engine testing is recommended.
3. A similar fuel character effects program is recommended for the TF41 Lamilloy®* combustion system.

*Lamilloy is a registered trademark of the General Motors Corporation.

REFERENCES

1. C. C. Gleason, T. L. Oller, M. W. Shayeson, and D. W. Bahr, Evaluation of Fuel Character Effects on J79 Engine Combustion System, final report for contract F33615-77-C-2042, June 1979.
2. C. C. Gleason, T. L. Oller, M. W. Shayeson, and D. W. Bahr, Evaluation of Fuel Character Effects on F101 Engine Combustion System, final report for contract F33615-77-C-2043, June 1979.
3. R. E. Vogel, DDA TF41 Combustion Rig Production Liner Baseline Testing, DDA TOR AF0320-044, November 1977.
4. W. F. Taylor and J. W. Frankenfeld, Development of High Stability Fuel, final report for Phase I, Contract No. N00140, 74-C-0618, NAPC, January 1975.
5. J. C. Presley, TF41/A7E Shipboard (and Shorebased) Mission Profile Data, Naval Air Systems Command, Memorandum AIR-53612B:COM, Ser. 8282, August 1978.
6. R. Roberts, A. Peduzzi, and G. Vitti, Experimental Clean Combustor Program, final report for Phase II, NASA CR-134969.
7. V. J. Sarli, D. C. Elier, and R. L. Marshall, Effects of Operating Variables on Gaseous Emissions, Air Pollution Control Association Conference, New Orleans, Louisiana, October 1975.
8. A. H. Lefebvre, Theoretical Aspects of Gas Turbine Combustion Performance, The College of Aeronautics, Cranfield, Co. A, Note Aero No. 163, August 1966.
9. W. S. Blazowski and T. A. Jackson, Evaluation of Future Jet Fuel Combustion Characteristics, AFAPL-TR-77-93, July 1978.

10. A. J. Verdouw, TF41 Combustor Wall Temperatures and Exit Temperature Patterns for 12 Experimental Fuels (Input for Life Studies), DDA EDR 9793B, February 1979.
11. T. G. Daehler, TF41 Combustor and Turbine Metal Temperature Trends for Alternate Fuels Study, DDA AX.0301-26, May 1979.
12. R. F. Pecca, Investigation of the Effect on the Life of the Combustion and Turbine Section Components of the TF41 Engine Resulting from the Use of Alternate Fuels, DDA AX.0301-027, May 1979.

APPENDIX A
GENERAL DATA SUMMARY

The following experimental data was obtained:

Performance

Idle

Altitude cruise

Sea-level dash

Sea-level takeoff

Flame stability

Fouling

Carboning

Sea-level starts

Ambient

Cold day

Altitude ignition

3.0 km

10.6 km

12.2 km

15.2 km

The thermocouple locations are illustrated in Figure A-1.

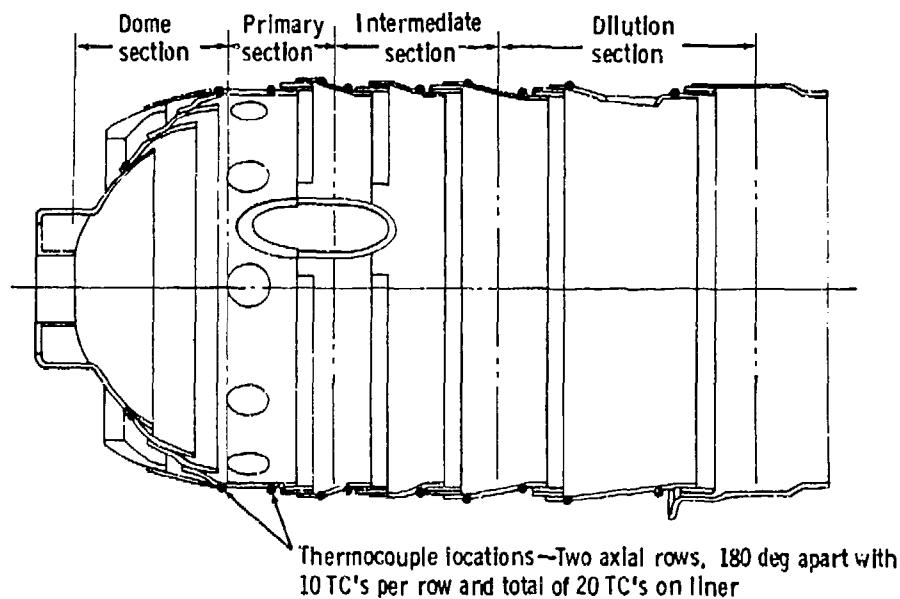
PERFORMANCE DATA SUMMARY

The performance data at idle, altitude cruise, sea level dash, and sea level takeoff are summarized in Tables A-1, -2, -3, and -4, respectively.

The following fuel schedule was employed in these performance tests:

- o 100% pilot fuel to 4.4 MPa pilot (approx 18.19 kg/hr)
- o Additional fuel is all main

The gas analysis results employed standard practice ARP 1256 and 1179. The NO_x EI is the sum of the measured NO and the measured NO_2 , the reported



TE-7127

Figure A-1. - TF41 Combustor Liner Thermocouple Locations.

combustion efficiency is the actual enthalpy increase resulting from combustion divided by the ideal enthalpy increase, assuming only CO_2 and H_2O combustion products. The gas analysis provided the enthalpy loss from combustion inefficiency from the measured CO , HC , NO , and NO_2 . The following expressions were used:

<u>Reactants</u>		<u>Products</u>	<u>JP-4 heating value (MJ/kg) at 25°C</u>
$\text{CO} + 1/2 \text{O}_2$	→	CO_2	-10.1
$\text{CH} + (1 + a/4) \text{O}_2$	→	$\text{CO}_2 + a/2 \text{H}_2\text{O}$	-42.0 to 43.5
$1/2 \text{N}_2 + 1/2 \text{O}_2$	→	NO	+3.0
$1/2 \text{N}_2 + \text{O}_2$	→	NO_2	+0.74

The gas analysis sample integrity was determined from a comparison of the combustor exhaust F/A ratio from the air and fuel flowmeters with the exhaust F/A ratio as determined from gas analysis. Tables A-1 through -4 compare "gas analysis" and "meter" combustor exhaust F/A ratios. JP-4 was tested first.

TABLE A-1
IDLE CONDITION PERFORMANCE DATA

Fuel No.	0	1	2	3	4	5	6	7	8	9	10	11	12
Base fuel	Facility	JP-4	JP-4	JP-4	JP-4	JP-4	JP-4	JP-8	JP-8	JP-8	JP-8	JP-8	JP-8
Additive fuel	JP-4	Special	+AR	+AR	+X	+X	+X+GM		+AR	+AR	+X	+X	+GM
Measured wt % H	14.5	14.4	12.0	12.9	11.9	13.0	13.9	13.9	11.9	12.9	12.0	12.9	13.9
Set point													
W_c , kg/sec	0.985	0.973	0.971	0.952	0.934	0.994	0.961	0.958	0.939	0.981	0.966	0.941	0.954
BIP, kPa	298.7	292.6	291.2	286.4	291.6	284.4	290.4	296.3	289.6	286.7	290.9	296.9	293.5
BIT, K	443.4	416.0	408.9	426.5	445.6	428.5	437.3	425.4	436.0	437.5	431.6	415.5	430.8
Fuel/air, g/kg	13.91	14.13	14.15	14.83	15.45	14.19	13.75	13.99	15.00	14.54	14.39	14.59	14.39
Gas analysis (corrected)*													
Comb eff, %	95.28	94.75	93.26	94.92	97.03	96.04	94.91	94.44	97.91	93.95	96.09	96.37	95.23
EICC, g/kg	64.50	72.13	91.18	67.77	58.73	65.10	60.12	69.42	52.92	65.66	67.04	68.76	72.32
EHC, g/kg	36.94	48.73	64.95	47.61	23.16	33.15	57.95	51.38	15.72	61.97	35.28	35.57	51.40
$EINO_x$, g/kg	1.92	5.26	3.80	1.30	2.71	2.49	2.53	2.27	3.15	1.87	2.83	2.98	3.09
SAE smoke number	16.2	17.5	59.9	36.8	45.1	36.2	15.0	29.7	41.2	34.6	53.5	27.9	26.3
Wall temperature, K													
Total avg	428.5	508.4	533.1	543.1	577.5	534.5	550.0	516.6	590.3	543.7	554.5	528.2	534.7
Total max	791.4	712.1	773.0	758.5	820.4	733.5	794.9	770.1	815.9	776.9	745.8	741.9	799.6
Dome avg	293.0	452.3	462.4	472.7	502.2	455.6	475.8	451.0	474.1	477.9	481.3	471.1	471.4
Dome max	306.3	477.1	497.5	506.3	526.6	478.9	489.6	461.2	495.1	504.0	489.6	508.3	478.9
PZ avg	298.7	446.1	466.8	475.1	491.9	459.3	458.0	451.4	475.8	470.6	468.7	452.7	466.9
PZ max	305.0	451.8	490.2	491.3	518.0	473.4	485.6	457.9	511.5	489.5	480.1	470.4	476.1
IZ avg	293.3	464.4	492.2	491.3	518.2	479.5	484.1	472.7	564.8	491.8	493.5	468.3	484.3
IZ max	301.2	475.9	508.3	504.8	537.6	492.5	496.2	483.9	644.0	503.1	512.5	480.5	497.3
DZ avg	394.5	467.1	487.3	490.1	519.0	480.9	487.0	476.7	547.1	493.8	497.7	467.9	484.6
DZ max	503.8	486.2	493.9	501.6	536.8	490.7	498.0	489.9	603.6	503.4	511.0	479.0	498.9
Trans avg	640.2	601.8	634.0	653.3	704.5	646.8	686.2	614.3	724.6	647.2	672.6	644.6	639.7
Trans max	791.4	712.1	773.0	758.5	820.4	733.5	794.9	770.1	815.9	776.9	745.8	741.9	799.6
Exit temperatures													
Ideal avg, K	982.6	965.4	945.7	990.7	1023.1	970.6	968.9	964.2	994.7	988.8	973.8	971.6	984.1
Mean avg, K	1002.1	955.5	930.3	985.3	1029.3	958.8	1002.5	856.6	1024.8	1003.2	985.1	991.6	952.1
Mean max, K	1323.4	1201.8	1252.4	1158.0	1221.6	1106.1	1224.3	1252.2	1191.0	1185.4	1149.5	1235.0	1295.9
Stat max, K	1300.8	1306.7	1230.4	1236.5	1302.1	1194.4	1252.5	1472.0	1270.0	1250.7	1195.6	1309.1	1400.5
Total PF	0.6306	0.4253	0.5253	0.2735	0.3077	0.2284	0.4718	0.5174	0.3067	0.3288	0.2862	0.4440	0.5491
PF (90% span)	0.0236	-0.0725	0.0012	-0.1008	-0.1566	-0.1214	-0.1364	0.2505	-0.1159	-0.0990	-0.0708	-0.1878	0.1271
PF (70% span)	0.0394	0.0538	0.0280	0.0064	-0.0552	-0.0036	-0.0525	0.3084	-0.0339	0.0117	0.0199	-0.0311	0.1611
PF (50% span)	0.0820	0.1670	0.0733	0.1299	0.0650	0.1075	0.0757	0.3175	0.0804	0.1273	0.0882	0.1163	0.1540
PF (30% span)	0.0653	0.1722	0.0802	0.1319	0.1975	0.1618	0.1877	0.1916	0.1730	0.1275	0.1037	0.1856	0.1015
PF (10% span)	-0.2105	-0.3205	-0.1832	-0.1682	-0.0709	-0.1448	-0.0741	-1.0684	-0.1036	-0.1674	-0.1404	-0.0830	-0.5445
Fuel/air ratios, g/kg													
Chemical		16.15	16.28	16.73	17.70	15.82	17.58	15.44	18.93	16.64	17.08	19.01	18.79
Mechanical		14.13	14.15	14.83	15.45	14.19	13.75	13.99	15.00	14.54	14.39	14.59	14.39
% difference		14.3	15.1	12.8	14.6	11.5	27.9	10.4	26.2	14.5	18.7	30.3	30.6

*CO, UHC, and NO_x values are corrected per the technique described in Section IV-A.

TABLE A-2
CRUISE CONDITION PERFORMANCE DATA

Fuel No.	0	1	2	3	4	5	6	7	8	9	10	11	12
Base fuel	Facility	JP-4	JP-4	JP-4	JP-4	JP-4	JP-4	JP-8	JP-8	JP-8	JP-8	JP-8	JP-8
Additive fuel	JP-4	Special	+AR	+AR	+X	+X	+X+GM		+AR	+AR	+X	+X	+GM
Measured wt % H	14.5	14.4	12.0	12.9	11.9	13.0	13.9	13.9	11.9	12.9	12.0	12.9	13.9
Set point													
W _c , kg/sec	1.565	1.580	1.523	1.635	1.583	1.594	1.545	1.562	1.583	1.533	1.572	1.587	1.581
BIP, MPa	513.6	512.9	501.0	514.9	505.9	509.9	519.8	529.7	509.2	514.2	522.8	524.1	513.7
BIP, K	563.9	575.1	584.9	604.2	577.3	578.5	582.3	578.2	569.8	577.1	582.8	569.9	574.9
Fuel/air, g/kg	15.27	15.15	15.96	15.11	15.35	15.25	15.55	15.11	15.75	15.33	15.68	15.42	14.73
Gas analysis (corrected)													
Comb eff, %	98.95	98.95	98.70	98.65	99.01	99.06	99.21	99.08	99.14	98.77	99.03	99.43	99.33
RICO, g/kg	25.20	27.42	27.92	20.63	28.14	23.12	17.11	23.99	25.58	25.72	22.97	16.52	18.77
RIBC, g/kg	4.61	5.52	8.29	11.34	4.75	5.36	5.15	4.61	3.73	8.15	6.02	2.80	4.28
EDNO ₂ , g/kg	6.32	5.74	6.53	6.00	7.24	6.58	6.49	6.31	7.59	5.4 ^c	6.80	7.71	7.53
SAR smoke number	29.4	28.9	36.0	28.9	29.6	39.0	12.0	26.9	31.1	34.9	48.0	18.9	25.7
Wall temperature, K													
Total avg	494.6	686.0	749.6	748.0	725.0	714.0	715.8	688.6	742.3	710.6	739.0	711.3	712.5
Total max	894.5	899.4	939.9	943.9	929.0	890.7	946.5	939.1	1145.4	956.5	940.6	909.6	895.6
Dome avg	309.0	627.4	667.6	658.6	627.9	631.6	614.8	623.6	637.7	627.7	643.9	609.4	631.8
Dome max	349.4	645.9	718.4	677.3	645.4	652.4	629.4	636.1	664.1	639.2	662.5	624.4	639.1
PZ avg	297.8	643.8	706.6	699.2	676.6	653.7	670.5	640.2	683.4	674.5	667.1	664.2	641.9
PZ max	358.5	663.9	732.8	709.2	703.1	673.3	718.8	654.1	782.4	705.8	694.0	715.6	662.0
IZ avg	293.3	658.7	724.4	716.0	699.7	680.4	669.4	661.6	713.0	695.4	710.4	667.9	670.2
IZ max	301.3	676.7	760.7	752.6	727.6	711.0	683.7	678.5	756.3	719.5	757.5	693.7	693.7
DZ avg	485.1	648.1	692.9	696.4	675.8	665.1	659.1	651.0	672.4	674.4	697.2	651.5	662.5
DZ max	686.3	660.0	716.6	720.4	694.1	686.9	679.6	661.6	702.3	689.5	723.9	669.2	682.1
Trans avg	782.6	759.1	837.1	843.5	815.3	807.6	819.0	767.1	854.0	778.0	834.5	815.7	820.1
Trans max	994.5	899.4	939.9	943.9	929.0	890.7	946.5	939.1	1145.4	956.5	940.6	909.6	895.6
Exit temperatures													
Ideal avg, K	1133.3	1138.5	1158.4	1153.2	1132.9	1136.1	1155.8	1134.4	1136.6	1142.5	1146.9	1132.6	1119.9
Mean avg, K	1141.1	1063.4	1246.1	1137.4	1130.2	1106.7	1157.0	1038.3	1134.7	1128.3	1157.6	1129.8	1124.8
Mean max, K	1313.3	1311.4	1330.4	1299.9	1306.0	1336.1	1324.4	1310.3	1281.1	1343.0	1330.4	1287.1	1319.5
Stat max, K	1342.8	1641.9	1378.0	1329.8	1340.0	1422.1	1351.5	1528.2	1213.3	1334.2	1369.5	1333.8	1358.6
Total FF	0.3143	0.3050	0.2630	0.2450	0.2766	0.3355	0.2862	0.3011	0.2148	0.3276	0.2875	0.2486	0.3536
FF (90% span)	-0.0246	0.1786	-0.0494	-0.0092	0.0101	-0.0740	-0.0063	0.2271	0.0140	0.0635	-0.0477	-0.0336	-0.0935
FF (70% span)	0.0125	0.2290	0.0235	0.0506	0.0436	0.0312	0.0418	0.2782	0.0351	0.0840	0.0360	0.0361	0.0184
FF (50% span)	0.0962	0.2591	0.0887	0.1080	0.0763	0.1170	0.0786	0.2506	0.0713	0.0784	0.0945	0.0823	0.0971
FF (30% span)	0.0927	0.2116	0.0952	0.0745	0.0832	0.1255	0.0693	0.1482	0.0685	0.0051	0.0807	0.0777	0.1131
FF (10% span)	-0.1769	-0.8788	-0.1577	-0.2239	-0.2132	-0.1994	-0.1831	-0.9246	-0.1889	-0.2306	-0.1635	-0.1629	-0.1353
Fuel/air ratios, g/kg													
Chemical	16.62	17.27	16.75	17.27	16.92	17.30	16.32	17.72	16.91	17.72	18.12	18.67	
Mechanical	15.15	15.96	15.11	15.35	15.25	15.55	15.11	15.75	15.53	15.66	15.42	14.73	
% difference		9.7	8.2	10.9	12.5	10.9	11.2	8.0	12.5	8.9	13.2	17.5	26.7

^cCO, UHC, and NO_x values are corrected per the technique described in Section IV-A.

TABLE A-3
SL DASH CONDITION PERFORMANCE DATA

Fuel No.	0	1	2	3	4	5	6	7	8	9	10	11	12
Base fuel	Facility	JP-4	JP-4	JP-4	JP-4	JP-4	JP-4	JP-8	JP-8	JP-8	JP-8	JP-8	JP-8
Additive fuel	JP-4	Special	+AR	+AR	+X	+X	+X+CM		+AR	+AR	+X	+X	+CM
Measured wt X H	14.5	14.4	12.0	12.9	11.9	13.0	13.9	13.9	11.9	12.9	12.0	12.9	13.9
Set point													
W _c , kg/sec	5.139	5.125	5.001	5.089	5.133	5.109	5.122	5.104	5.147	5.118	5.128	5.070	5.081
HTP, mPa	1815.1	1819.5	1835.5	1821.3	1812.4	1847.0	1847.8	1832.2	1840.6	1828.9	1838.7	1849.6	1828.9
BIT, K	740.5	749.3	743.5	744.5	743.8	749.4	744.0	739.1	744.0	740.6	745.0	738.9	743.1
Fuel/air, g/kg	18.62	18.62	19.58	19.23	18.93	19.02	18.52	18.69	19.19	19.14	19.17	19.34	18.71
Gas analysis (corrected)													
Comb eff, %	99.80	99.87	99.80	99.65	99.80	99.83	99.85	99.85	99.77	99.82	99.80	99.83	99.84
EICO, g/kg	1.63	0.78	2.16	1.96	1.93	1.18	1.09	1.60	2.07	2.01	1.81	1.24	1.08
EHNC, g/kg	0.43	0.11	0.65	2.90	0.53	0.66	0.60	0.34	1.15	0.42	0.80	0.31	0.67
EMO _x , g/kg	25.99	23.69	26.83	23.96	28.99	20.73	26.38	22.71	27.31	24.20	26.72	29.20	24.51
SAE smoke number	36.6	35.6	42.8	47.4	48.2	36.2	35.5	42.3	36.8	49.1	45.2	46.3	32.5
Wall temperature, K													
Total avg	932.0	933.9	979.1	969.4	968.7	965.5	956.8	927.7	1116.0	939.6	978.9	963.0	957.7
Total max	1155.6	1175.3	1204.3	1184.0	1182.9	1166.4	1158.6	1165.8	1221.4	1163.9	1176.6	1181.4	1158.2
Dome avg	875.6	887.7	901.0	882.8	925.5	889.4	930.6	889.3	989.8	896.1	932.9	925.1	907.1
Dome max	955.1	988.4	980.4	966.0	982.6	961.9	1014.5	985.0	1156.8	1005.4	988.8	983.5	950.2
PZ avg	886.5	884.1	918.4	899.3	909.4	904.6	890.5	888.5	1086.9	887.5	912.8	900.2	891.2
PZ max	932.3	927.3	973.3	947.5	955.5	955.1	930.4	930.6	1148.9	936.0	962.0	945.0	931.8
IZ avg	929.8	933.0	974.0	954.4	963.5	952.0	937.7	935.0	1148.9	935.3	970.9	956.6	939.2
IZ max	963.0	970.4	1019.1	995.7	1009.1	995.5	985.2	965.3	1163.6	983.7	1020.4	992.3	983.1
DZ avg	904.1	902.1	934.9	927.5	920.0	922.5	902.6	895.0	1133.7	907.6	930.5	911.0	907.7
DZ max	938.0	934.1	970.1	970.7	949.3	961.6	935.5	914.6	1144.4	945.1	969.9	935.1	947.5
Trans avg	988.5	989.9	1059.5	1062.6	1039.4	1046.6	1035.5	971.0	1153.4	988.4	1049.2	1036.0	1042.0
Trans max	1155.6	1175.3	1204.3	1184.0	1182.9	1166.4	1158.6	1165.8	1221.4	1163.9	1176.6	1181.4	1158.2
Exit temperatures													
Ideal avg, K	1394.1	1401.2	1409.1	1406.2	1390.6	1404.2	1390.9	1388.5	1395.2	1398.5	1398.6	1403.2	1394.0
Mass avg, K	1381.0	1343.5	1402.8	1407.4	1409.6	1396.0	1411.1	1370.9	1404.3	1376.8	1412.3	1406.5	1407.9
Mass max, K	1596.4	1607.9	1633.4	1601.4	1612.5	1585.8	1591.6	1583.5	1613.9	1551.6	1607.0	1629.0	1574.4
Stat max, K	1645.2	1746.1	1670.3	1698.6	1633.1	1647.9	1623.2	1619.3	1640.6	1603.8	1636.1	1628.2	1607.3
Total PF	0.3080	0.3151	0.3005	0.2734	0.3087	0.2563	0.3027	0.2860	0.2946	0.2093	0.2836	0.3141	0.2637
PF (90% span)	0.0368	-0.0054	0.0117	0.0035	0.0029	-0.0278	-0.0211	0.0318	0.0147	0.0031	-0.0035	0.0081	-0.0331
PF (70% span)	0.0790	0.0503	0.0555	0.0611	0.0482	0.0377	0.0456	0.0810	0.0612	0.0728	0.0506	0.0554	0.0355
PF (50% span)	0.0999	0.0823	0.0940	0.1036	0.0840	0.0920	0.0776	0.0942	0.0925	0.1140	0.0821	0.0786	0.0815
PF (30% span)	0.0331	0.0645	0.0517	0.0413	0.0559	0.0724	0.0553	0.0521	0.0516	0.0280	0.0539	0.0436	0.0666
PF (10% span)	-0.2486	-0.1913	-0.2130	-0.2095	-0.1907	-0.1578	-0.1572	-0.2589	-0.2204	-0.2177	-0.1833	-0.1859	-0.1509
Fuel/air ratios, g/kg													
Chemical		19.92	22.78	22.53	21.57	20.27	24.31	21.17	22.57	20.71	22.81	22.22	22.41
Mechanical		18.62	19.58	19.23	18.93	19.02	18.52	18.69	19.19	19.14	19.17	19.34	18.71
X difference		7.0	16.4	17.1	14.0	6.6	31.3	13.2	17.6	8.2	19.0	14.9	15.8

*CO, UHC, and NO_x values are corrected per the technique described in Section IV-A.

TABLE A-4
SLTO CONDITION PERFORMANCE DATA

Fuel No.	0	1	2	3	4	5	6	7	8	9	10	11	12
Base fuel	Facility	JP-4	JP-4	JP-4	JP-4	JP-4	JP-4	JP-8	JP-8	JP-8	JP-8	JP-8	JP-8
Additive fuel	JP-4	Special	+AR	+AR	+X	+X	+X+GM		+AR	+AR	+X	+X	+GM
Measured wt X B	14.5	14.4	12.0	12.9	11.9	13.0	13.9	13.9	11.9	12.9	12.0	12.9	13.9
Set point													
W _c , kg/sec	5.002	4.977	5.064	4.950	5.020	4.988	4.991	5.033	5.049	4.941	5.001	4.983	4.953
P _{IP} , MPa	1817.5	1843.0	1845.1	1838.9	1860.1	1839.4	1871.5	1859.6	1847.0	1839.6	1860.8	1823.6	1857.7
P _{IT} , K	761.3	759.0	756.3	759.4	761.4	756.3	760.3	758.4	760.0	766.8	762.4	756.8	762.3
Fuel/air, g/kg	21.19	21.24	21.66	21.94	21.60	21.49	21.18	21.41	21.81	21.93	22.23	21.67	21.16
Gas analysis (corrected)													
Comb eff, %	99.82	99.88	99.81	99.82	99.81	99.83	99.85	99.85	99.80	99.85	99.82	99.82	99.83
CO, g/kg	0.68	0.96	1.89	1.72	1.84	1.68	1.15	1.57	1.92	1.61	1.98	1.15	1.51
UHC, g/kg	0.27	0.10	0.40	0.53	0.33	0.47	0.46	0.21	0.50	0.15	0.42	0.26	0.31
NO _x , g/kg	28.23	18.42	30.02	27.63	29.87	21.78	28.53	25.92	31.81	26.07	28.34	31.55	28.46
SAE smoke number	43.4	42.1	43.9	45.4	58.3	43.4	35.4	40.4	53.9	49.3	45.0	41.2	39.3
Wall temperature, K													
Total avg	971.9	964.3	1007.8	1005.1	1012.9	994.8	995.6	967.6	1146.2	992.2	1022.3	1000.0	997.5
Total max	1221.0	1237.5	1251.3	1247.1	1253.5	1219.3	1221.0	1233.7	1244.3	1236.1	1249.3	1234.8	1218.3
Dome avg	899.8	892.7	908.7	897.8	947.2	895.8	937.5	907.5	1000.0	923.6	941.0	942.2	928.4
Dome max	985.4	946.8	978.3	979.0	1007.1	956.8	1012.0	1005.1	1160.0	1034.8	983.0	1000.5	974.8
PZ avg	912.7	897.4	932.0	917.3	931.0	915.0	912.7	911.4	1136.6	954.4	933.9	921.4	915.0
PZ max	963.0	947.0	989.9	969.7	985.0	968.1	961.4	958.7	1157.5	1088.8	988.0	970.4	961.5
IZ avg	967.5	960.9	998.1	982.5	1007.8	976.8	979.7	972.2	1161.3	981.5	1010.2	994.9	978.6
IZ max	1001.7	995.5	1041.7	1030.0	1045.4	1015.6	1019.0	1007.6	1177.6	1022.5	1050.1	1028.6	1013.6
DZ avg	947.5	938.9	970.3	965.4	975.0	955.8	950.8	945.6	1150.9	963.3	982.5	957.8	952.1
DZ max	985.7	975.4	1009.5	1010.2	1014.3	1000.1	990.5	974.2	1164.0	1009.2	1028.1	987.3	995.7
Trans avg	1041.6	1038.2	1104.0	1118.7	1099.4	1091.1	1088.5	1025.5	1194.6	1050.7	1112.8	1083.8	1095.4
Trans max	1221.0	1237.5	1251.3	1247.1	1253.5	1219.3	1221.0	1233.7	1244.3	1236.1	1249.3	1234.8	1218.3
Exit temperatures													
Ideal avg, K	1492.0	1491.2	1483.2	1501.8	1487.2	1486.0	1487.6	1489.0	1488.3	1506.0	1505.6	1489.7	1486.3
Mass avg, K	1474.8	1491.8	1473.5	1495.0	1508.4	1475.3	1508.9	1469.6	1496.5	1477.4	1487.9	1487.9	1502.6
Mass max, K	1719.9	1747.1	1726.5	1718.9	1765.8	1697.7	1727.9	1726.8	1731.0	1705.5	1768.9	1743.6	1697.0
Stat max, K	1773.7	1767.2	1765.6	1761.1	1776.8	1819.8	1755.2	1758.0	1771.0	1741.9	1832.8	1751.2	1732.9
Total PF	0.3102	0.3471	0.2992	0.2712	0.3503	0.2696	0.3227	0.3107	0.2933	0.2461	0.3183	0.3206	0.2796
PF (90% span)	0.0411	0.0102	0.0103	0.0215	0.0134	-0.0286	-0.0182	0.0277	0.0162	0.0070	-0.0094	0.0160	-0.0300
PF (70% span)	0.0769	0.0388	0.0565	0.0691	0.0556	0.0298	0.0462	0.0742	0.0623	0.0744	0.0456	0.0600	0.0381
PF (50% span)	0.0996	0.0838	0.0938	0.1059	0.0898	0.0915	0.0811	0.0846	0.0972	0.1161	0.0884	0.0786	0.0837
PF (30% span)	0.0353	0.0629	0.0545	0.0328	0.0544	0.0739	0.0604	0.0523	0.0547	0.0304	0.0626	0.0401	0.0675
PF (10% span)	-0.2552	-0.2162	-0.2147	-0.2291	-0.2133	-0.1669	-0.1694	-0.2385	-0.2301	-0.2277	-0.1869	-0.1929	-0.1591
Fuel/air ratios, g/kg													
Chemical		21.08	25.15	25.60	23.47	22.57	28.10	24.65	25.75	24.80	27.36	22.94	23.29
Mechanical		21.24	21.66	21.94	21.60	21.49	21.18	21.41	21.81	21.93	22.23	21.67	21.16
% difference		-0.7	16.1	16.7	8.7	5.0	32.7	15.1	18.1	13.1	23.1	5.9	10.1

*CO, UHC, and NO_x values are corrected per the technique described in Section IV-A.

Gas analysis F/A ratios on the high side are expected because the gas sample rakes sample the flow core and not the cooling air-containing wall film. The gas analysis probe locations were left undisturbed for the program balance based on the excellent JP-4 results. As shown in Tables A-1 through -4 some of the experimental fuels had much larger disagreements between chemical and meter F/A ratios. Large disagreements appeared to be associated with JP-8 based fuels, and with mineral seal oil addition, suggesting the possibility of a temperature pattern shift with fuel volatility. However, the outlet temperature pattern results do not appear to indicate such a shift. On an average basis (at idle, cruise, dash, and SLTO) most of the fuels have chemical analysis F/A ratio deviations within 15% of JP-4. Because virtually all gas sample F/A ratios were greater than meter F/A ratios, the exhaust emissions reported in this program are conservative, i.e., perfect sampling would result in lower reported emissions.

In addition to overall average and maximum combustor wall temperatures, Tables A-1 through -4 also provide the following combustor wall temperatures (average and maximum):

- o Dome
- o Primary Zone (PZ)
- o Intermediate Zone (IZ)
- o Dilution Zone (DZ)
- o Transition (TRANS)

Tables A-1 through A-4 also provide the following combustor outlet temperature pattern information:

- o Ideal average temperature
- o Measured average temperature
- o Measured maximum temperature
- o Statistical maximum temperature
- o Total Pattern Factor (PF)
- o Radial PF (various % span)

The ideal average temperature is based on actual BIT, F/A ratio, fuel heating value and hydrogen content, and 100% combustion efficiency. The statistical maximum temperature is a statistical projection of the 3000 BOT data points obtained in the five depth temperature traverse to yield (to a 99% confidence level) the hot spot that would actually be measured with an infinitely detailed temperature survey. The statistical maximum temperature is considered more stable and reliable than the actually measured hot spot temperature. The statistical method has been exclusively used on all recent TF41 temperature traverse work. The "total PF" is based on the statistical hot spot. The statistical hot spot was calculated as follows:

$$T_{HS} = T_{AV} + K\sigma$$

where T_{HS} = statistically projected hot spot
 T_{AV} = average measured temperature
 K = selected constant (2.326 for 99% confidence level)
 σ = temperature standard deviation, determined from the 3000 point survey

The combustor pattern factor is defined as follows:

$$PF = \frac{T_{MAX} - T_{AVG}}{T_{AVG} - T_{IN}}$$

T_{MAX} = maximum statistical temperature, K
 T_{AVG} = average measured exit temperature, K
 T_{IN} = combustor inlet temperature, K

The reported radial PF values were calculated from measured maximum and average radial temperatures. The various percent spans are from hub to tip.

FLAME STABILITY DATA SUMMARY

Flame stability was determined at idle, and altitude cruise conditions. Results are summarized in Table A-5. LBO F/A ratios were determined at idle and cruise flow conditions. Minimum ignition F/A ratio was determined at idle

TABLE A-5
IGNITION AND FLAME STABILITY SUMMARY

Condition	Idle	Cruise	SL cold	SL amb	3,048 M	10,668 M	12,192 M	15,240 M
Fuel 1								
Inlet parameters								
Airflow, kg/sec	1.066	1.131	0.717	0.704	0.686	0.337	0.475	0.337
Temperature, K	419.8	375.4	271.5	279.8	282.0	278.7	278.7	278.7
Pressure, kPa	291.3	342.1	119.9	119.9	148.5	92.8	79.2	62.0
Flow factor, (kg-√K)/(sec-kPa)	0.075	0.079	0.098	0.098	0.100	0.102	0.100	0.031
Ignition								
Fuel flow, kg/hr	21.64	---	22.45	23.77	21.68	22.77	17.19	14.33
Avg fuel/air, g/kg	5.491	---	8.650	9.164	6.760	10.975	9.661	11.156
θ	27.02 × 10 ⁴	---	11.39 × 10 ¹	10.59 × 10 ¹	41.84 × 10 ¹	59.03	67.32	48.35
Lean blow out								
Fuel flow, kg/hr	4.08	4.08	8.44	9.93	7.62	10.82	9.66	8.82
Avg fuel/air, g/kg	1.064	1.003	3.270	3.920	2.388	5.304	5.646	7.281
θ	11.60 × 10 ⁸	73.01 × 10 ¹⁰	96.72 × 10 ⁶	13.74 × 10 ⁵	17.35 × 10 ⁵	11.06 × 10 ³	19.60 × 10 ²	15.06 × 10 ¹
Fuel 2								
Inlet parameters								
Airflow, kg/sec	1.080	1.147	0.706	0.681	0.662	---	---	---
Temperature, K	416.5	380.9	273.1	287.6	287.6	---	---	---
Pressure, kPa	292.9	338.7	116.2	118.2	148.5	---	---	---
Flow factor, (kg-√K)/(sec-kPa)	0.075	0.080	0.100	0.098	0.099	---	---	---
Ignition								
Fuel flow, kg/hr	20.64	---	21.73	19.64	20.68	---	---	---
Avg fuel/air, g/kg	5.153	---	8.417	7.851	6.477	---	---	---
θ	25.96 × 10 ⁷	---	13.48 × 10 ¹	21.02 × 10 ¹	91.67 × 10 ¹	---	---	---
Lean blow out								
Fuel flow, kg/hr	6.17	5.49	11.16	10.70	9.39	---	---	---
Avg fuel/air, g/kg	1.387	1.330	4.392	4.365	3.026	---	---	---
θ	10.13 × 10 ⁸	39.70 × 10 ¹⁰	99.35 × 10 ⁴	18.91 × 10 ⁵	22.24 × 10 ⁵	---	---	---
Fuel 3								
Inlet parameters								
Airflow, kg/sec	1.071	1.150	0.700	0.691	0.875	0.553	---	---
Temperature, K	416.5	366.5	271.5	280.9	282.0	284.3	---	---
Pressure, kPa	292.	348.8	117.2	117.9	147.3	93.1	---	---
Flow factor, (kg-√K)/(sec-kPa)	0.075	0.078	0.098	0.098	0.100	0.100	---	---
Ignition								
Fuel flow, kg/hr	20.00	---	25.85	20.37	21.14	24.63	---	---
Avg fuel/air, g/kg	5.116	---	10.081	8.002	6.577	11.284	---	---
θ	50.24 × 10 ⁶	---	83.81	16.93 × 10 ¹	61.66 × 10 ¹	55.75	---	---
Lean blow out								
Fuel flow, kg/hr	6.53	4.08	10.93	10.93	10.66	11.84	---	---
Avg fuel/air, g/kg	1.693	0.986	4.338	4.393	3.382	4.444	---	---
θ	10.21 × 10 ⁸	32.05 × 10 ¹⁰	95.18 × 10 ⁴	14.20 × 10 ⁵	17.32 × 10 ⁵	54.32 × 10 ¹	---	---

TABLE A-5 (Continued)

Condition	Idle	Cruise	SL cold	SL end	3,043 M	10,668 M	12,192 M	15,240 M
Fuel 4								
Inlet parameters								
Airflow, kg/sec	1.066	1.122	0.702	0.694	0.884	---	---	---
Temperature, K	424.8	577.6	272.0	278.7	279.3	---	---	---
Pressure, kPa	294.6	338.7	117.5	118.5	149.0	---	---	---
Flow factor, (kg- \sqrt{K})/(sec-kPa)	0.075	0.086	0.098	0.098	0.099	---	---	---
Ignition								
Fuel flow, kg/hr	18.78	---	22.72	23.41	24.36	---	---	---
Avg fuel/air, g/kg	4.858	---	8.978	9.159	7.665	---	---	---
ϕ	14.46×10^8	---	11.39×10^1	11.53×10^1	25.25×10^1	---	---	---
Lean blow out								
Fuel flow, kg/hr	6.30	4.08	10.84	11.02	10.84	---	---	---
Avg fuel/air, g/kg	1.613	1.011	4.291	4.412	3.408	---	---	---
ϕ	14.46×10^8	79.05×10^{10}	98.03×10^4	13.07×10^5	15.67×10^5	---	---	---
Fuel 5								
Inlet parameters								
Airflow, kg/sec	1.067	1.122	0.725	0.708	0.893	0.548	---	---
Temperature, K	422.0	577.6	270.9	277.6	277.6	279.8	---	---
Pressure, kPa	292.9	338.7	119.9	117.2	150.7	93.1	---	---
Flow factor, (kg- \sqrt{K})/(sec-kPa)	0.075	0.080	0.100	0.101	0.099	0.098	---	---
Ignition								
Fuel flow, kg/hr	17.46	---	23.68	24.27	25.27	24.77	---	---
Avg fuel/air, g/kg	4.370	---	8.990	9.455	7.693	12.097	---	---
ϕ	12.80×10^8	---	10.77×10^1	98.06	23.02×10^1	56.23	---	---
Lean blow out								
Fuel flow, kg/hr	5.31	4.08	10.09	9.05	9.19	25.24	---	---
Avg fuel/air, g/kg	1.382	1.011	3.865	3.552	2.858	12.786	---	---
ϕ	12.80×10^8	79.05×10^{10}	93.47×10^4	12.02×10^5	14.80×10^5	52.55	---	---
Fuel 6								
Inlet parameters								
Airflow, kg/sec	1.062	1.149	0.726	0.678	0.380	0.559	0.454	0.353
Temperature, K	433.4	577.6	273.7	289.8	282.0	277.4	281.1	278.7
Pressure, kPa	294.6	355.6	118.5	118.5	149.0	93.1	79.2	62.3
Flow factor, (kg- \sqrt{K})/(sec-kPa)	0.075	0.078	0.099	0.097	0.039	0.100	0.096	0.095
Ignition								
Fuel flow, kg/hr	---	---	26.81	21.54	22.82	24.54	18.05	15.01
Avg fuel/air, g/kg	---	---	10.472	8.655	7.209	11.974	10.431	11.693
ϕ	---	---	78.02	11.62×10^1	30.15×10^1	54.20	63.54	44.08
Lean blow out								
Fuel flow, kg/hr	5.60	4.54	10.80	9.68	11.39	11.75	10.68	9.84
Avg fuel/air, g/kg	1.465	1.096	4.246	3.970	3.594	5.835	6.542	7.748
ϕ	18.12×10^8	54.02×10^{10}	10.52×10^5	20.88×10^5	17.58×10^5	13.98×10^2	37.37×10^1	11.40×10^1

TABLE A-5 (Continued)

Condition	Idle	Cruise	SL cold	SL amb	3,048 M	10,668 M	12,192 M	15,240 M
Fuel 7								
Inlet parameters								
Airflow, kg/sec	1.063	1.146	0.704	0.682	0.879	0.557	0.461	---
Temperature, K	425.4	372.0	270.9	287.6	289.8	284.3	283.1	---
Pressure, kPa	292.9	348.8	118.5	118.5	150.0	93.1	78.9	---
Flow factor, (kg-√K)/(sec/kPa)	0.075	0.079	0.098	0.098	0.100	0.101	0.098	---
Ignition								
Fuel flow, kg/hr	19.05	---	26.17	24.72	24.40	26.90	26.94	---
Avg fuel/air, g/kg	4.977	---	10.164	9.650	7.711	12.383	16.142	---
ϕ	55.27×10^{-7}	---	81.23	10.18×10^1	23.76×10^1	53.83	37.48	---
Lean blow out								
Fuel flow, kg/hr	4.08	4.72	11.66	11.27	11.04	17.83	16.03	---
Avg fuel/air, g/kg	1.067	1.143	4.603	4.590	3.490	8.897	10.133	---
ϕ	14.68×10^8	65.23×10^{10}	94.47×10^4	18.98×10^5	24.31×10^5	97.12	65.32	---
Fuel 8								
Inlet parameters								
Airflow, kg/sec	1.043	1.129	0.722	0.704	0.871	0.542	---	---
Temperature, K	435.9	372.0	269.3	282.0	288.7	287.6	---	---
Pressure, kPa	287.9	338.7	120.6	121.2	149.0	93.5	---	---
Flow factor, (kg-√K)/(sec-kPa)	0.076	0.080	0.098	0.098	0.099	0.098	---	---
Ignition								
Fuel flow, kg/hr	24.04	---	28.53	28.94	24.95	23.86	---	---
Avg fuel/air, g/kg	6.401	---	10.966	11.277	7.945	11.925	---	---
ϕ	19.88×10^3	---	75.00	79.30	23.61×10^1	61.83	---	---
Lean blow out								
Fuel flow, kg/hr	5.26	4.08	13.99	13.04	11.73	13.59	---	---
Avg fuel/air, g/kg	1.401	1.004	5.383	5.142	3.734	6.962	---	---
ϕ	22.12×10^8	62.89×10^{10}	27.90×10^3	72.46×10^4	23.16×10^5	36.55×10^1	---	---
Fuel 9								
Inlet parameters								
Airflow, kg/sec	1.063	1.122	0.723	0.670	0.839	0.557	---	---
Temperature, K	410.9	377.6	268.7	294.7	302.0	279.8	---	---
Pressure, kPa	294.6	338.7	117.9	118.5	149.7	93.5	---	---
Flow factor, (kg-√K)/(sec/kPa)	0.073	0.080	0.100	0.098	0.097	0.100	---	---
Ignition								
Fuel flow, kg/hr	22.68	---	25.40	23.54	24.95	27.12	---	---
Avg fuel/air, g/kg	5.928	---	9.730	9.604	8.263	6.758	---	---
ϕ	48.03×10^3	---	86.50	11.77×10^1	22.10×10^1	34.19×10^1	---	---
Lean blow out								
Fuel flow, kg/hr	7.26	5.24	11.36	11.16	9.75	27.12	---	---
Avg fuel/air, g/kg	1.897	1.297	4.368	4.623	3.230	13.516	---	---
ϕ	83.22×10^7	79.05×10^{10}	83.32×10^4	30.11×10^5	41.38×10^5	48.94	---	---

TABLE A-5 (Concluded)

Condition	Idle	Cruise	SL cold	SL amb	3,048 M	10,668 M	12,192 M	15,240 M
Fuel 10								
Inlet parameters								
Airflow, kg/sec	1.067	1.122	0.742	0.683	0.864	---	---	---
Temperature, K	422.0	577.6	272.0	287.6	287.6	---	---	---
Pressure, kPa	292.9	338.7	119.9	118.9	149.0	---	---	---
Flow factor, (kg-√K)/(sec-kPa)	0.075	0.080	0.102	0.097	0.098	---	---	---
Ignition								
Fuel flow, kg/hr	20.73	---	25.17	20.37	21.95	---	---	---
Avg fuel/air, g/kg	5.197	---	9.259	7.793	6.915	---	---	---
ϕ	11.98×10^{-7}	---	10.26×10^{-1}	21.89×10^{-1}	51.54×10^{-1}	---	---	---
Lean blow out								
Fuel flow, kg/hr	6.49	4.08	11.93	10.57	10.39	---	---	---
Avg fuel/air, g/kg	1.689	1.011	4.477	4.298	3.361	---	---	---
ϕ	12.80×10^{-8}	79.05×10^{-10}	95.57×10^{-6}	19.04×10^{-5}	22.37×10^{-5}	---	---	---
Fuel 11								
Inlet parameters								
Airflow, kg/sec	1.067	1.123	0.722	0.722	0.900	0.559	---	---
Temperature, K	422.0	577.6	272.0	272.0	272.0	272.6	---	---
Pressure, kPa	292.9	338.7	121.6	121.6	149.0	93.5	---	---
Flow factor, (kg-√K)/(sec-kPa)	0.075	0.080	0.098	0.098	0.100	0.099	---	---
Ignition								
Fuel flow, kg/hr	25.49	---	26.40	26.40	22.68	22.82	---	---
Avg fuel/air, g/kg	6.578	---	9.882	9.882	7.469	11.073	---	---
ϕ	88.31×10^{-2}	---	90.39	90.39	24.37×10^{-1}	60.65	---	---
Lean blow out								
Fuel flow, kg/hr	7.42	4.03	12.59	12.59	11.29	13.59	---	---
Avg fuel/air, g/kg	1.931	1.010	4.845	4.845	3.486	6.747	---	---
ϕ	12.80×10^{-8}	78.99×10^{-10}	10.07×10^{-5}	10.07×10^{-5}	11.52×10^{-5}	31.83×10^{-1}	---	---
Fuel 12								
Inlet parameters								
Airflow, kg/sec	1.064	1.147	0.708	0.703	0.875	0.555	---	---
Temperature, K	422.0	569.3	272.0	278.1	278.7	284.3	---	---
Pressure, kPa	292.9	348.8	119.2	118.5	150.4	93.3	---	---
Flow factor, (kg-√K)/(sec-kPa)	0.075	0.078	0.098	0.099	0.097	0.100	---	---
Ignition								
Fuel flow, kg/hr	18.42	---	24.31	22.95	24.63	24.77	---	---
Avg fuel/air, g/kg	4.608	---	9.357	9.002	8.297	12.117	---	---
ϕ	12.84×10^{-8}	---	96.59	10.95×10^{-1}	16.82×10^{-1}	35.65	---	---
Lean blow out								
Fuel flow, kg/hr	7.14	5.17	11.23	11.14	11.36	12.70	---	---
Avg fuel/air, g/kg	1.866	1.253	4.407	4.402	3.605	6.360	---	---
ϕ	12.04×10^{-8}	58.35×10^{-10}	99.18×10^{-6}	12.63×10^{-5}	15.71×10^{-5}	53.06×10^{-1}	---	---

Avg F/A are arithmetic averages of IGM/NO IGM or LBO1/LBO2 F/A ratios.

 $\phi = (\text{BIP})^{1.75} \text{ Ar } b \cdot (\text{BIP}/b)^{1/4} / u_A$ with minimum $b = 25 \text{ K}$, and based on average IGM F/A or average LBO F/A ratios.

only. Stability and ignition data (as well as combustion efficiency) may be correlated against the combustor loading parameter, θ . It is defined as follows:

$$\theta = \frac{P^{1.75} Ar h e^{T/b}}{W_c}$$

where

- P = combustor annulus pressure, MPa
- Ar = combustor reference area (area between cases), m²
- h = combustor annulus height, or combustor dia, m
- e = base of natural logarithms
- T = combustor inlet temperature, K
- b = function of combustion zone equivalence ratio
- W_c = combustor airflow, kg/s

For ignition/stability correlation, optimum results would be expected for a stoichiometric combustion zone. Under such conditions, b may be taken as 300. Other fixed values for TF41 are:

$$\begin{aligned} Ar &= 0.223 \text{ m}^2 \\ h &= 13.2 \text{ cm} \end{aligned}$$

The fuel schedule for these data follows:

- o 100% pilot fuel up to 4.48 MPa pilot (approx 19 kg/hr)
- o Additional fuel is all main

FOULING DATA SUMMARY

A 1-hr fouling and carboning test was run for each fuel at SLTO conditions. Severe fouling conditions were established at the nozzle by the following measures:

- o Heated main fuel to 93°C
- o An unusually low pilot fuel rate (4.5 kg/hr vs 18.6 kg/hr normal) to establish severe pilot passage fuel interface temperatures
- o Slotted nozzles to prevent pilot passage cooling by conduction to the main fuel

These severe conditions in 1 hr give the fuel fouling expected in 75 hr of typical mission operation.

The fouling results are summarized in Table A-6. This tabulation shows pre-test and posttest pilot and main nozzle passage flow numbers, as well as flow numbers at 15 min intervals during the fouling test. The pilot passage flow was momentarily increased to obtain accurate pilot nozzle passage flow number data.

After each pilot test flow bench calibration the nozzles were disassembled, and any passage deposit was carefully removed mechanically and weighed to provide another fouling indication. These results are given in Table A-7.

SEA LEVEL STARTS DATA SUMMARY

Ignition and LBO F/A ratios were determined at sea-level start conditions, over a nominal temperature range from 274 to 282 K. Combustor flow factor, $W_a \sqrt{T/P}$, was held constant. Results are given in Table A-5.

ALTITUDE IGNITION DATA SUMMARY

As previously discussed, altitude ignition data were obtained at flow conditions corresponding to 3 sec out engine conditions at 0.6 flight M_N , at 3, 11, 12 and 15 km conditions.

The procedure was to establish airflow conditions and then establish the minimum ignition F/A ratio through a series of attempted lights. Approximately 30 sec were allowed to achieve ignition, as indicated by a temperature rise. The maximum overall F/A ratio attempted was 30.0, well beyond stoichiometric in the combustion zone.

The LBO F/A ratio was determined by reducing fuel flow slowly and noting the extinction fuel flow, based on temperature rise. Airflow conditions were allowed to change as F/A ratio changed. Airflow conditions at extinction were reported.

The altitude ignition data are summarized in Table A-5.

TABLE A-6
SLTO FOULING AND CARBONING DATA

Fuel		Flow	Combustor rig operating time, min					Flow	Passage
Fuel	nozzle	bench						bench	rbon
No.	serial number	pretest	0	15	30	45	60	posttest	mg
Measured pilot nozzle flow numbers, kg/sec/ $\sqrt{\text{MPa}}$ *									
1	2	12.78	9.72	9.77	9.72	9.67	9.72	13.11	1.0
2	1	11.96	11.03	11.03	11.03	10.98	11.03	11.85	0.4
3	2	13.11	12.40	12.40	12.35	12.45	12.51	13.22	1.3
4	3	10.98	12.40	12.40	12.51	12.40	13.00	11.36	0.3
5	2	13.27	10.22	10.22	10.22	10.27	10.22	10.98	4.0
6	3	11.64	12.78	12.70	12.89	12.95	12.84	11.91	5.8
7	1	12.89	11.14	11.14	11.14	11.14	11.09	12.07	0.3
8	3	10.60	12.89	12.89	12.95	13.17	13.00	10.54	0.4
9	3	11.74	12.51	12.51	12.56	12.67	12.45	10.32	0.2
10	2	13.66	10.82	10.82	10.65	10.60	10.65	11.47	4.5
11	1	11.42	13.27	13.27	13.38	13.49	14.20	11.47	3.1
12	2	12.62	16.75	14.75	15.57	13.98	14.15	13.11	2.1
Measured main nozzle flow numbers, kg/sec/ $\sqrt{\text{MPa}}$ *									
1	2	276.4	240.9	242.5	240.4	240.4	240.4	275.3	0.0
2	1	257.8	240.9	241.5	241.5	240.9	241.5	243.1	0.0
3	2	275.3	250.2	250.7	250.2	250.2	249.6	278.6	0.0
4	3	258.4	238.2	232.2	232.2	232.2	230.0	257.8	0.0
5	2	277.0	246.4	246.9	245.8	248.0	246.9	276.4	0.0
6	3	257.8	231.1	242.5	244.2	244.2	246.4	258.4	0.0
7	1	274.8	234.9	237.6	238.7	237.6	236.0	255.7	0.0
8	3	257.8	246.4	242.5	242.0	244.2	243.6	259.5	0.0
9	3	255.7	244.7	239.3	239.3	238.7	239.8	257.8	0.0
10	2	280.2	243.1	242.0	243.1	243.1	241.5	260.6	0.0
11	1	236.7	243.6	238.2	235.4	237.1	237.6	255.1	0.0
12	2	276.4	263.8	266.6	264.4	263.8	264.4	276.4	0.0

$$\text{flow number} = \frac{\text{Flow rate, kg/sec}}{\sqrt{\text{pressure, MPa}}}$$

*Nonflammable test fluid used on flow bench, viscosity different than test fuels

TABLE A-7
FUEL FOULING TEST RESULTS--FUEL DEPOSIT INVESTIGATION

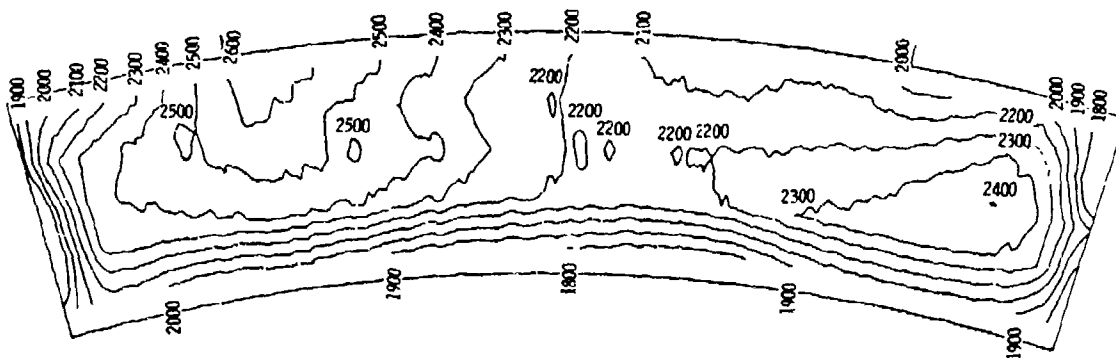
<u>Fuel No.</u>	<u>Initial* weight</u>	<u>Final* weight</u>	<u>Fuel deposit* weight</u>	<u>Comments</u>
1	6.36	6.40	0.0010	Very light carbon-- pilot; main--clean
2	6.29	6.30	0.0004	Small amount wet & dry deposits--pilot & main
3	6.33	6.36	0.0013	Slight amount wet & dry deposits--pilot & main
4	6.46	6.46	0.0003	Pilot--small amount wet & dry deposits; main--clean
5	6.34	6.35	0.0040	Pilot--black granular deposits and light carbon; main--clean
6	6.43	6.44	0.0058	Pilot--black granular deposits; main--clean
7	6.20	6.20	0.0003	Essentially no deposits
8	6.39	6.39	0.0004	Small amount of wet & dry deposits--main & pilot
9	6.23	6.23	0.0002	No deposits, slight amount of metal removed
10	6.44	6.44	0.0045	Pilot--black granular deposits & carbon; main--clean
11	6.43	6.43	0.0031	Pilot--black granular deposits & light carbon; main--light carbon
12	6.30	6.31	0.0021	Pilot--black granular deposits & carbon; main--light carbon

*Measurements in grams (taken with gramatic balance).

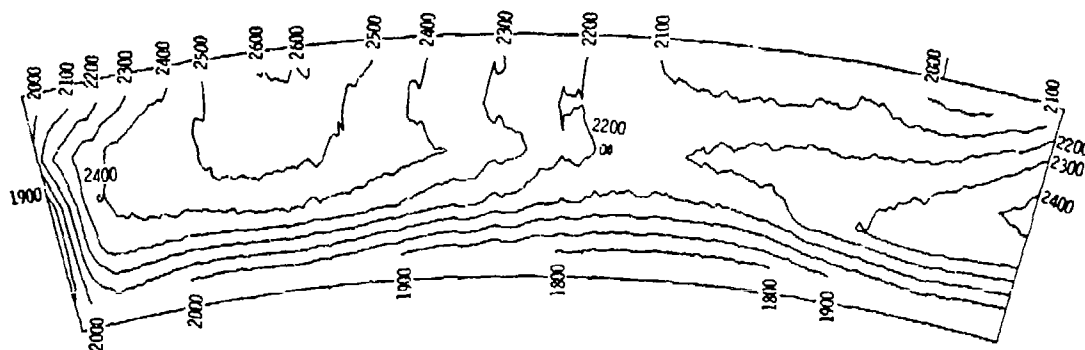
APPENDIX B

COMBUSTOR OUTLET TEMPERATURE PATTERNS

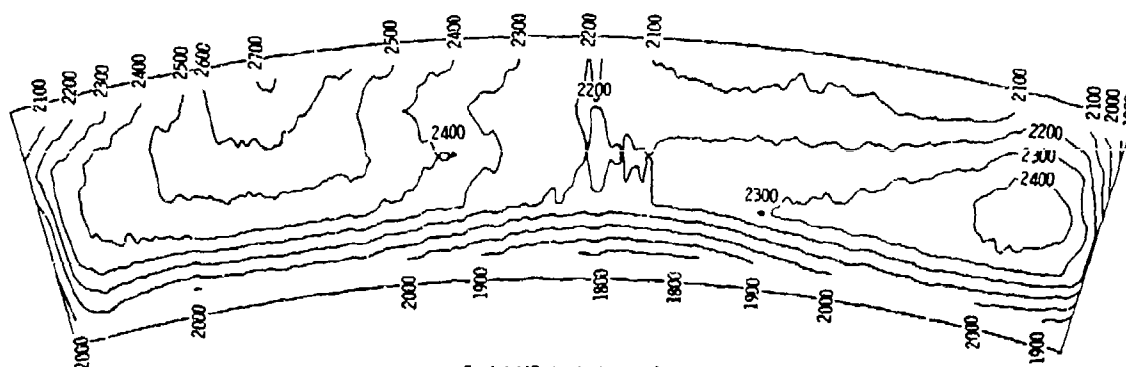
Combustor exit temperature distributions at SLTO conditions (normalized to 1502 K) as presented for all test fuels in Figures B-1 and -2.



Fuel 2 (JP-4 + Aromatic Solvent, 12% H)



Fuel 3 (JP-4 + Aromatic Solvent, 13% H)

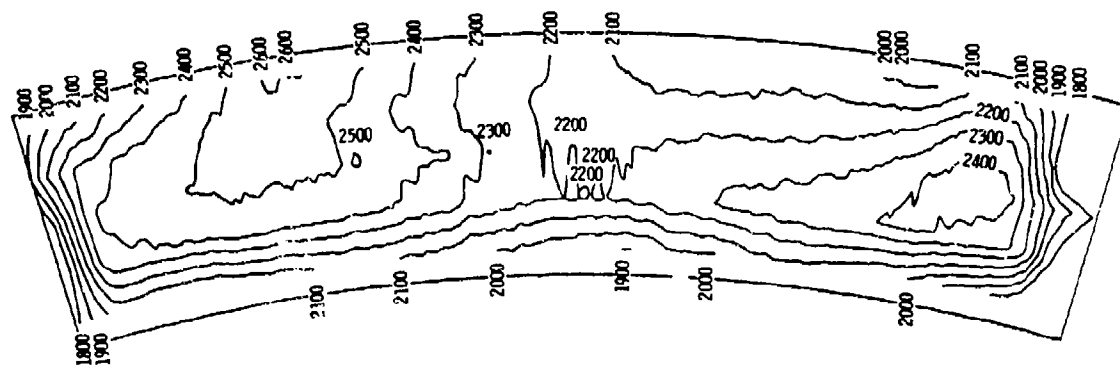


Fuel 4 (JP-4 + Xylene, 12% H)

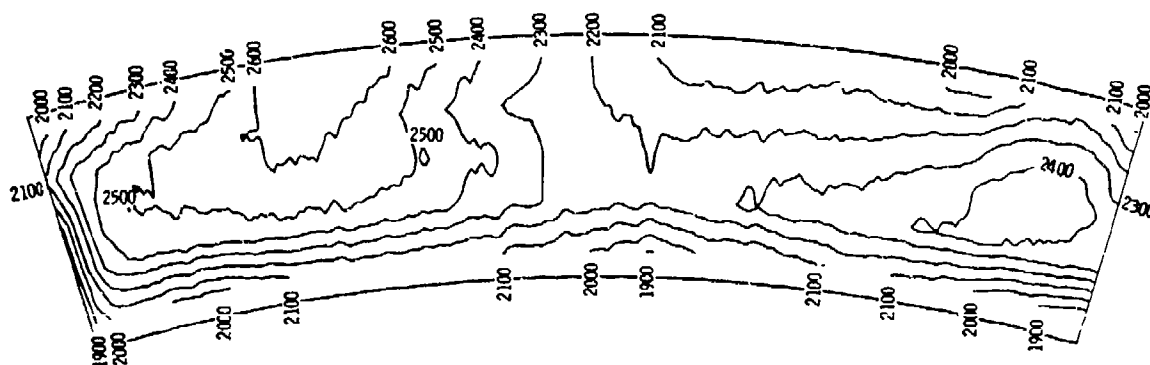
Plots shown
are °F

TE-7489-1

Figure B-1. - SLTO Combustor Outlet Temperature Patterns---Fuels 2 through 6.



Fuel 5 (JP-4 + Xylene, 13% H)

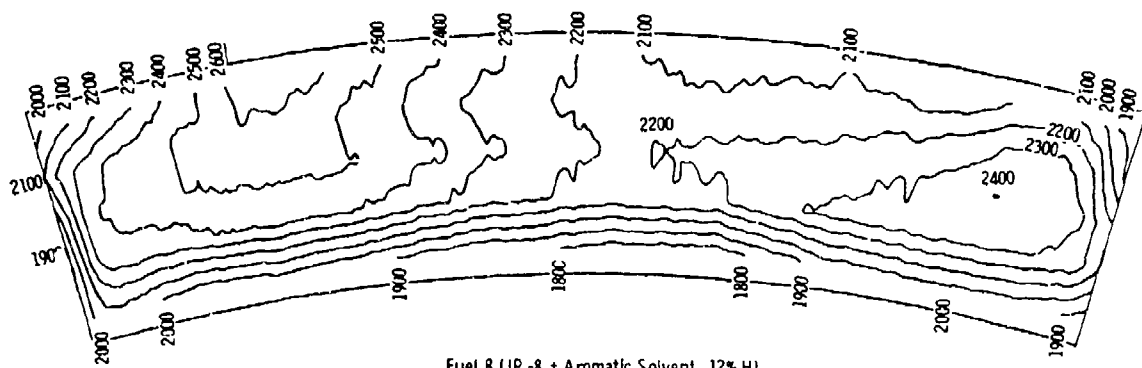


Fuel 6 (JP-4 + Xylene + GM)

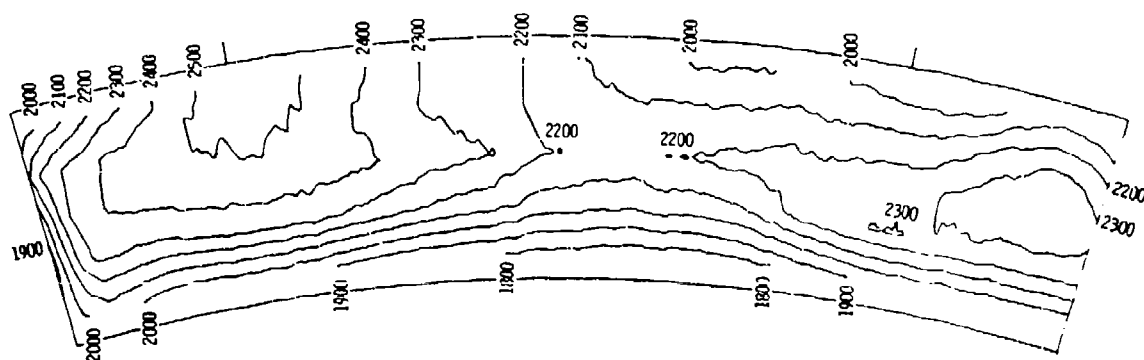
Plots shown
are "F"

Figure B-1 (Concluded).

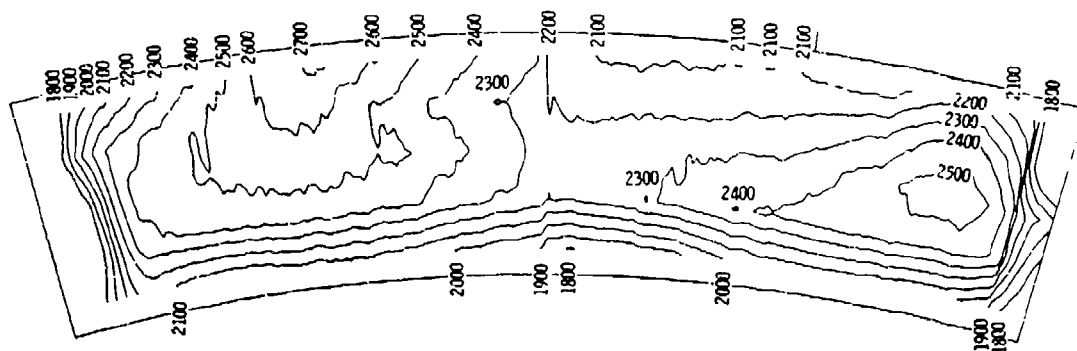
TE-7489-2



Fuel 8 (JP-8 + Aromatic Solvent, 12% H)



Fuel 9 (JP-8 + Aromatic Solvent, 13% H)

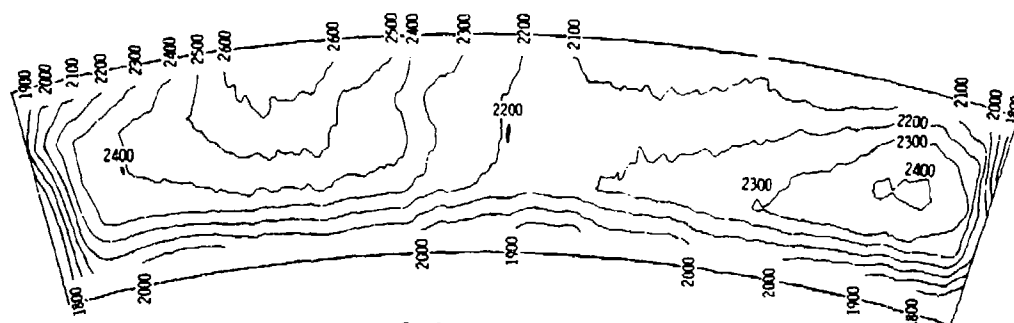


Fuel 10 (JP-8 + Xylene, 12% H)

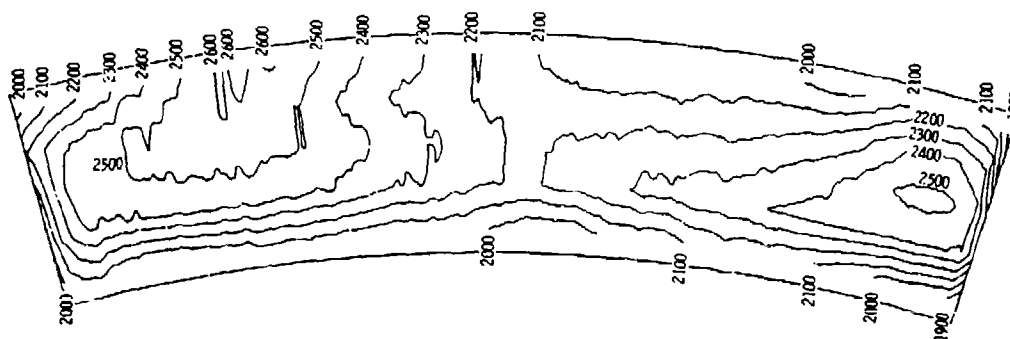
Plots shown
are °F

TE-7491-1

Figure B-2. - SLTO Combustor Outlet Temperature Patterns--Fuels 8 through 12.



Fuel 11 (JP-8 + Xylene, 13% H)



Fuel 12 (JP-8 + GM)

Plots shown are "F

TE-7491-2

Figure B-2 (Concluded).

APPENDIX C
CARBONING DATA SUMMARY

Fuel nozzle and combustor dome carboning characteristics were determined during a special 1-hr test at SLTO conditions. A special low thermal shock shutdown procedure was employed to preserve any carbon deposits. Posttest photographs showing carbon deposition include Figures C-1 through -10.

PRECEDING PAGE BLANK-NOT FILMED

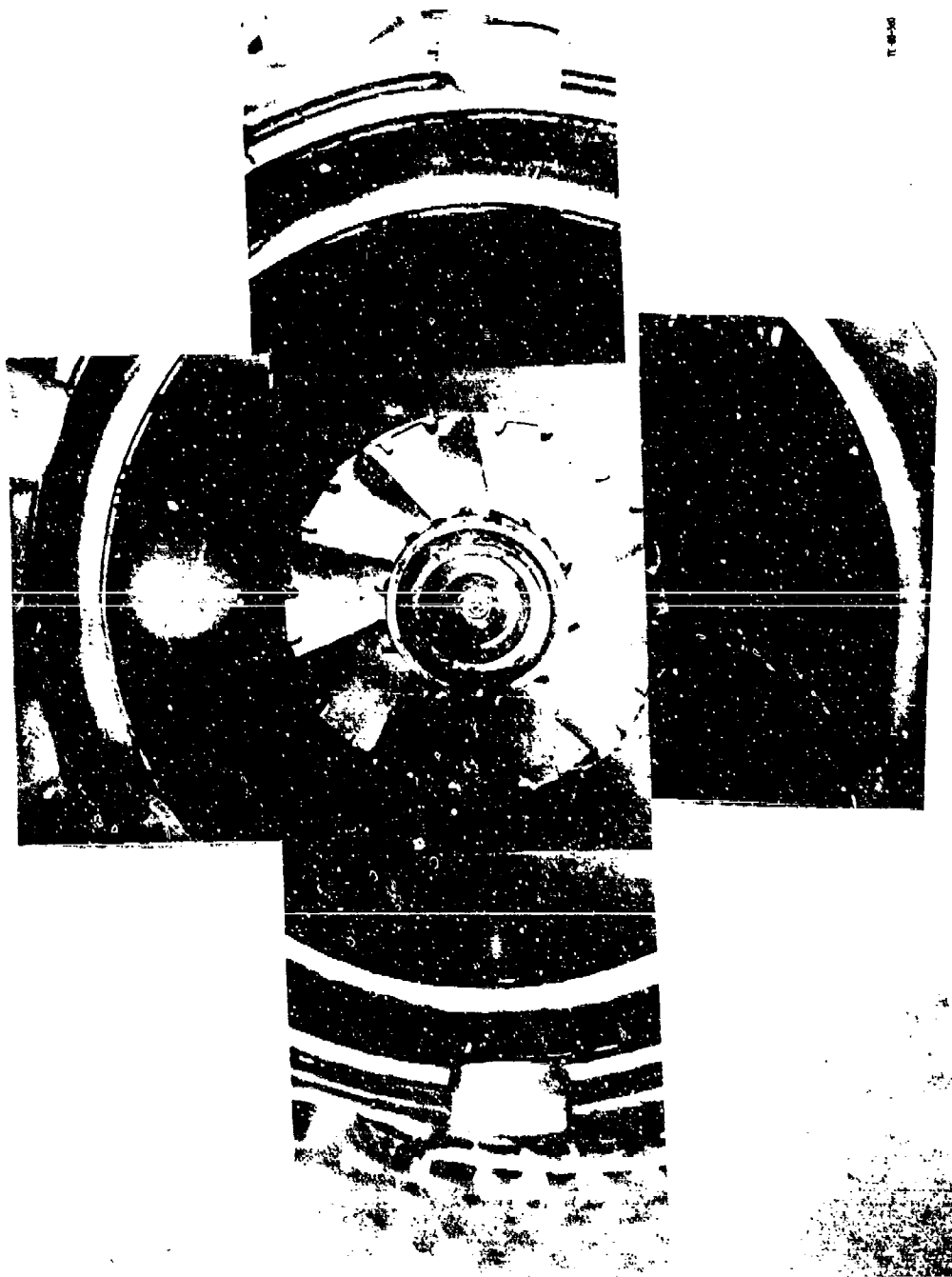


Figure C-1. - Posttest Photograph of Carbon Deposition--Fuel 2.

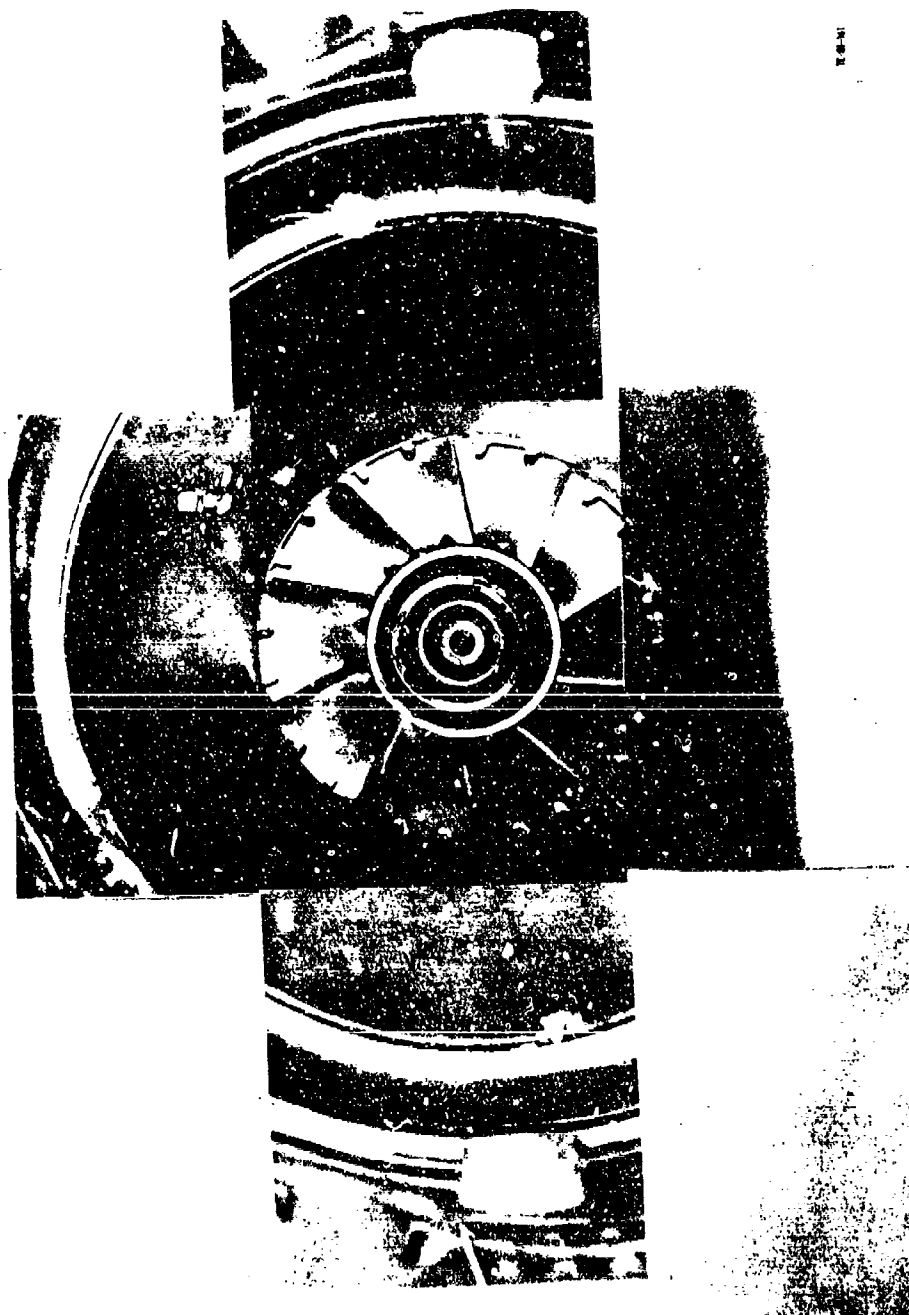


Figure C-2. - Posttest Photograph of Carbon Deposition--Fuel 3.



Figure C-3. - Posttest Photograph of Carbon Deposition--Fuel 4.

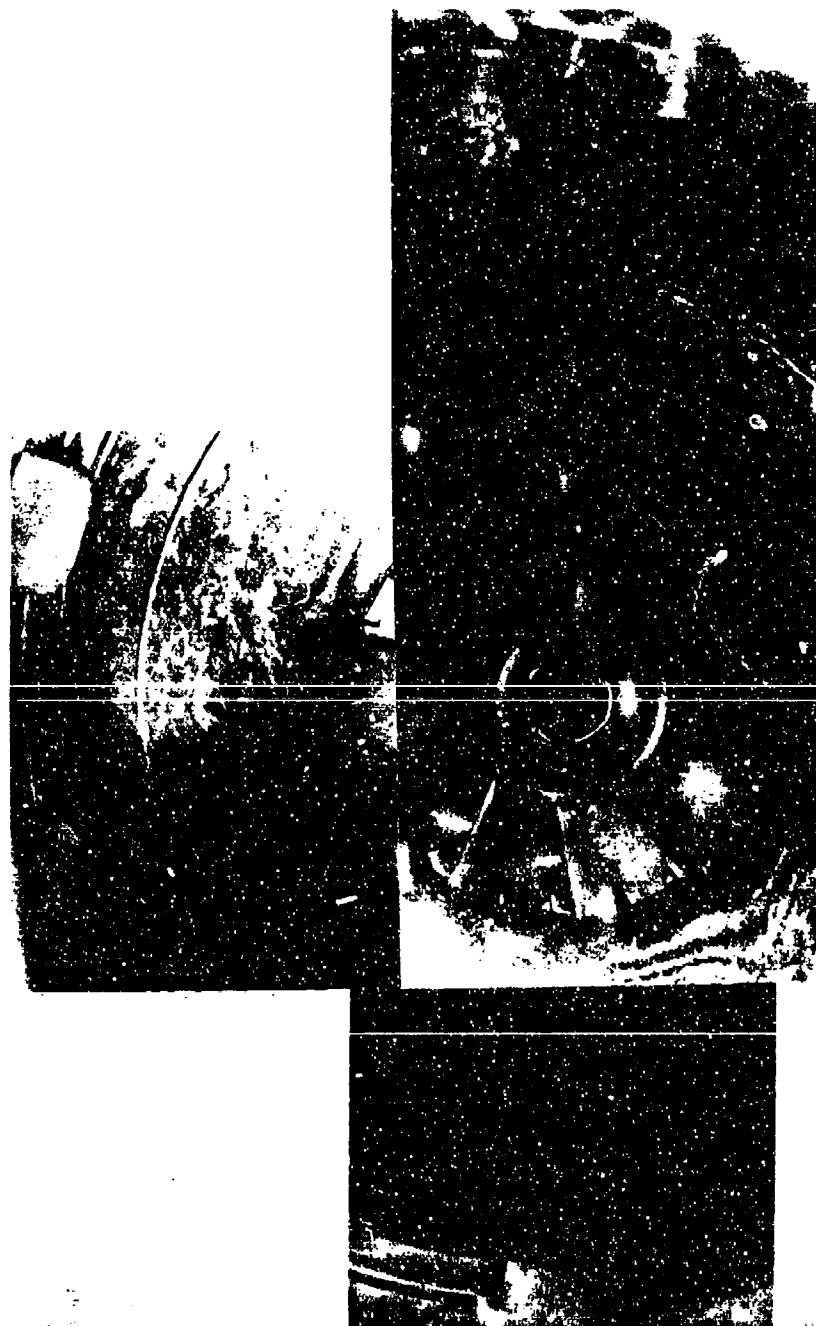


Figure C-4. - Posttest Photograph of Carbon Deposition--Fuel 5.

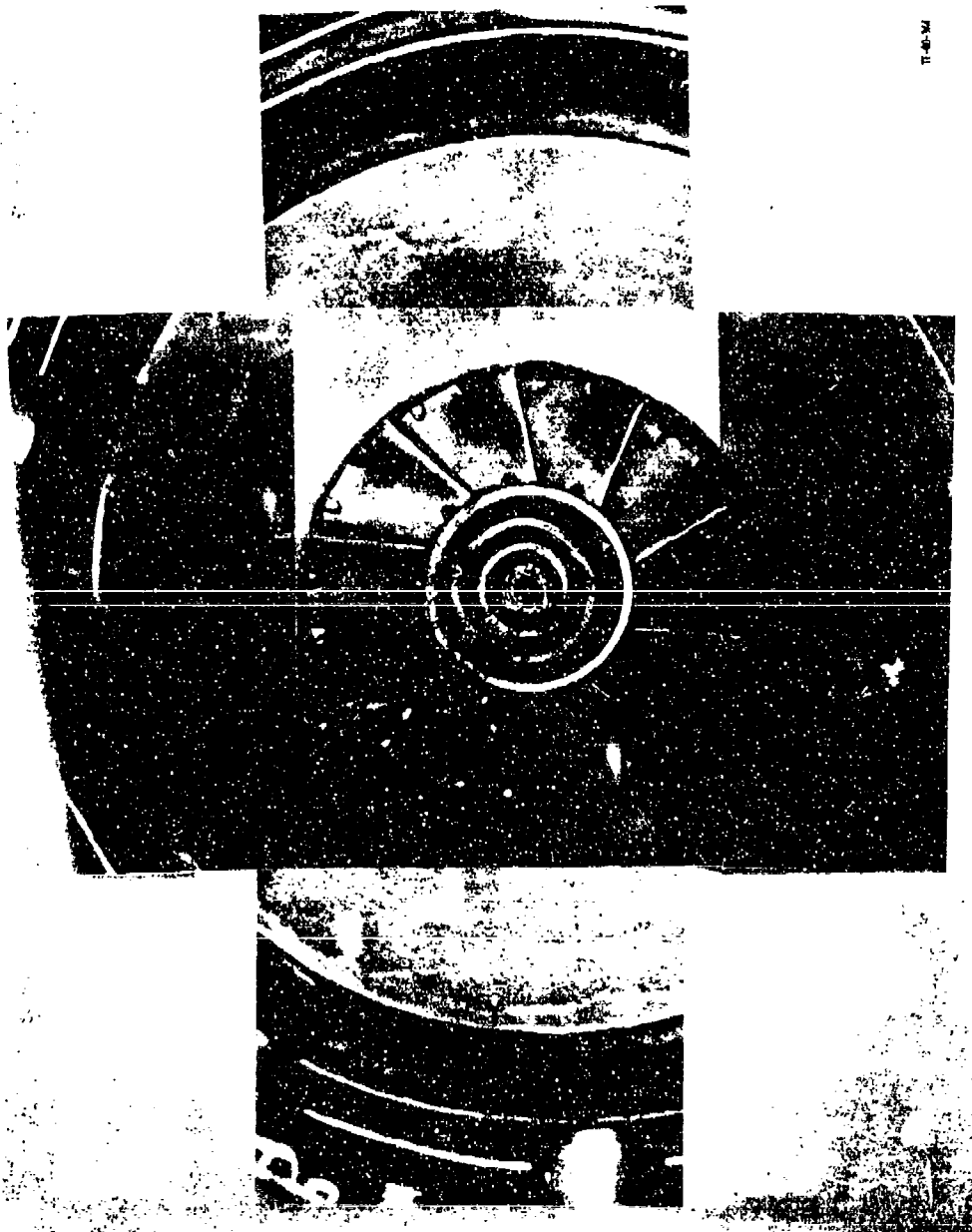


Figure C-5. - Posttest Photograph of Carbon Deposition--Fuel 6.

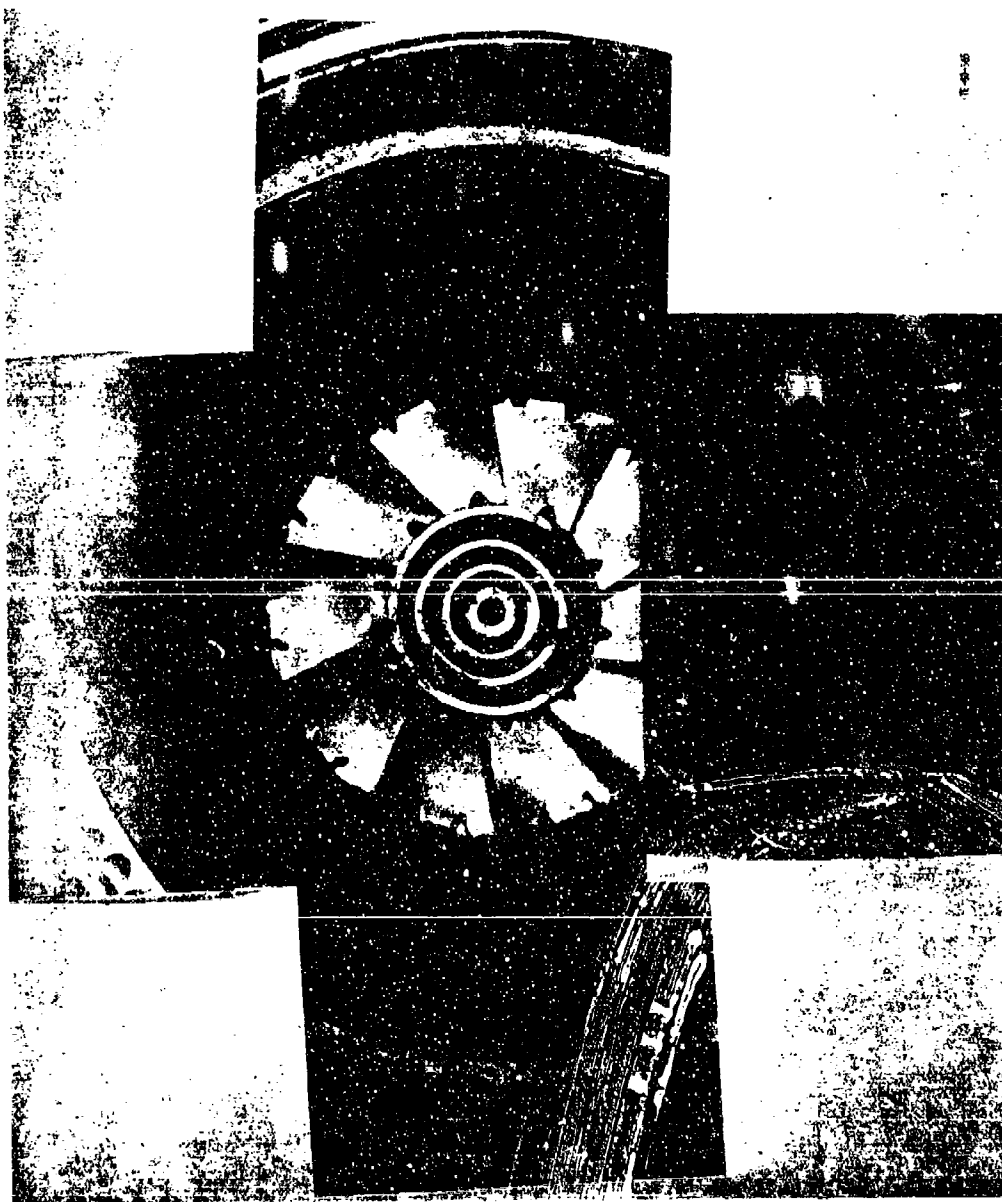


Figure C-6. - Posttest Photograph of Carbon Deposition--Fuel 8.



Figure C-7. - Posttest Photograph of Carbon Deposition--Fuel 9.



Figure C-8. - Posttest Photograph of Carbon Deposition--Fuel 10.

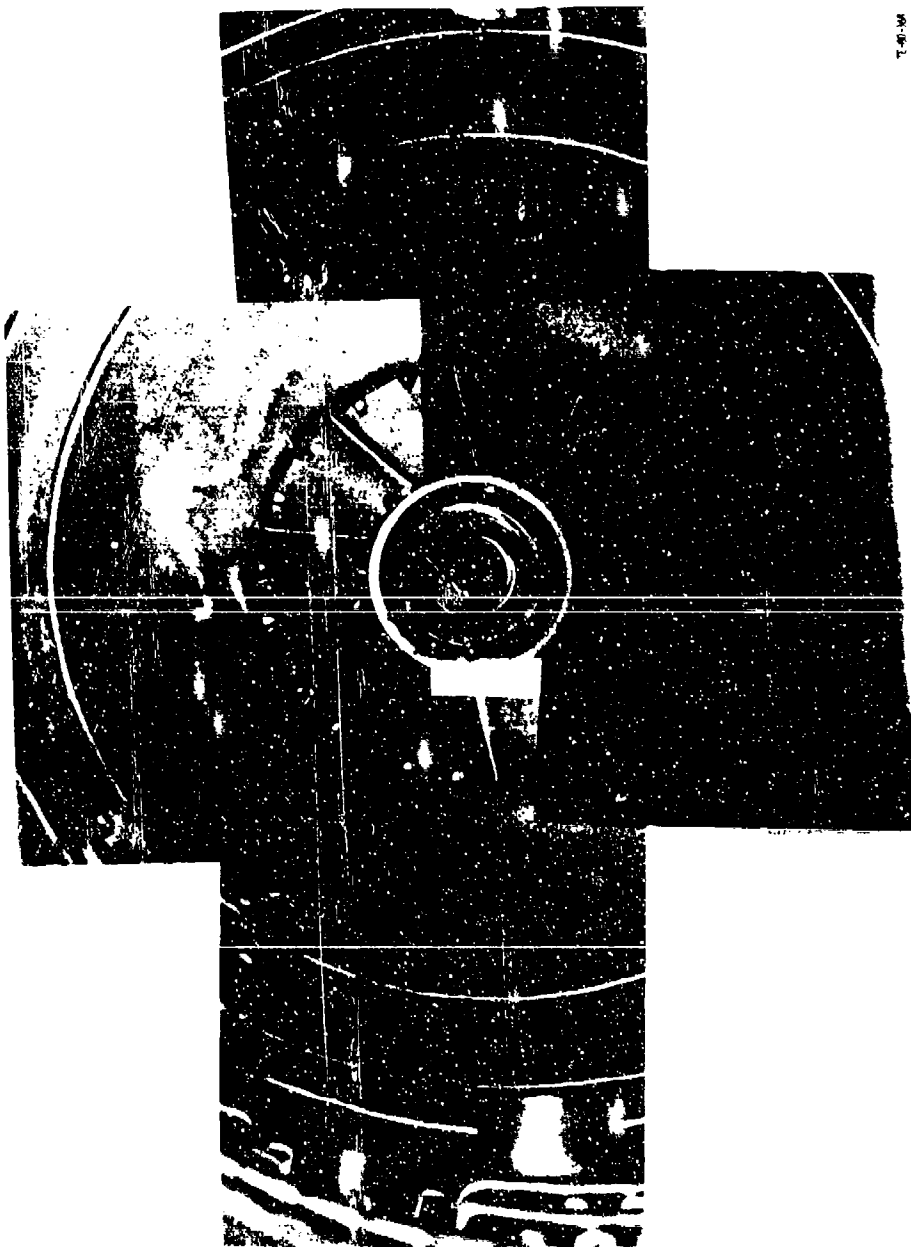


Figure C-9. - Posttest Photograph of Carbon Deposition--Fuel 11.

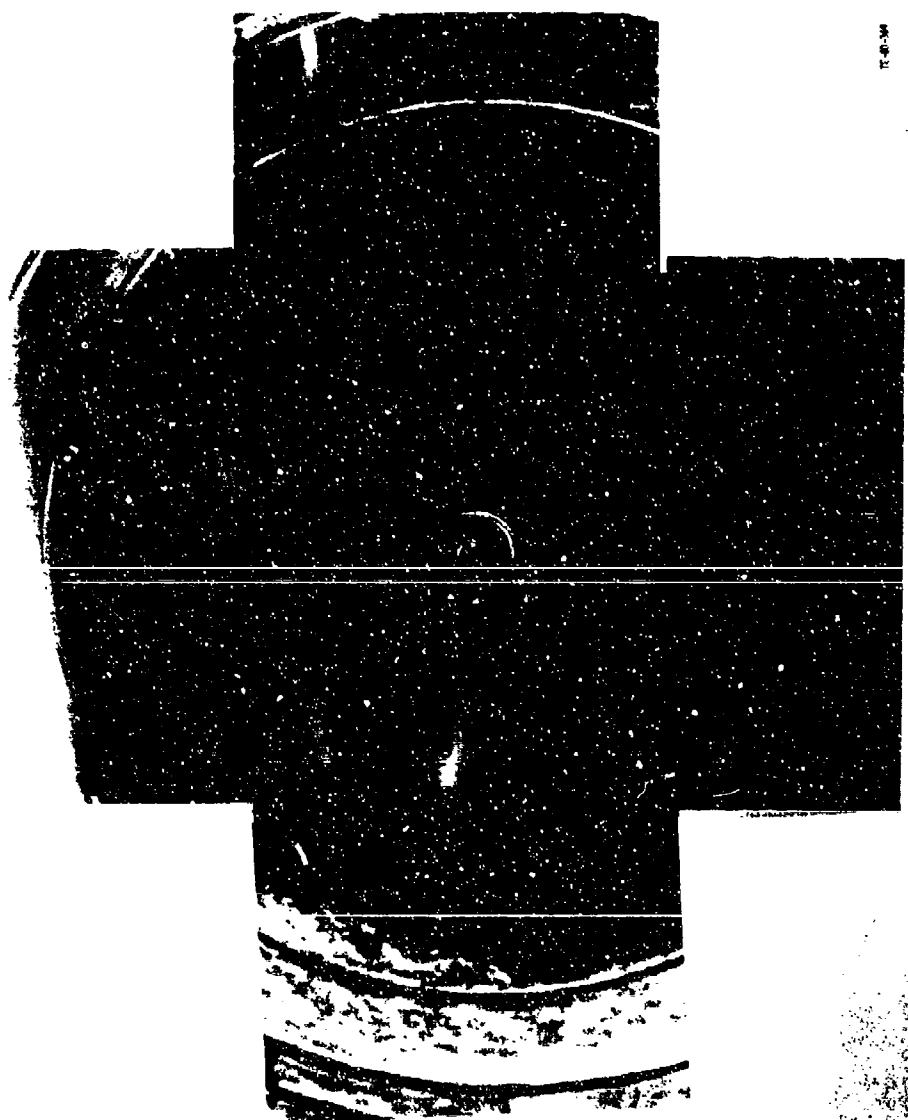


Figure C-10. - Posttest Photograph of Carbon Deposition--Fuel 12.

APPENDIX D

STRESS LIFE ANALYSIS

A calculated life analysis was performed on the life limiting component of the TF41 combustion system - the discharge nozzle - for four of the test fuels, Fuels 1, 7, 8, and 10. The maximum von Mises equivalent stress and the maximum component stresses for each of the four fuels is shown in Table D-1. These stresses can be compared to the yield and ultimate strength of the Nimonic 263 material in Figure D-1. The location of these stresses is shown in Figures D-2 and -3 depending on whether they occur on the inner or outer surface. These figures also show the mathematical model used in the analysis. The computer program used assumes elastic behavior, and the stresses in Table D-1 are equivalent elastic stresses, i.e., the elastic stress that is compatible with the calculated strain. Normally the equivalent elastic stress range is considered to be a valid representation of the strain range; however, in the case of the combustor where large portions of the wall exceed the proportional limit, the calculated strains and equivalent elastic stresses could be unconservatively in error especially in the hottest regions and should be used only in a relative sense to compare one fuel with another. Only Fuel 10 has an equivalent stress higher than Fuel 1, the baseline. Fuel 8, because of its lower gradient, has an equivalent stress well below the others.

PRECEDING PAGE BLANK-NOT FILMED

TABLE D-1
MAXIMUM STRESSES IN THE TRANSITION SECTION OF THE TF41 COMBUSTOR
FOR TYPICAL TEST FUELS

	Fuel 1 (JP-4 baseline)		Fuel 7		Fuel 8		Fuel 10	
	Stress, MPa	Temp, K	Stress, MPa	Temp, K	Stress, MPa	Temp, K	Stress, MPa	Temp, K
von Mises equivalent	651	1127	582	1102	418	1152	658	1154
σ_x								
max tension	681	889	643	883	399	1033	662	866
max compress	618	1116	554	1091	403	1172	650	1142
σ_y								
max tension	454	889	436	883	283	1033	410	911
max compress	487	1043	450	1027	358	1141	395	1020
σ_z								
max tension	465	889	438	883	256	1124	426	911
max compress	470	889	450	883	266	1191	422	911

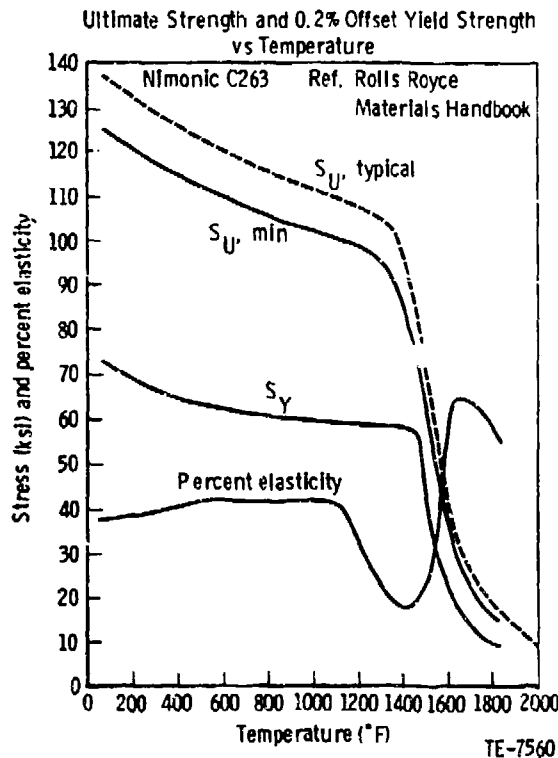


Figure D-1. - Strength Versus Temperature--N263 Material.
146

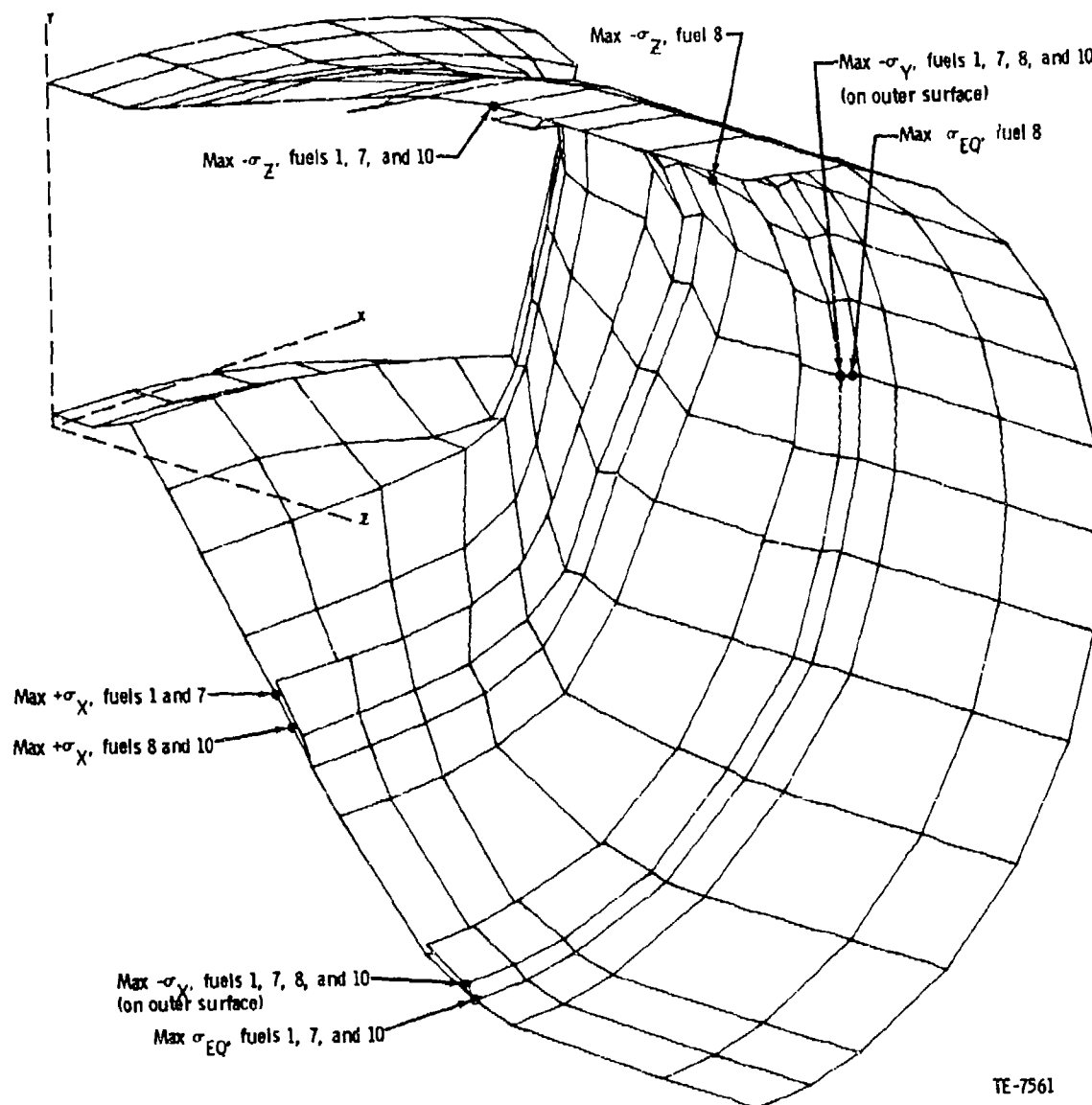
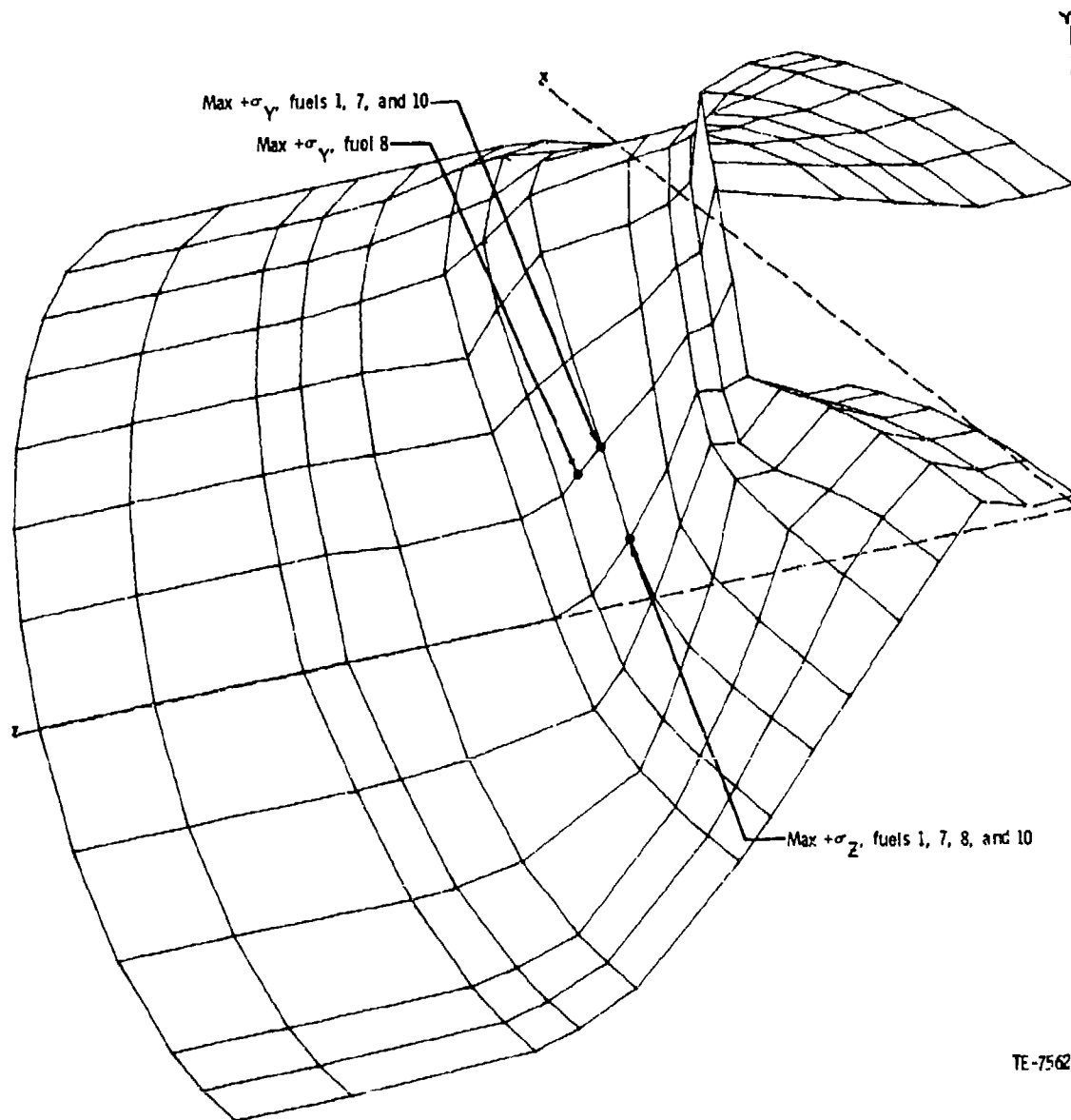


Figure D-2. - Computer-Simulated Discharge Nozzle Inner Surface
(STRATA Model).



TE-7562

Figure D-3. - Computer-Simulated Discharge Nozzle Outer Surface
(STRATA Model).